Report to
THE NATIONAL SCIENCE FOUNDATION
(RANN)
Grant No. GI-43880

STRUCTURAL WALLS IN EARTHQUAKE
RESISTANT STRUCTURES

Experimental Program

PROGRESS REPORT

By: J. E. Carpenter, A. E. Fiorato, G. B. Barney
        P. H. Kaar, R. G. Oesterle, H. G. Russell,
                    W. G. Corley

Date: August 29, 1975

Submitted by
RESEARCH AND DEVELOPMENT
CONSTRUCTION TECHNOLOGY LABORATORIES
PORTLAND CEMENT ASSOCIATION
Old Orchard Road
Skokie, Illinois   60076

50272-101

REPORT DOCUMENTATION PAGE	1. REPORT NO. NSF-RA-E-75-276	2.	3. Recipient's Accession No.
4. Title and Subtitle Structural Walls in Earthquake Resistant Structures, Experimental Program, Progress Report			**5. Report Date** August 29, 1975
			6.
7. Author(s) J. Carpenter, A. Fiorato, G. Barney et al			**8. Performing Organization Rept. No.**
9. Performing Organization Name and Address Portland Cement Association Old Orchard Road Skokie, Illinois 60076			**10. Project/Task/Work Unit No.**
			11. Contract(C) or Grant(G) No. (C) (G) GI43880
12. Sponsoring Organization Name and Address Applied Science and Research Applications (ASRA) National Science Foundation Washington, D.C. 20550			**13. Type of Report & Period Covered** Progress
			14.

15. Supplementary Notes

16. Abstract (Limit: 200 words)

An experimental program is presented to develop design criteria for reinforced concrete walls used as lateral bracing in earthquake resistant buildings. The primary concern is the ductility, energy dissipation, and strength of the walls. The program is divided into three parts--reversing loads applied to isolated walls, reversing loads applied to wall-systems, and testing of elements of systems. Each is discussed in detail, including descriptions of test specimens, apparatus and results, as well as interim conclusions and recommendations. Isolated walls represent an element of a structural wall system, and are being tested to determine their strength, ductility, and energy dissipation capacity. The ability of structural wall systems to resist lateral loads is being investigated to evaluate structural details necessary to assure intended interaction between the walls and the rest of the structure. Tests are being performed on specimens representing the compression zones of structural walls to evaluate the effect of confinement reinforcement and to determine the effective stress-strain curve of confined concrete.

17. Document Analysis   a. Descriptors

Concrete reinforcement
Concrete construction
Walls

Earthquakes
Earthquake resistant construction
Structural design

b. Identifiers/Open-Ended Terms

c. COSATI Field/Group

18. Availability Statement NTIS	19. Security Class (This Report)	21. No. of Pages 153
	20. Security Class (This Page)	22. Price

(See ANSI–Z39.18)   See Instructions on Reverse   OPTIONAL FORM 272 (4–77)
(Formerly NTIS–35)
Department of Commerce

TABLE OF CONTENTS

STRUCTURAL WALLS* IN EARTHQUAKE RESISTANT STRUCTURES

EXPERIMENTAL PROGRAM – PROGRESS REPORT

by

J. E. Carpenter, A. E. Fiorato, G. B. Barney, P. H. Kaar
R. G. Oesterle, H. G. Russell, W. G. Corley**

INTRODUCTION

Purpose

An experimental program is being carried out to develop design criteria for reinforced concrete walls used as lateral bracing in earthquake resistant buildings. The primary concern in this investigation is the ductility, energy dissipation, and strength of the walls. In addition to an experimental program, an analytical investigation is being carried out. The experimental program is described in this part of the Progress Report.

Organization of the Experimental Program

The experimental program is divided into three parts. In Part I, reversing loads are being applied to isolated walls. In Part II, reversing loads will be applied to wall-systems. In Part III, elements of systems are being tested. Currently, Part III is limited to an investigation of the behavior of confined concrete.

---

*In conformity with the nomenclature soon to be adopted by both the Applied Technology Council and the Revision of Appendix A of ACI 318-71, Building Code Requirements for Reinforced Concrete, the term "structural wall" is used in place of "shear wall."

**Respectively, Principal Structural Engineer, Structural Engineer, Structural Engineer, Senior Structural Engineer, Associate Structural Engineer, Manager, Structural Development Section; Director Engineering Development Department, Portland Cement Association, Skokie, Illinois.

In this Introduction, the organization of the experimental program is briefly described and highlights are presented. Following the Introduction, a more detailed description of each part is given. Included are descriptions of the test specimens, test apparatus, test results, interim conclusions and recommendations.

Highlights of the Program to Date

Part I - Isolated Walls. The isolated walls represent an element of a structural wall system. They are being tested to determine their strength, ductility, and energy dissipation capacity.

The test specimens are approximately 1/3-scale models of actual walls. The model walls are 15-ft. high and have a horizontal length of 6 ft. 3 in. The web thicknesses are 4 in. All test specimens are subjected to in-plane horizontal reversing loads. The loads are applied alternately on one side and then on the other. A specimen and the testing apparatus are shown in Fig. 1.

Controlled variables covered in the program to date include the shape of the wall cross section, the amount of main flexural reinforcement, and the amount of hoop reinforcement around the main flexural reinforcement.

The following observations are based on a preliminary examination of the data from the tests of the first five specimens:
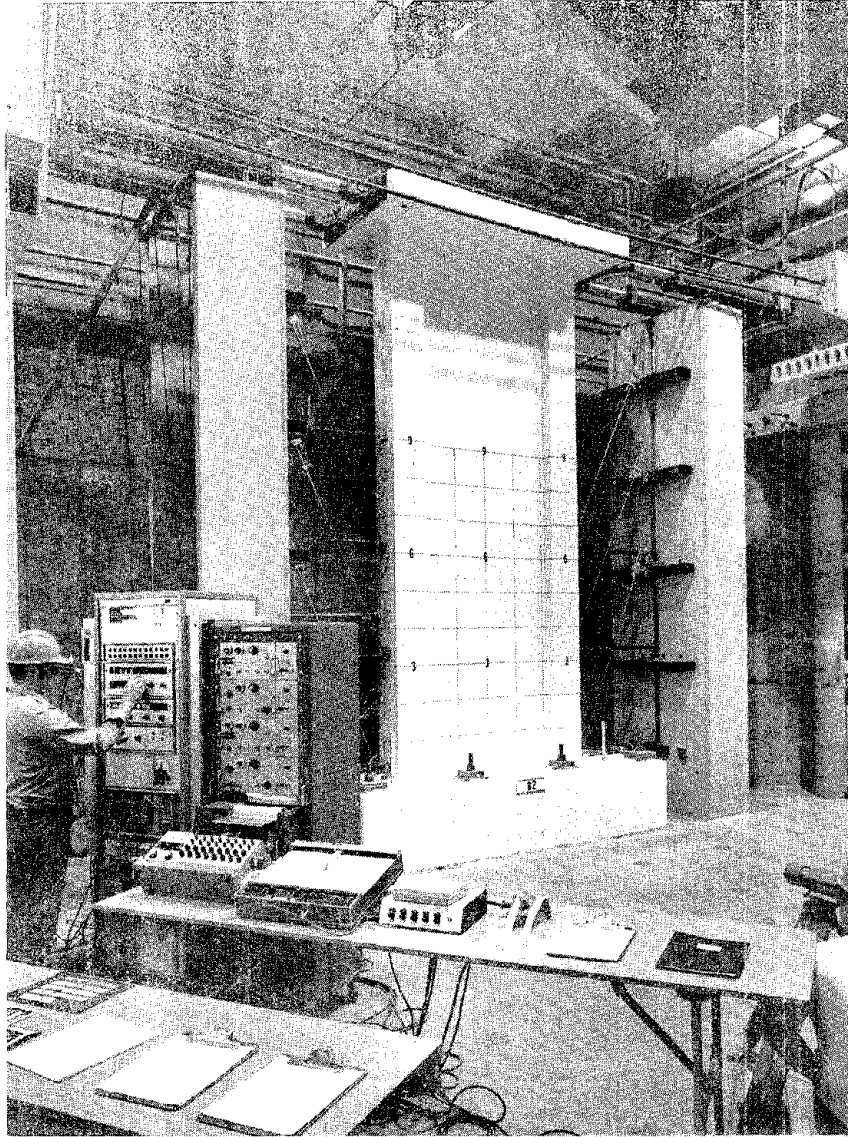
Fig. 1   Test Specimen and Test Apparatus

1. All specimens had a load capacity greater than predicted by the 1971 ACI Code[1] design for both flexure and shear.

2. All specimens had post-yield deflection capabilities under reversing load.

3. Two specimens were loaded relatively lightly in shear ($v_{max} < 3\sqrt{f'_c}$) and had ordinary column ties. Capacities of these specimens were governed by damage to the boundary elements as alternate tensile yielding and compressive buckling of the main flexural reinforcement occurred. Buckling of a bar was followed, within one to three loading cycles, by fracture of the bar. Strength loss in these specimens was associated with bar fractures and with the loss of broken concrete pieces not contained by the reinforcing cage.

4. Two specimens were loaded relatively heavily in shear ($v_{max} > 7\sqrt{f'_c}$). The failure mode for these specimens was associated with web shear distress. In one of these specimens, the test ended with severe web crushing at a nominal shear stress $v_{max} = 10.4\sqrt{f'_c}$. Six inelastic cycles were applied to the specimen prior to web crushing.

5. Lateral confinement reinforcement added around the main flexural reinforcement in the bound-

_____

[1] Numbers in parenthesis refer to References on pages 145 and 146.

-4-

ary elements of one specimen helped to limit
bar buckling. These hoops also contained
the broken pieces of concrete within the core
of the boundary elements. Even with the con-
finement, buckling of the main flexural rein-
forcement occurred. However, the length of
the buckled portion of the bar was shorter in
the confined specimen. Buckling was followed
by bar fracture within one to two loading
cycles. The specimen with confinement under-
went 29 inelastic cycles prior to bar frac-
tures. In comparison, the specimen without
confinement underwent 21 inelastic cycles.

6. The load capacity of the confined specimen was
   approximately the same as that for a companion
   specimen without confinement.

7. The confined specimen had an overall top deflec-
   tion ductility factor of about 50% greater than
   that for the companion specimen without con-
   finement.

8. For all specimens, the primary area of distress
   was within a height equal to the horizontal
   length of the wall.

9. The construction joint at the base of each
   specimen showed maximum slip in the range
   of 0.2 in. to 0.3 in. No specimen fail-
   ures could be attributed to construction
   joint performance.

10. Free vibration measurements taken at intervals throughout the test of each wall showed that the frequency decreased by a factor of about three from the uncracked state to the state where yielding had occurred. For the same conditions, damping increased from about 2% to about 10% of critical. After yielding no significant change in damping was observed.

Part II - Systems. Part II deals with structural wall systems to resist lateral loads. The investigation is being conducted to evaluate structural details necessary to assure intended interaction between the walls and the rest of the structure. Four systems will be tested. These are walls coupled with deep beams, walls coupled with slender beams, walls with openings, and wall-frame systems.

A major part of the investigation to date has been concerned with the proportioning and designing of the four test specimens. Tentative proportions for each of the four specimens have been established. Detailed design of the first specimen and of test apparatus are currently under way.

In the design of the four specimens, the following items were considered:

1. Details of the coupling beams were selected to provide adequate strength and ductility. A testing program to verify that the details are suitable is being developed for Part III - Elements.

2. Proportions of the coupling beams were
   selected so that flexural behavior and
   shear behavior will be equally important
   for the shorter beams. Flexural behavior
   will predominate for the longer beams.
   Overall length-thickness ratios of 2.5 to
   1 and 5 to 1 have been selected for the
   shorter and longer beams respectively.

3. Proportions of the specimens were selected
   to provide a specific hinging sequence.
   In the coupled wall specimens, the coupling
   beams were designed to hinge before the
   walls.

4. For ease of construction and testing, the
   proportions were selected to vary syste-
   matically from one specimen to the next.

   Part III - Elements. Tests have been performed on
specimens representing the compression zones of structural
walls. These tests are being performed to evaluate the ef-
fect of confinement reinforcement and to determine the ef-
fective stress-strain curve of confined concrete.

   The test specimen has been adapted from one developed
earlier for the determination of the stress-strain curves for
plain concrete.[2] Figure 2 shows a specimen being tested.
The controlled variables in the test program include spac-
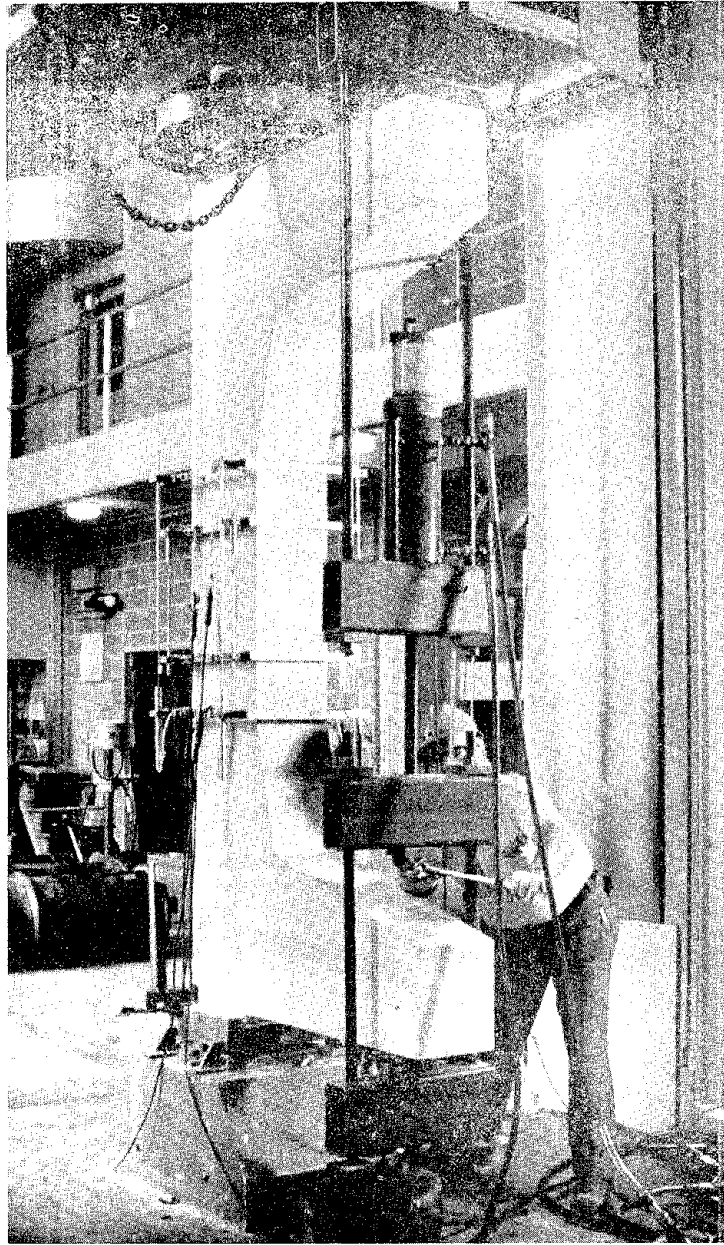ing and size of the confinement reinforcement, concrete

-7-

Fig. 2   Element Test Specimen

-8-

strength, amount of longitudinal reinforcement, and size of test specimen.

Based on a preliminary analysis of the test results, the following observations were made:

1. Confinement reinforcement was beneficial in providing higher concrete strains without substantial loss of ability to withstand compressive stress.

2. No. 4 bars at 4-in. spacing appeared to represent a transition point. Decreasing the bar size or increasing the bar spacing beyond this point showed a marked decrease in maximum concrete strain.

Future Course of the Investigation

Work in the next period of the project will continue as an extension of the present program. In Part I, the effects of confinement reinforcement, concrete strength and monotonic loading will be investigated. In Part II, construction of the systems specimens will continue and testing will begin. In Part III, tests of coupling beams will be completed and an investigation of splices will begin. Other tests will be included if the test program indicates areas for further investigation.

PART I - ISOLATED WALLS

Objective and Scope

The objectives of the experimental investigation of isolated walls are:

1. To determine the load-deformation characteristics for a wide range of configurations of wall specimens. This information will be used in the inelastic dynamic analyses.

2. To determine the ductility and energy dissipation capacity of walls subjected to reversing loads.

3. To determine the flexural and shear strengths of walls subjected to reversing loads, and to compare these strengths with the strengths under monotonic loading.

4. To determine means of increasing the energy dissipation capacity of walls where required.

5. To develop design procedures for walls of adequate strength and energy dissipation capacity.

To attain these objectives, an experimental program was developed to investigate the behavior of reinforced concrete walls to resist lateral loads.

The experimental program to date includes tests on five models of reinforced concrete walls. The test specimens represent approximately 1/3-scale models of full-scale walls, although no specific prototype walls were modeled.

All test specimens were subjected to in-plane lateral reversing loads.

The controlled variables in the program have been the shape of the wall cross-section, the amount of main flexural re-inforcement, and the amount of hoop reinforcement around the main flexural reinforcement.

Table 1 provides a summary of the specimens tested.

Test Program

Introduction. A detailed description of the geo-metric and material properties of the first five specimens tested are given in this section. In addition, the construction, instrumentation, and testing procedures are described.

Description of Test Specimens. The dimensions of the test specimens are shown in Fig. 3. Height of the wall, from the top of the base block to the center of the top slab, is 15 ft. The horizontal length of the wall is 6 ft. 3 in. and its web thickness is 4 in.

Three different wall cross-sections have been tested. These are flanged, barbell, and rectangular sections. The nomi-nal cross-sectional dimensions of the three sections are shown in Fig. 4.

The 2x4x10-ft. base block shown in Fig. 3 is used to secure the specimens to the laboratory floor during testing. The slab on top of the wall, also shown in Fig. 3, is used to transfer the loads to the test specimen. Both the base block and the top slab were designed to ensure that no premature

TABLE 1.   SUMMARY OF TESTS

Specimen Mark	Shape*	Reinforcement Percentage		
		Flexural**	Shear	Confinement (ρ_s)+
F1	Flanged	3.89	0.71	—
B1	Barbell	1.11	0.31	—
B2	Barbell	3.67	0.63	—
R1	Rectangular	1.47	0.31	—
B3	Barbell	1.11	0.31	1.28

* Shapes of Cross Sections are shown in Fig. 4

** Based on area of boundary element

+ $\rho_s = 2\,A_{sh}/\ell_h\,s_h$

where

ρ_s = ratio of volume of spiral reinforcement to total volume of core

A_{sh} = area of transverse hoop bar (one leg)

ℓ_h = maximum unsupported length of rectangular hoop

s_h = center-to-center spacing of hoops
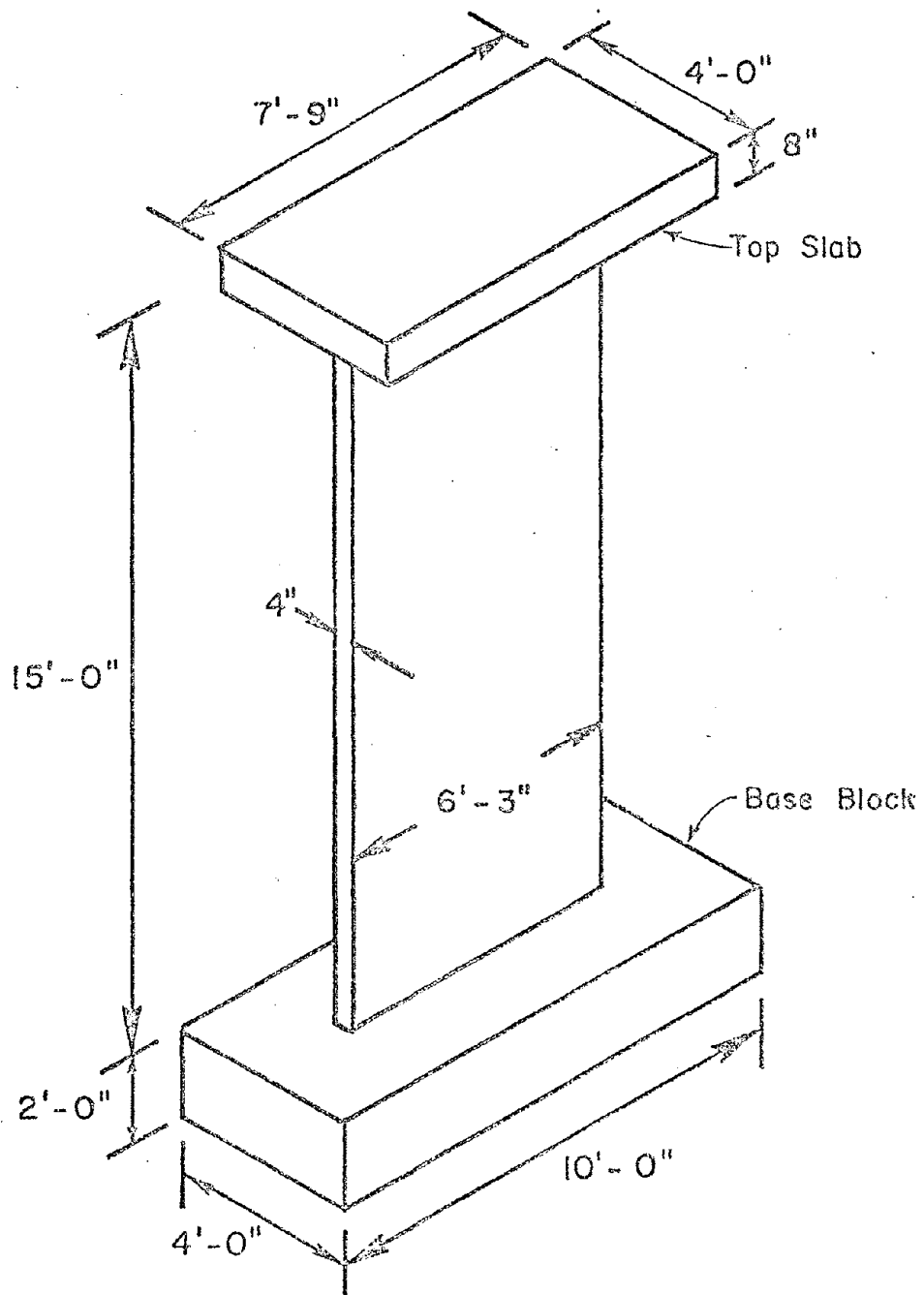
Fig. 3 Nominal Dimensions of Test Specimen
With Rectangular Cross Section
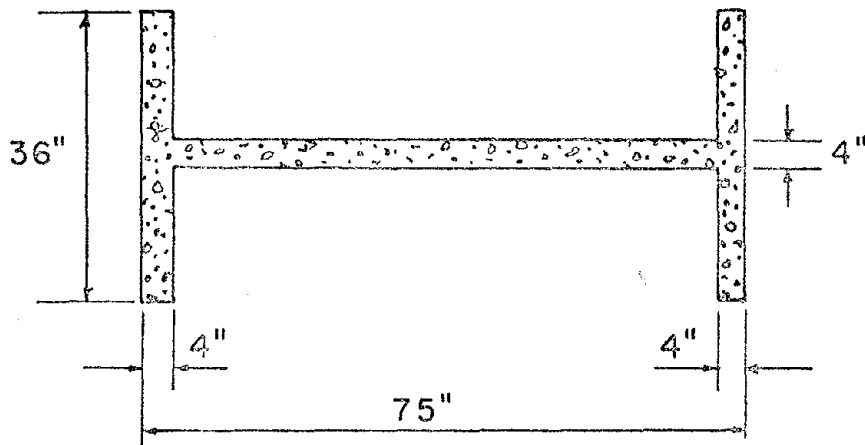
(a) Flanged Section
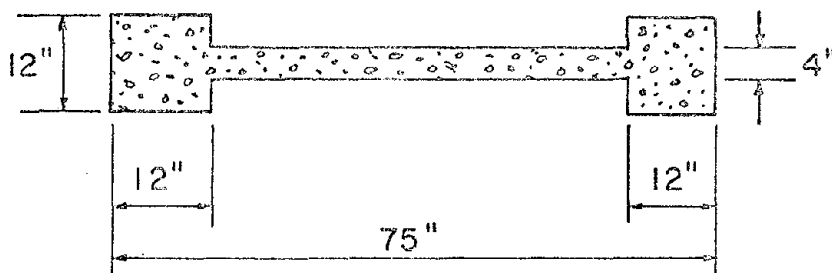
(b) Barbell Section
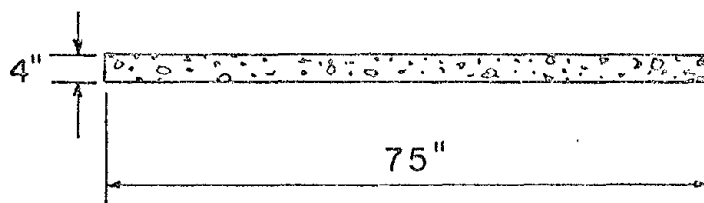
(c) Rectangular Section

Fig. 4 Nominal Cross-Sectional Dimensions
of Test Specimens

termination of the test would occur because of a failure of these loading or supporting elements.

Design of Test Specimens. The following procedure was used in designing the test specimens. First, a nominal percentage of main flexural reinforcement was selected. This was either 1% or 4% based on the area of the boundary element. For rectangular sections, the "boundary element" was taken to extend 7.5 in. from each end of the wall. The percentages of flexural reinforcement were chosen to bound the range of values commonly encountered in practice.

Nominal vertical web reinforcement provided in the walls was 0.25% of the gross concrete area of the horizontal wall section. This is the minimum amount permitted by the 1971 ACI Code, Section 10.2.[1] Design yield stress of the steel was taken as 60,000 psi and design concrete strength was taken as 6000 psi. Strain hardening of the steel, according to ACI Code assumptions, was neglected in calculating the moment capacity.

Horizontal shear reinforcement was designed to develop the moment capacity. The shear design was made according to the 1971 ACI Code, Section 11.16.[1]

The vertical and horizontal reinforcement was constant over the height of the specimens.

Details of Reinforcement. Reinforcing details for the five specimens tested are shown in Fig. 5 through Fig. 19. All reinforcing steel was detailed and fabricated according to standard practice.[1,3]
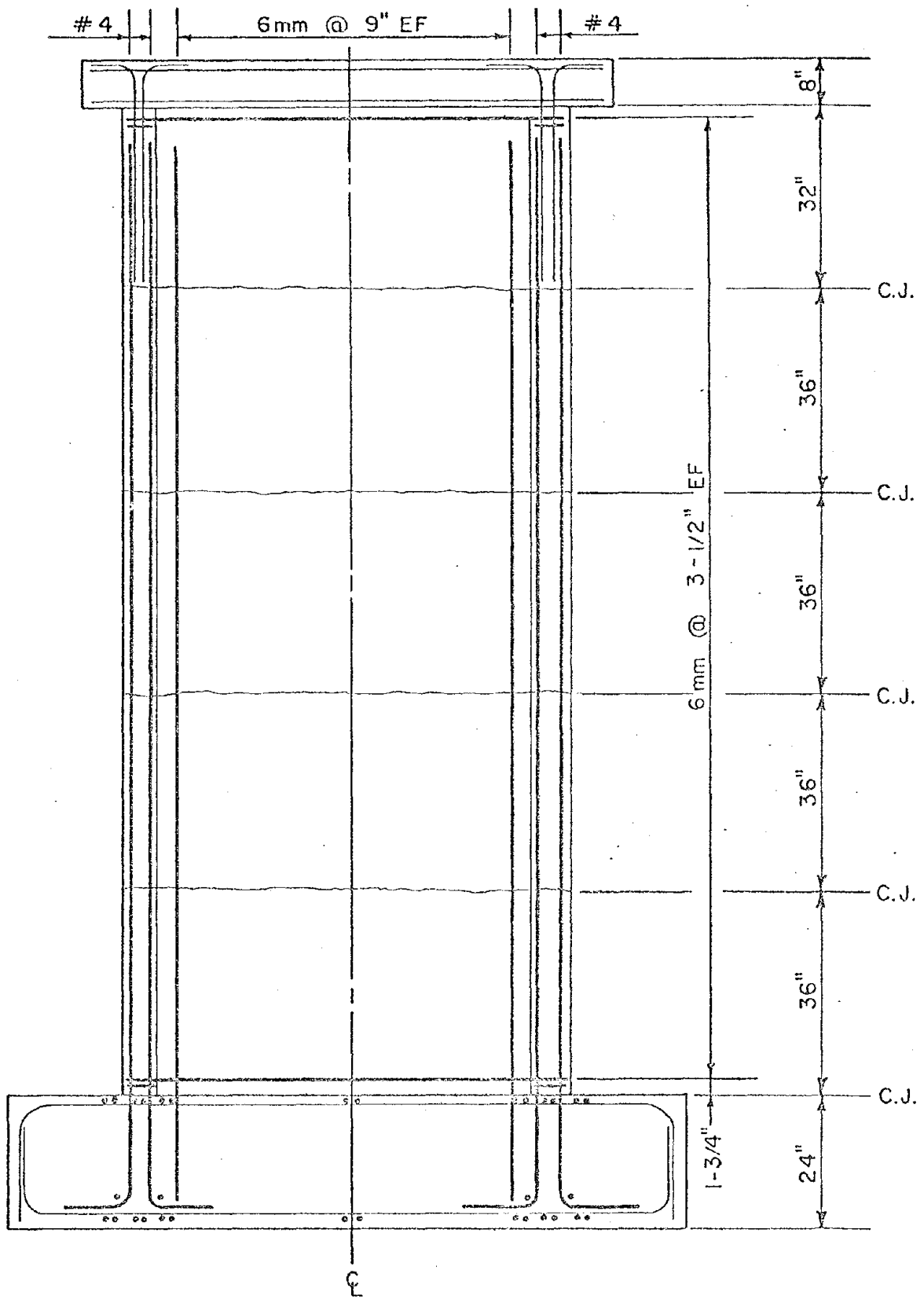
Fig. 5   Elevation of Specimen F1

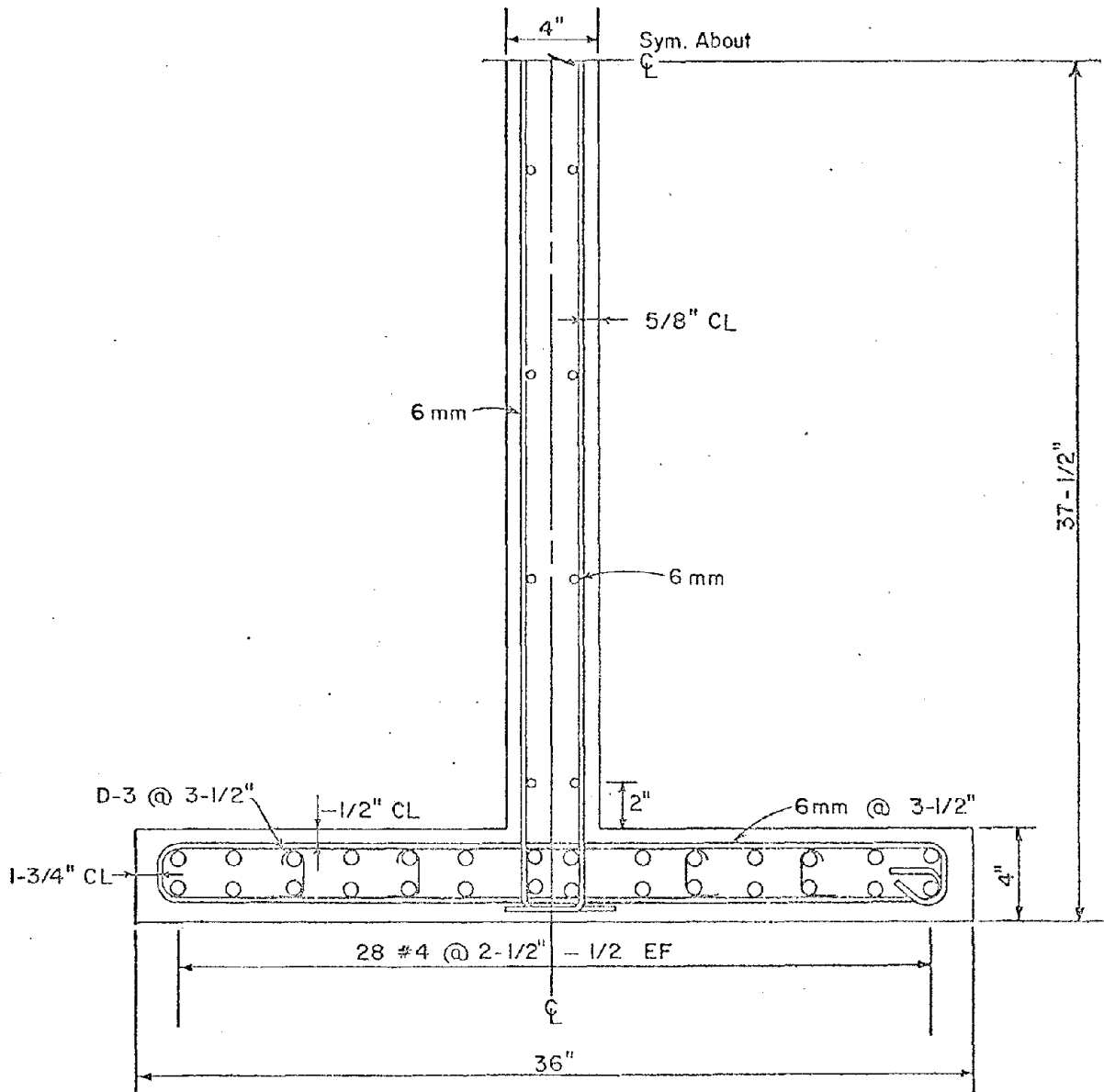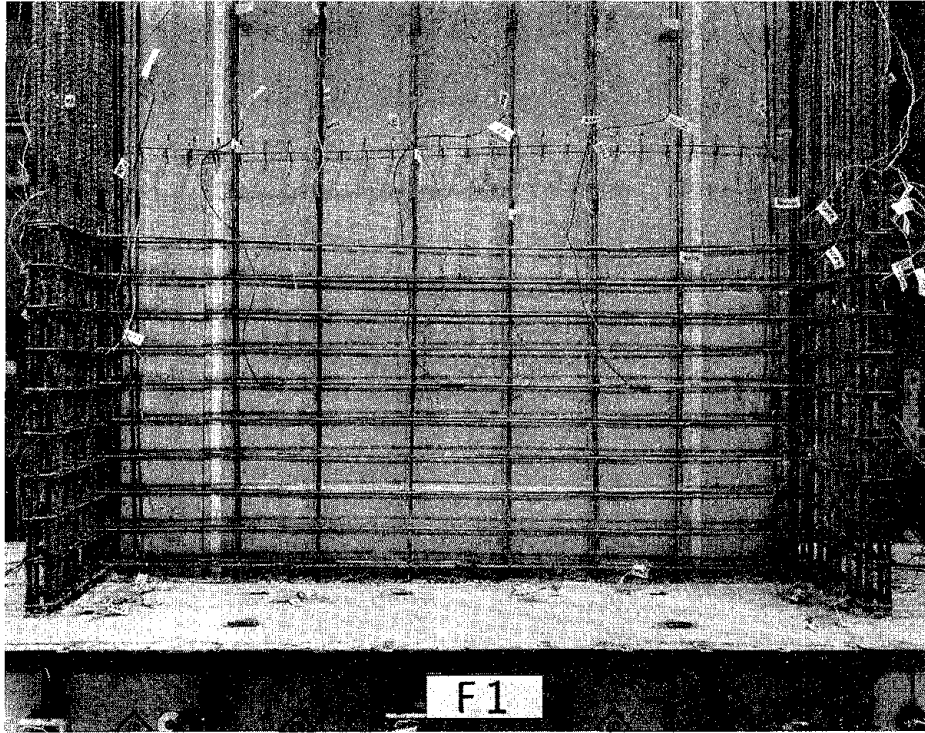Fig. 6   Cross Section of Specimen F1

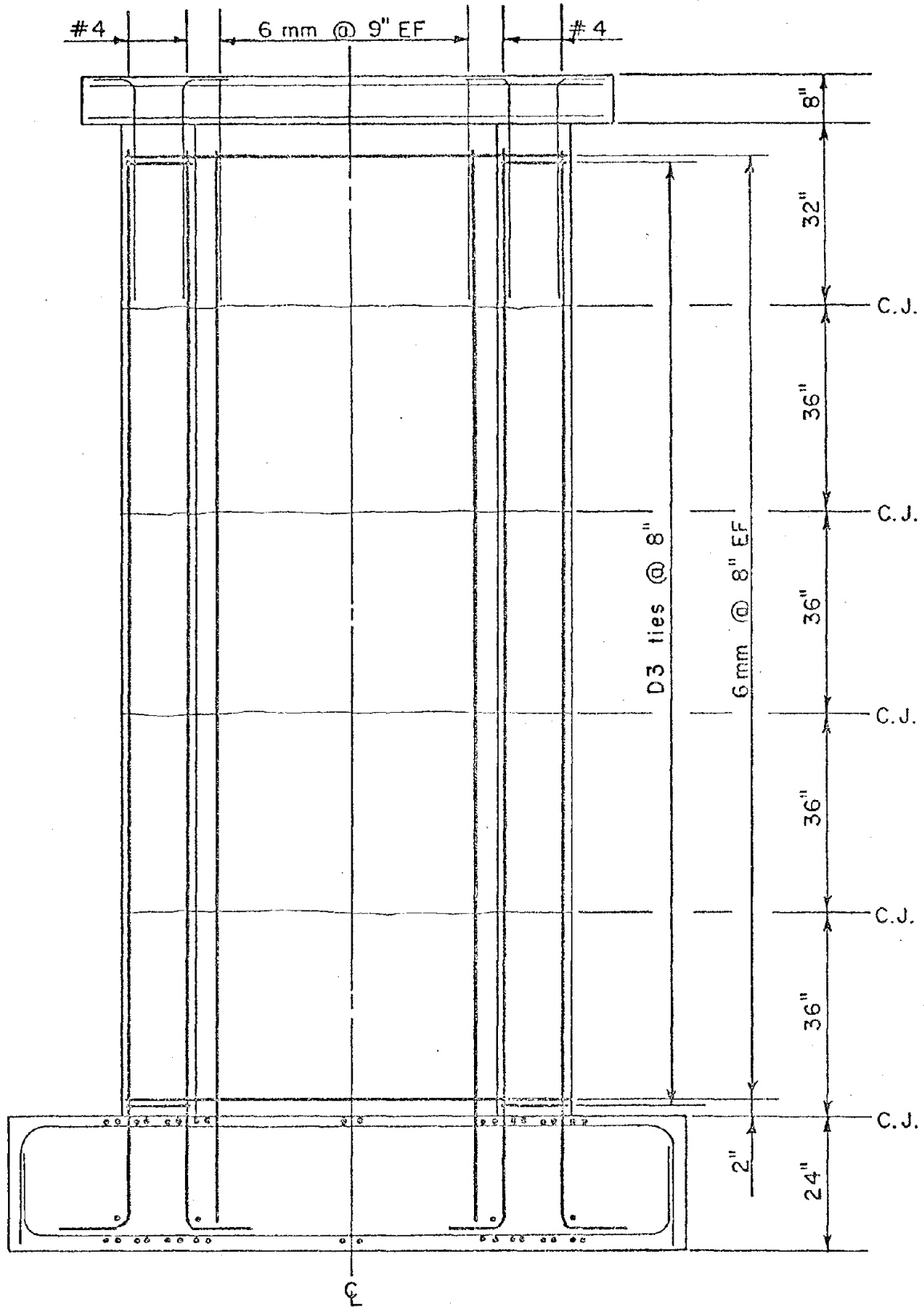Fig. 7   Reinforcement for First Wall Lift
of Specimen F1

Fig. 8   Elevation of Specimen Bl

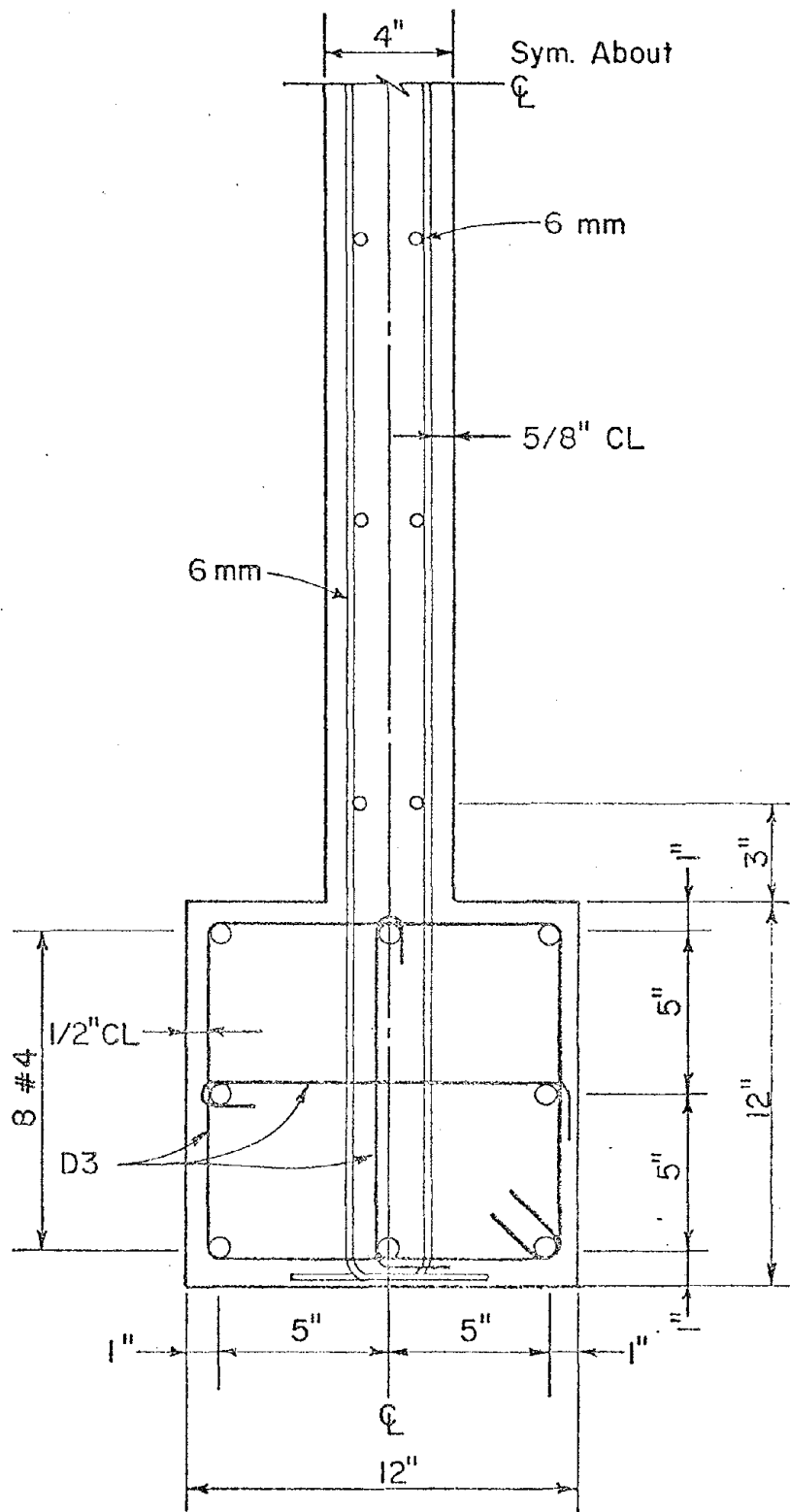Fig. 9 Cross Section of Specimen B1

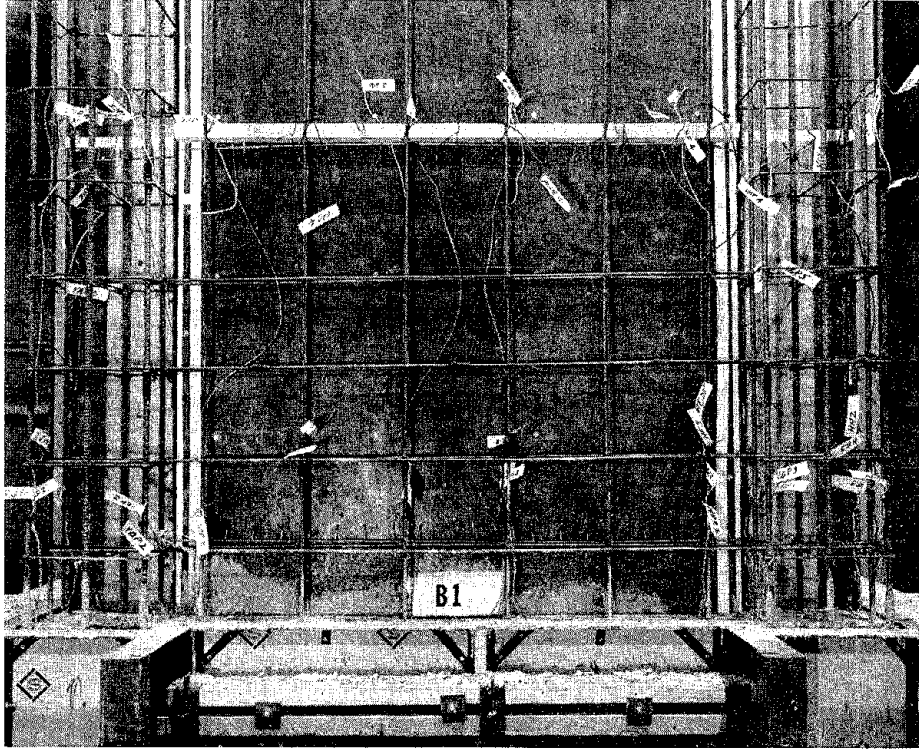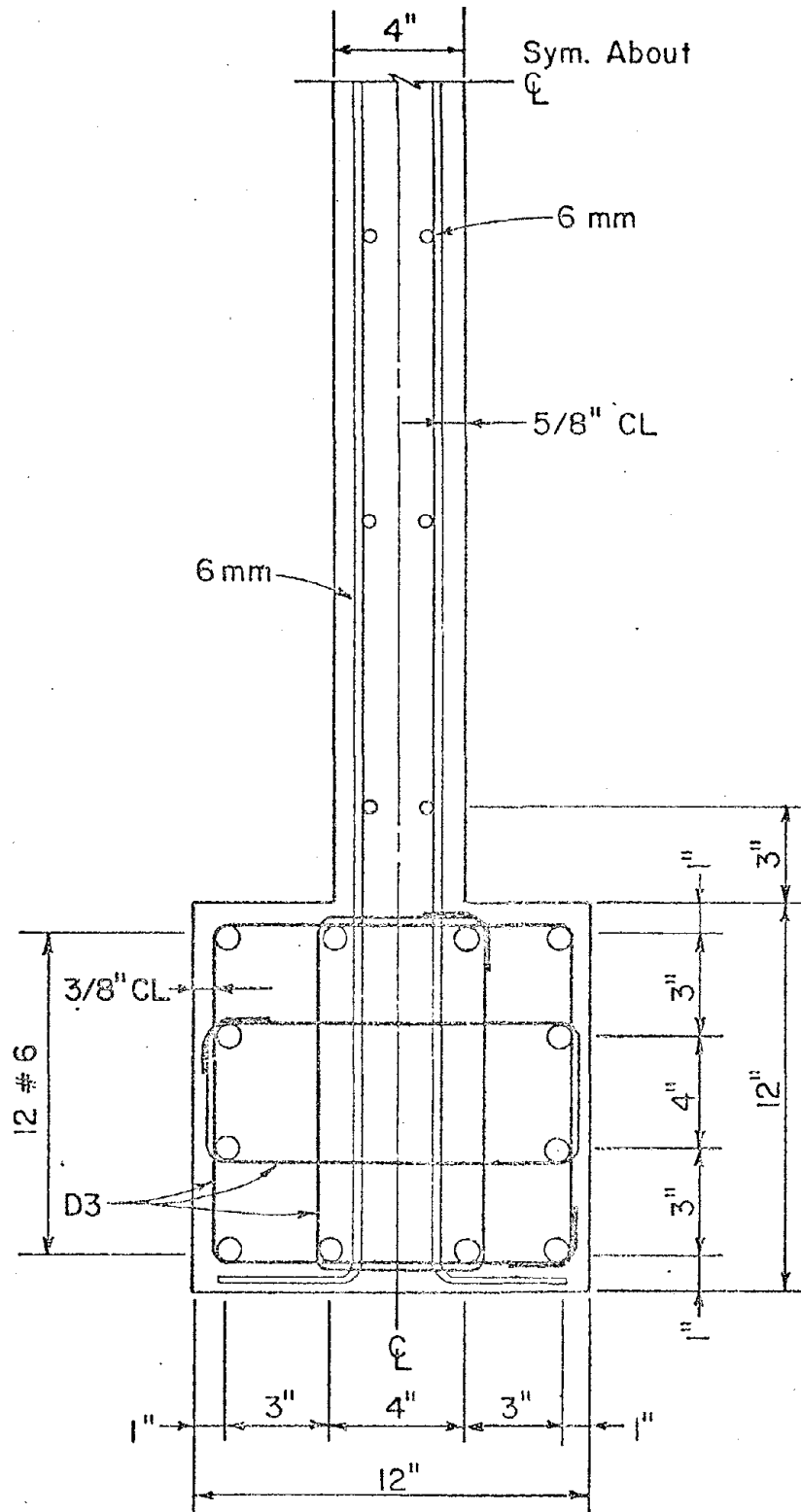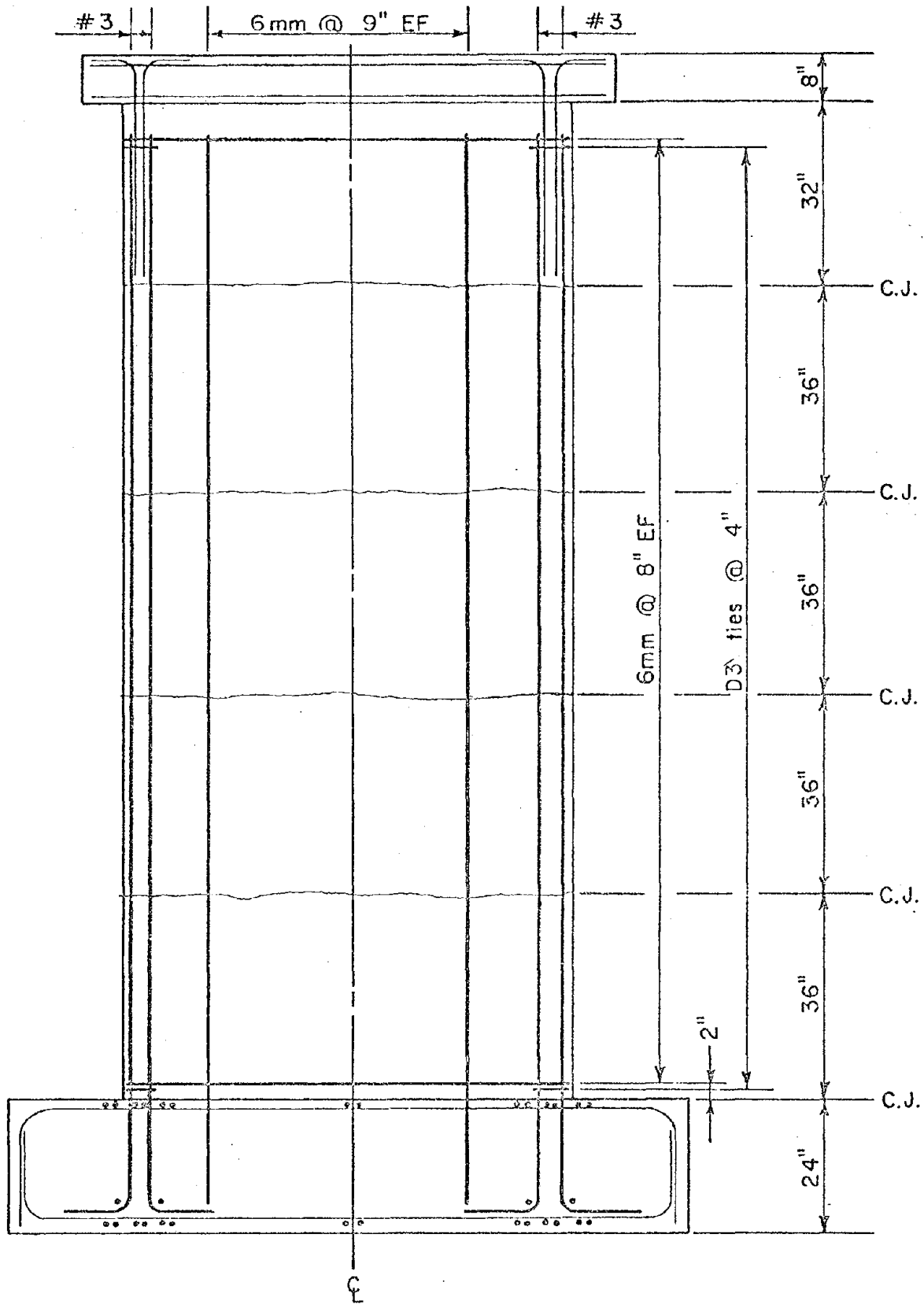Fig. 10   Reinforcement for First Wall Lift
of Specimen B1

Fig. 11   Elevation of Specimen B2

Fig. 12   Cross Section of Specimen B2

Fig. 13   Reinforcement for First Wall Lift
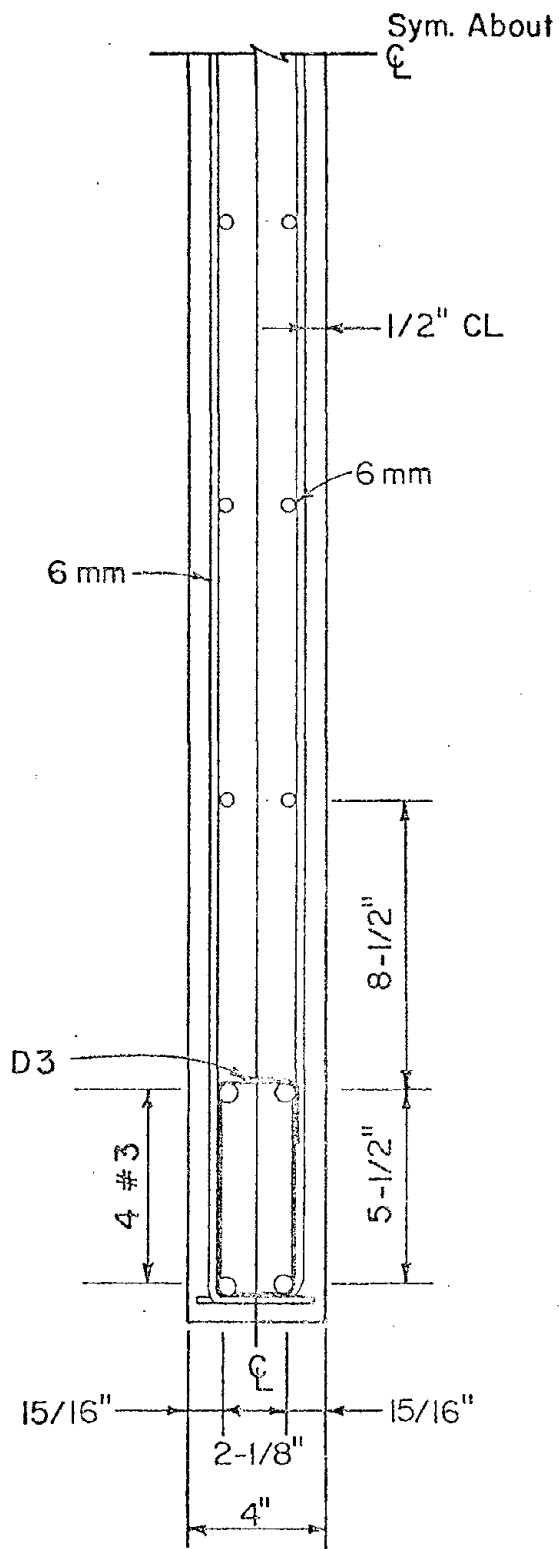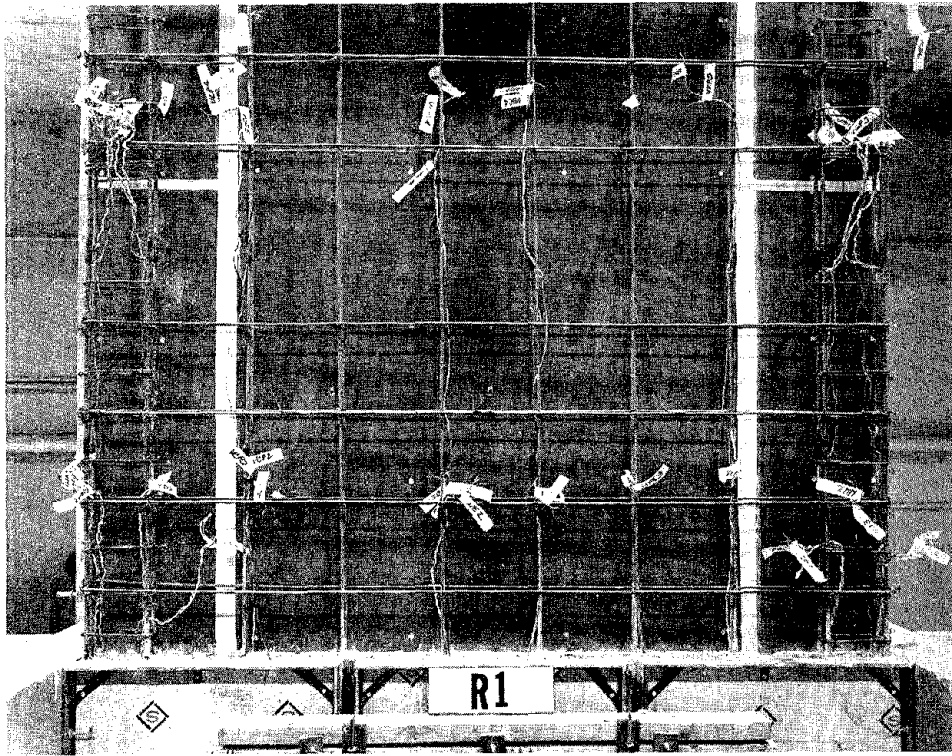of Specimen B2

Fig. 14   Elevation of Specimen Rl

Sym. About
C

1/2" CL

6 mm

6 mm

8-1/2"

5-1/2"

D3

4 #3

C

15/16"   15/16"

2-1/8"

4"

Fig. 15   Cross Section of Specimen R1

-26-

Fig. 16   Reinforcement for First Wall Lift
of Specimen R1

-27-

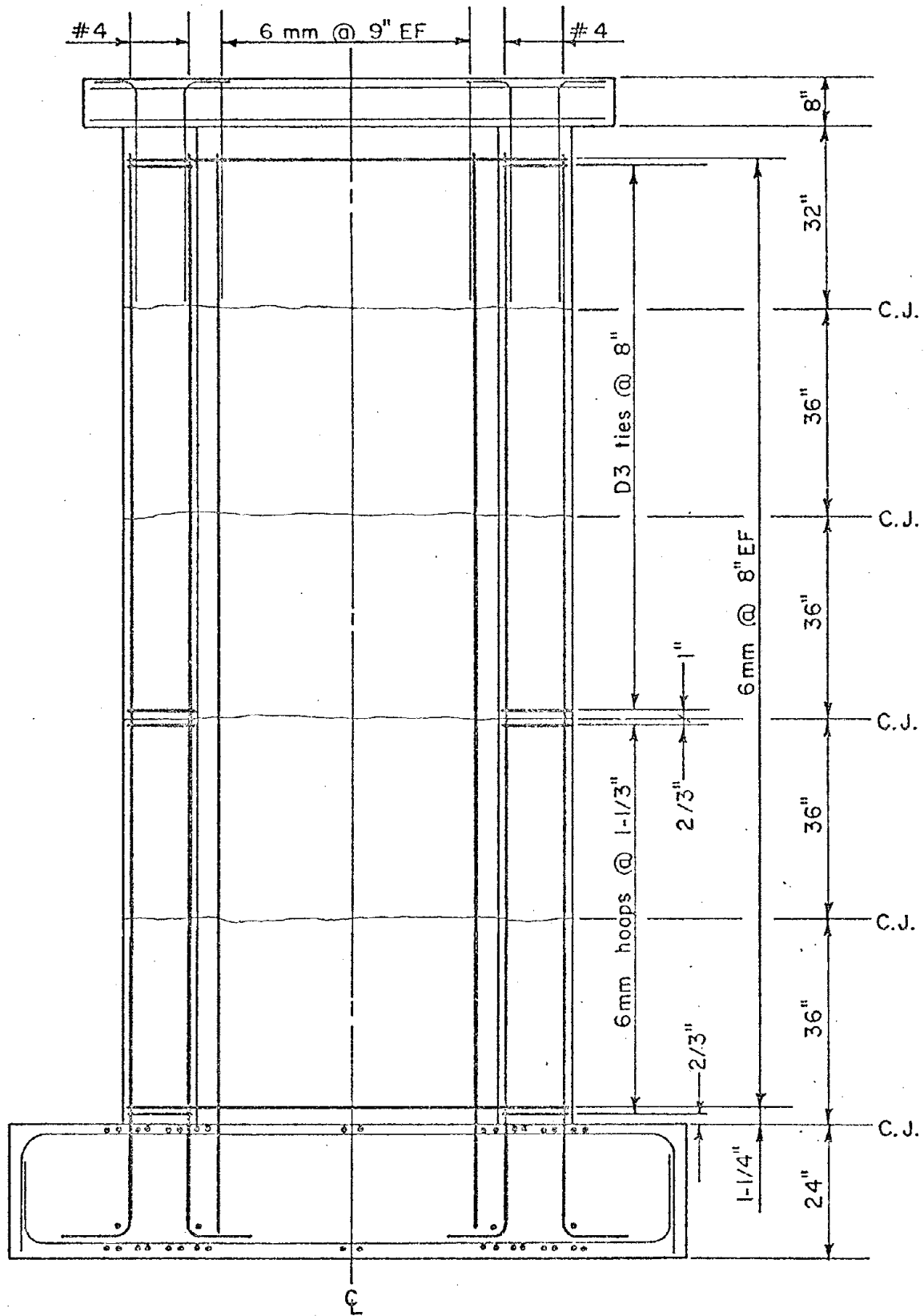Fig. 17 Elevation of Specimen B3

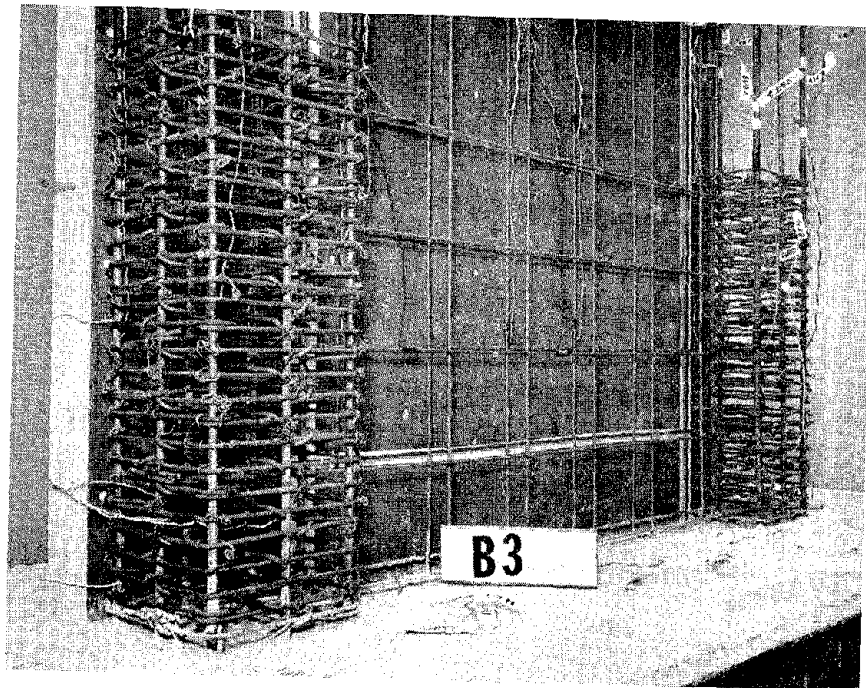Fig. 18   Cross Section of First Two Lifts of Specimen B3

Fig. 19   Reinforcement for First Wall Lift
of Specimen B3

Except for Specimen B3, no special reinforcing details were used. Tie spacings were selected according to the 1971 ACI Code, Section 7.12.[1]

Specimen B3 was constructed with confinement reinforcement in the boundary elements of the first two wall lifts. In all other respects, Specimen B3 was nominally the same as Specimen B1. The confinement hoops were designed according to Appendix A of the 1971 ACI Code.[1]

Concrete. A concrete mix using a maximum aggregate size of 3/8 in. was selected for the walls. Type I cement, sand, and coarse aggregate were combined to provide concrete with a slump of $3 \pm 1/2$ in. Aggregate gradation curves for the sand and coarse aggregate are given in Fig. 20.

Physical properties of the concrete used in each specimen are given in Table 2. Compressive strength and modulus of elasticity of the concrete were determined from compressive tests on 6x12-in. cylinders. The modulus of rupture was determined from tests on 6x6x30-in. beams. A representative stress-strain relationship for the concrete is shown in Fig. 21.

Reinforcement. In the specimens, No. 3, No. 4, and No. 6 bars conforming to ASTM Designation A615 Grade 60 were used as reinforcement. Deformed 6mm hot rolled bars with properties similar to Grade 60 were also used. Deformed wire, size D-3, was used to represent smaller bar sizes. This wire was heat-treated to obtain stress-strain characteristics similar to those of Grade 60 bars.
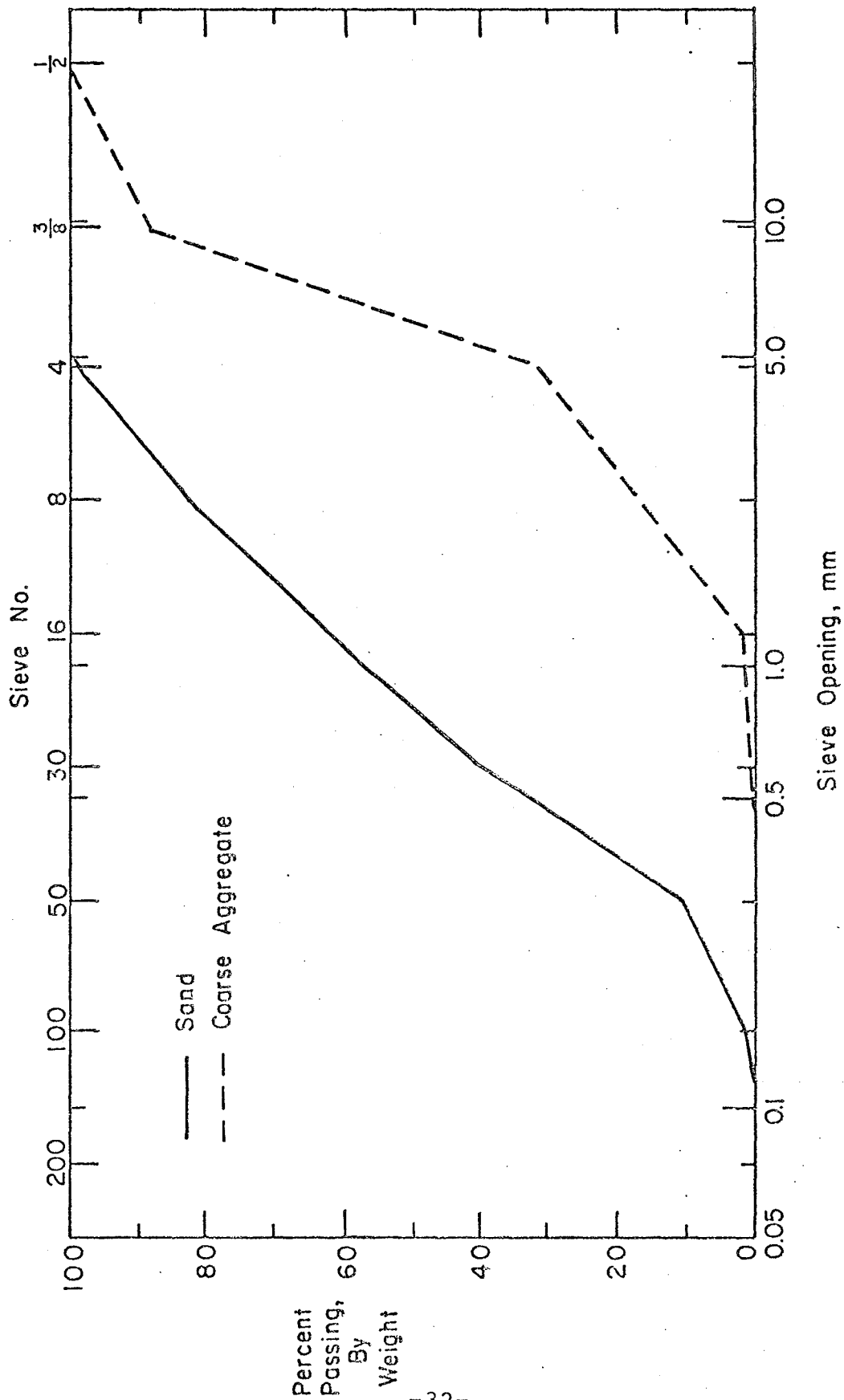
Fig. 20 Aggregate Gradation Curves

-32-

TABLE 2. CONCRETE PROPERTIES FOR TEST SPECIMENS

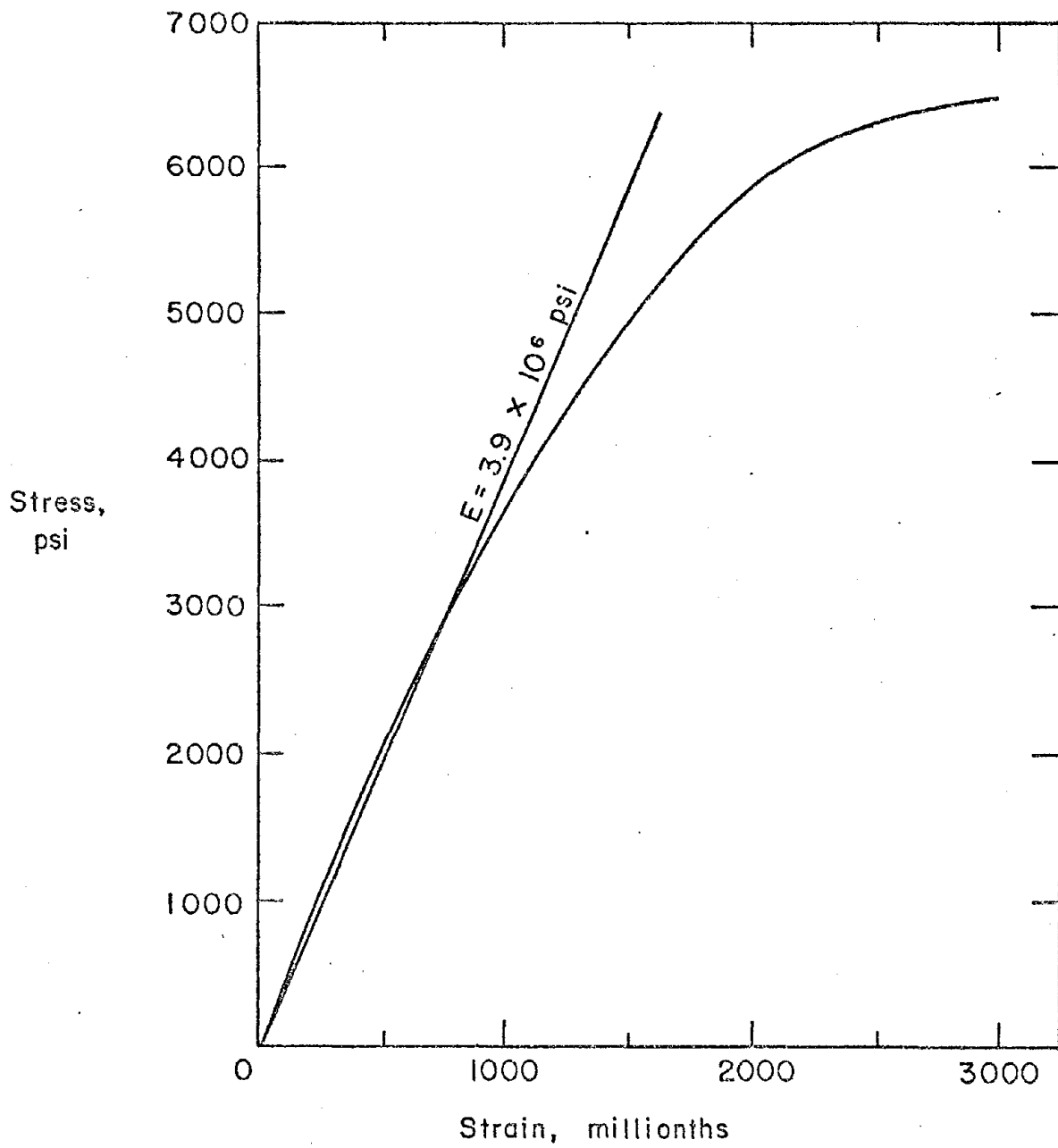| Specimen	Lift Number	Age (Days)	Compressive Strength f'_c (psi)	Modulus of Rupture f_r (psi)	Modulus of Elasticity E_c (psi x 10^6)
F1	2	70	5620	660	3.62
	3	65	5530	610	3.76
	4	60	5780	590	3.71
	5	53	6120	620	3.95
B1	2	56	7780	730	4.20
	3	54	7590	730	3.95
	4	49	7080	750	4.14
	5	46	6980	750	3.93
B2	2	49	7900	680	4.19
	3	44	7650	740	4.20
	4	41	7260	730	3.74
	5	36	7270	670	3.81
R1	2	50	6540	670	4.14
	3	45	6440	640	3.92
	4	43	6630	640	3.78
	5	36	6050	610	3.76
B3	2	56	6940	685	3.98
	3	51	6783	587	3.94
	4	45	6795	620	3.81
	5	43	6370	575	3.84

Fig. 21 Stress versus Strain Relationship for Concrete

The physical properties of the reinforcement used in the test specimens are summarized in Table 3. Representative stress-strain relationships for the reinforcement are shown in Fig. 22.

Construction of Test Specimens. Test specimens were constructed in the vertical position. The formwork system shown in Fig. 23 was designed to facilitate construction. Stationary formwork served to maintain the vertical position of the specimen. Each wall was cast in six lifts as shown in Fig. 24.

At the start of construction, a heavy reinforcing cage for the base block was constructed. This cage was placed on the level base platform of the formwork. The vertical wall reinforcement was then placed in the base cage and supported against the stationary formwork. After the vertical reinforcement was secured, the base block was cast. This casting was designated Lift 1.

Following casting of the base block, the construction joint was prepared and the horizontal reinforcement for Lift 2 was placed. Then the removable formwork for Lift 2 was set, and Lift 2 was cast. Subsequent wall lifts were constructed in the same manner. The wall lifts were 36-in. in height. Figure 25 shows Specimen B1 during construction.

Construction joints between lifts were made following standard practice.[4] The surface of the concrete was roughened with a cold chisel, and cleaned of laitance and loose particles prior to placing the adjoining concrete.

TABLE 3.   REINFORCING STEEL PROPERTIES FOR TEST SPECIMENS

Size	Properties	Specimen				
		F1	B1	B2	R1	B3
D3*	f_y (ksi)	69.7	68.7	67.1	66.0	69.0
	f_{su} (ksi)	76.6	75.1	74.4	72.0	75.8
	E_s (psix10^6)	32.8	33.0	33.8	30.6	32.5
	Elong. (%)	10.3	11.0	9.4	5.9	8.9
6mm**	f_y (ksi)	76.2	75.5	77.2	75.7	69.4
	f_{su} (ksi)	102.2	100.8	101.6	101.5	95.5
	E_s (psix10^6)	31.3	32.5	32.1	31.4	30.4
	Elong. (%)	10.4	10.7	10.2	12.2	11.7
No.3	f_y (ksi)	–	–	–	74.2	–
	f_{su} (ksi)	–	–	–	111.0	–
	E_s (psix10^6)	–	–	–	27.8	–
	Elong. (%)	–	–	–	9.8	–
No.4	f_y (ksi)	64.5	65.2	–	–	63.5
	f_{su} (ksi)	102.6	102.7	–	–	101.0
	E_s (psix10^6)	28.1	28.3	–	–	25.9
	Elong. (%)	11.5	11.7	–	–	10.9
No.6	f_y (ksi)	–	–	59.5	–	–
	f_{su} (ksi)	–	–	100.8	–	–
	E_s (psix10^6)	–	–	30.2	–	–
	Elong. (%)	–	–	13.3	–	–

*A = 0.03 sq. in. d_b = 0.195 in.

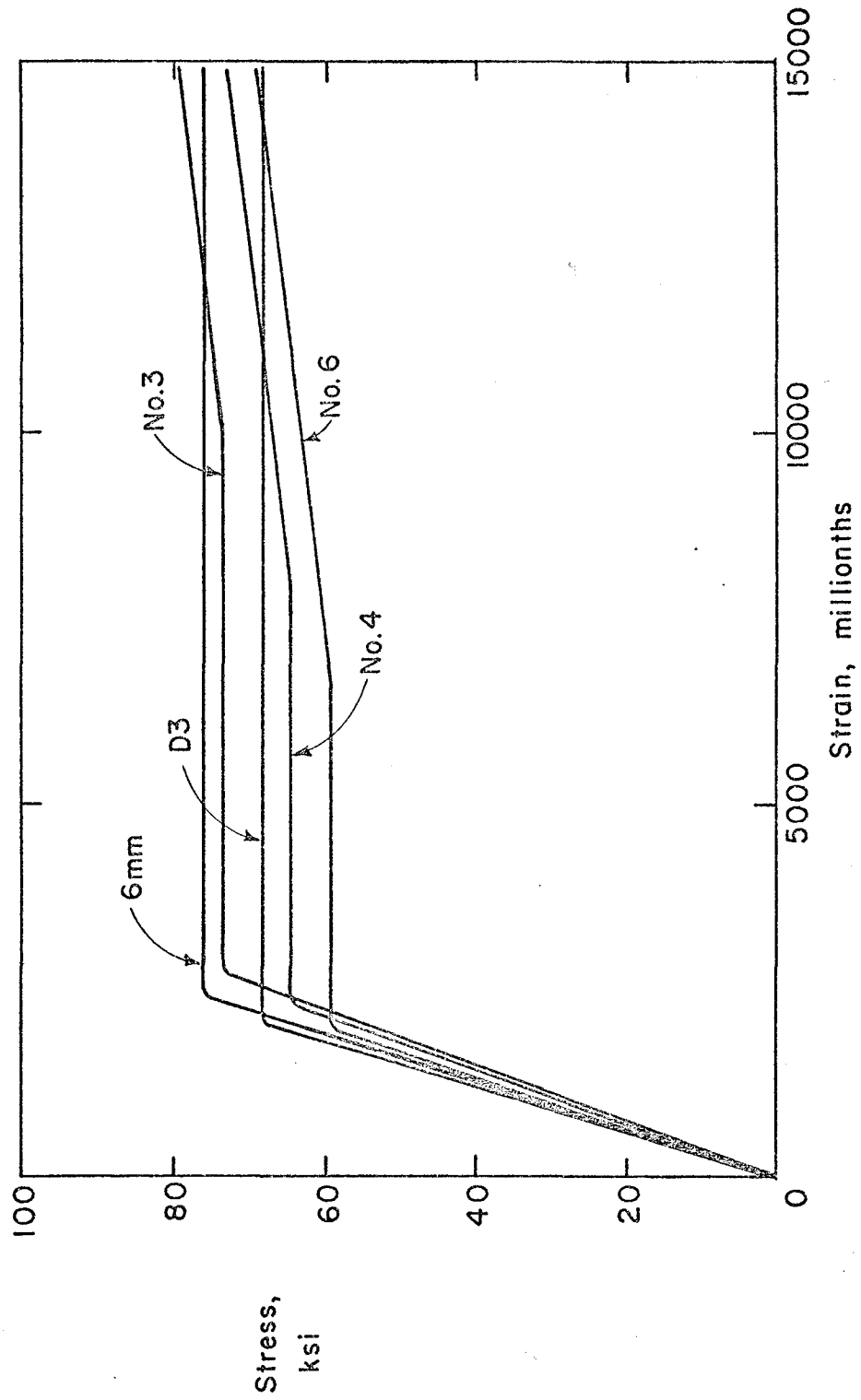**A = 0.05 sq. in. d_b = 0.25 in.

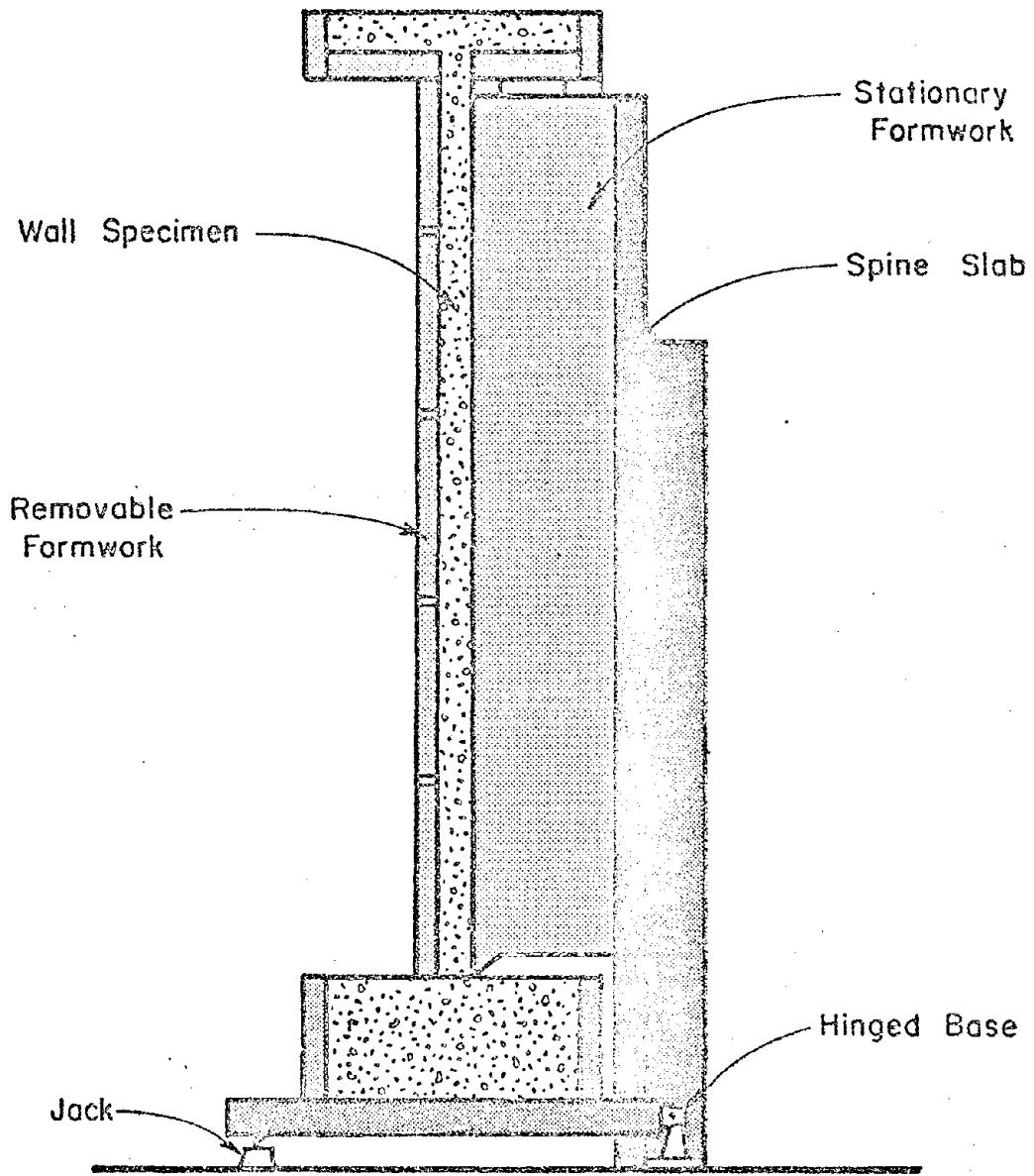Fig. 22 Stress versus Strain Relationships for Reinforcement
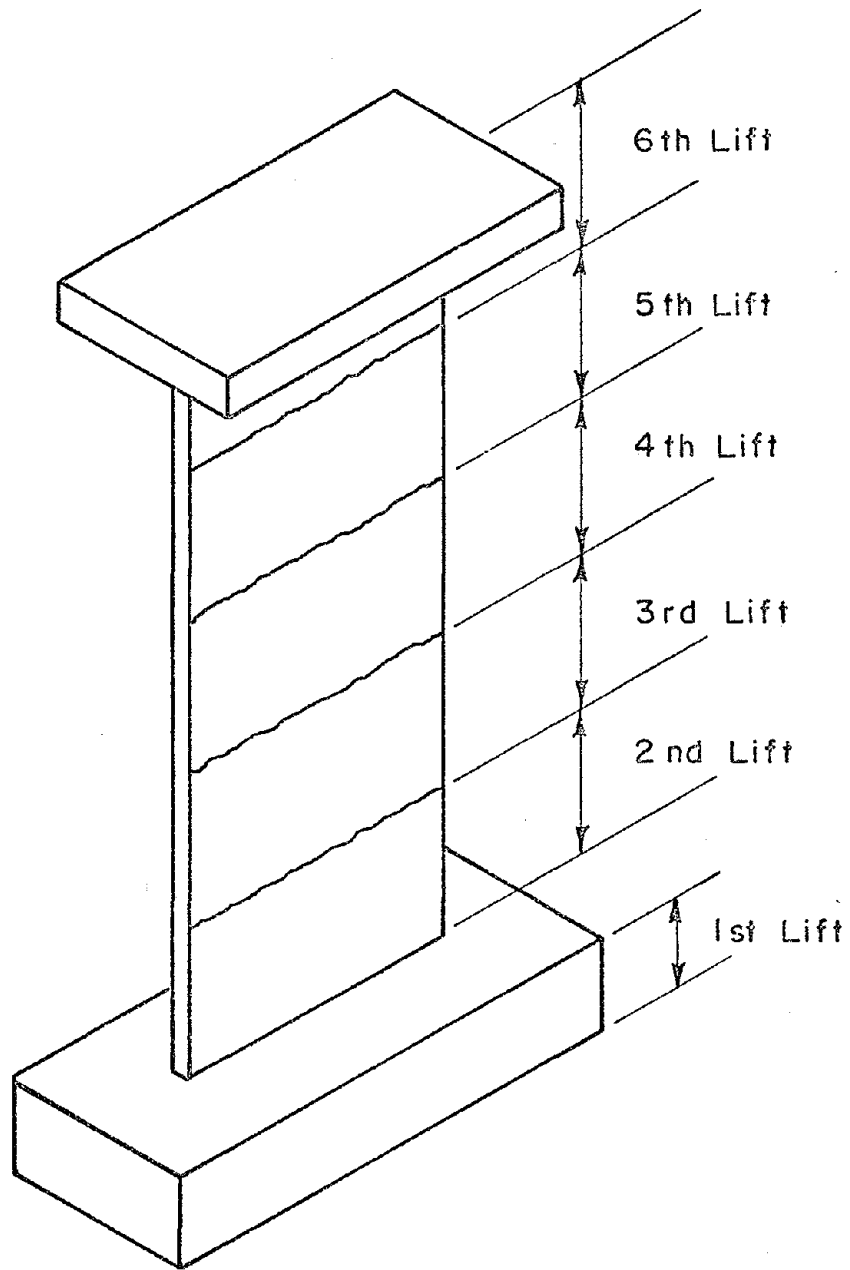
Fig. 23 Formwork System for Casting Test Specimens

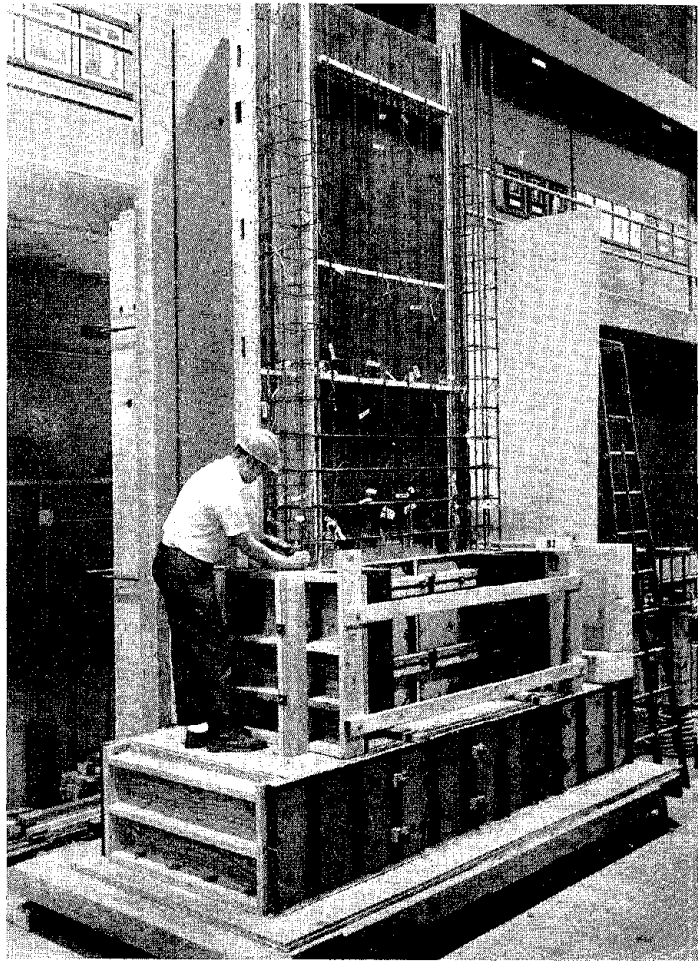Fig. 24 Lift Designations for Casting Test Specimens

Fig. 25   Specimen B1 During Construction

The sixth lift was cast in two segments. First, the wall segment was cast in the morning, then the slab segment was cast in the afternoon. The delay between segments was to avoid problems caused by plastic shrinkage of the slab.

Approximately two days after casting the sixth lift, the removable formwork was stripped. Following this operation, a special lifting rig was placed on the specimen. This rig allowed the specimen to be lifted through rods attached to the base block. Prior to lifting, the base platform of the formwork was rotated to tilt the specimen away from the stationary formwork; thus essentially stripping the specimen from the stationary form. The specimen could then be lifted away from the stationary formwork and placed in position on the test floor.

Test Apparatus. The apparatus for testing the shear wall models is shown in Fig. 26. A photograph of test set up is shown in Fig. 27.

Each test specimen is post-tensioned to the floor using eight 1-3/8-in. diameter Stressteel bars.

Loads are applied to the specimen as a vertical canti-lever with concentrated forces at the top. Hydraulic rams on each side of the specimen alternately apply force to first one side then the other side of the top slab. Reactions from the applied loads are transferred to the test floor through a large infilled reaction frame. This load transfer occurs directly when the rams closest to the reaction frame are acti-vated, and indirectly through the remote support column and
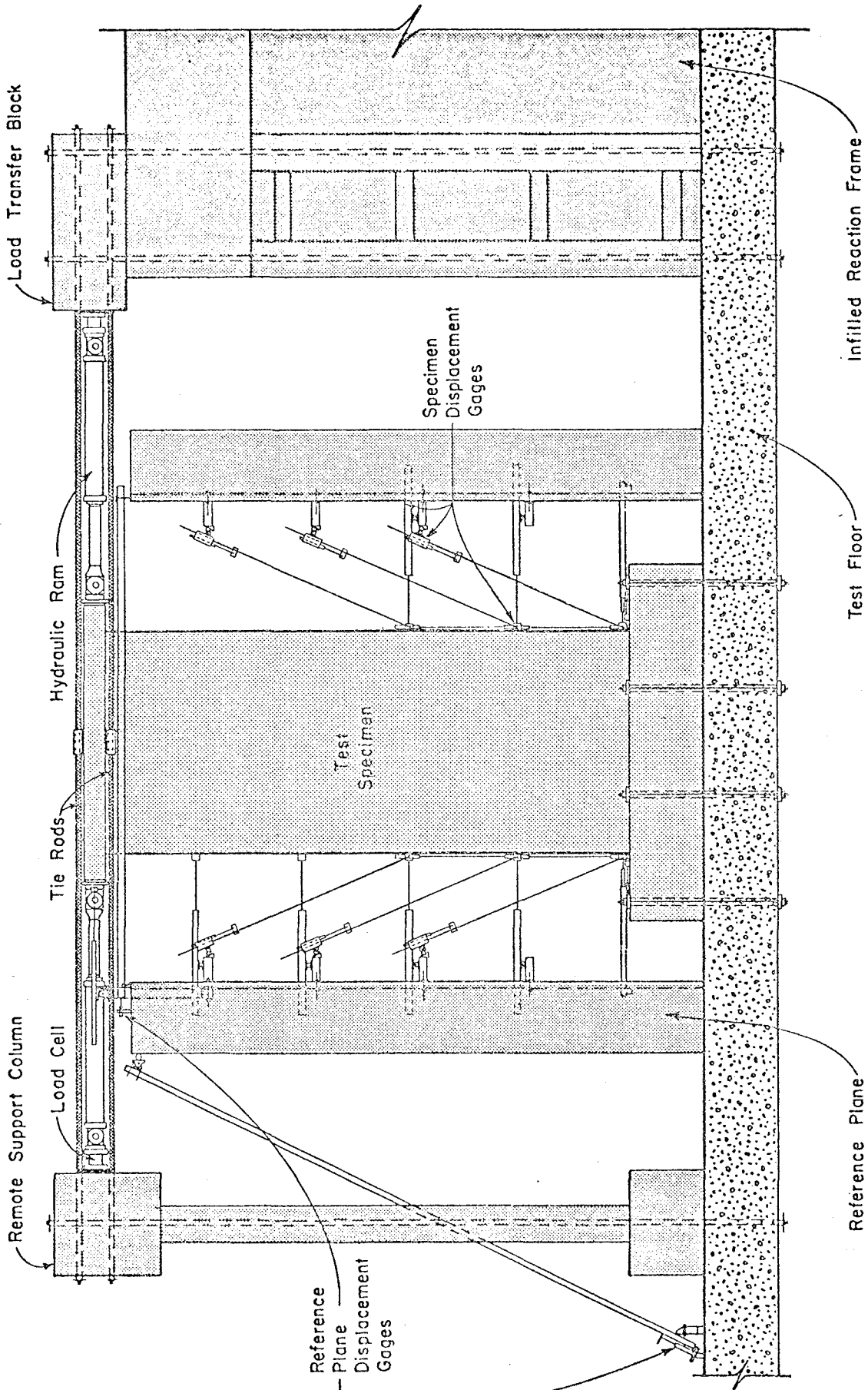
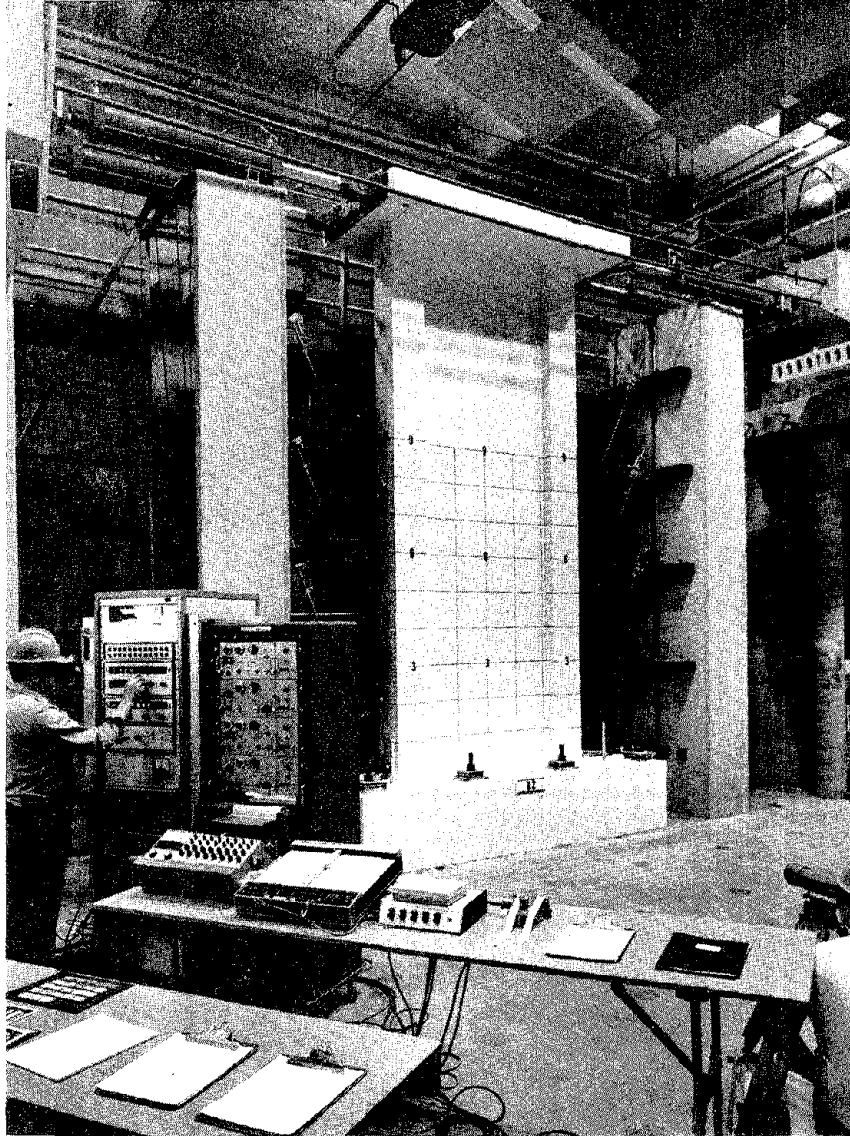Fig. 26 Test Apparatus

-42-

Fig. 27   Isolated Wall Test

tie rods, when the rams farthest from the reaction frame are activated. A system of one or two rams on each side of the specimen are used depending on the anticipated capacity of each specimen. The hydraulic rams have a capacity of 200 kips and a stroke of 36 in. At each end of the ram, a clevis bracket and pin arrangement is attached to form a link assembly.

Instrumentation. During each test, applied loads, displacements, rotations, and steel strains are measured.

The applied loads are measured by load cells attached to one end of each ram. The load cells have a capacity of 200 kips in compression and can measure loads to within about 20 lb.

Horizontal displacements are measured at six levels, as shown in Fig. 26. For the lower three levels, measurements are made at each end of the wall. Diagonal displacements are also made at the lower three levels to define the geometry of the deformed wall. Using this system, both flexural and shearing distortions can be determined.

As shown in Fig. 26, the horizontal and vertical displacement gages are supported on reference planes located on each side of the test specimen. As a check, the reference planes are instrumented to monitor any possible movement. For the first five tests, movements of the reference planes were negligible.

Rotations in the lower 6 ft. of the wall are obtained by measuring vertical displacements along each end of the wall. Three sets of measurements are made. The first set is made be-

tween the top of the base block and the bottom of the wall over a nominal gage length of 3 in. The other two sets of measurments are made over nominal gage lengths of 36 in.

Displacement measurements are made using linear potentiometers and direct current differential transducers (DCDT's). These gages have resolutions from 0.001 in. to 0.003 in.

Strain gages are placed on both the vertical and the horizontal reinforcement. The basic strain gage layout is shown in Figs. 28 and 29. In addition, strains are measured on several of the hoops and supplementary cross ties of the confinement reinforcement of Specimen B3.

Output from the load cells, potentiometers, DCDT's, and strain gages is recorded on both printed and punched paper tape using a VIDAR Digital Data Acquisition System. Raw data from the punched paper tape is transferred to disc storage to facilitate data reduction and analysis.

In addition to the instrumentation previously described, dial gages are used to measure relative slip at construction joints. Figure 30 shows the location of the dial gages, which have a sensitivity of 0.001 in.

Crack widths are measured during testing with a hand microscope containing a scale with graduations of 0.001 in.

A complete photographic record is kept for each test. In addition to color slides and black and white photographs, three time-lapse cameras running at one frame per second record each cycle of loading.
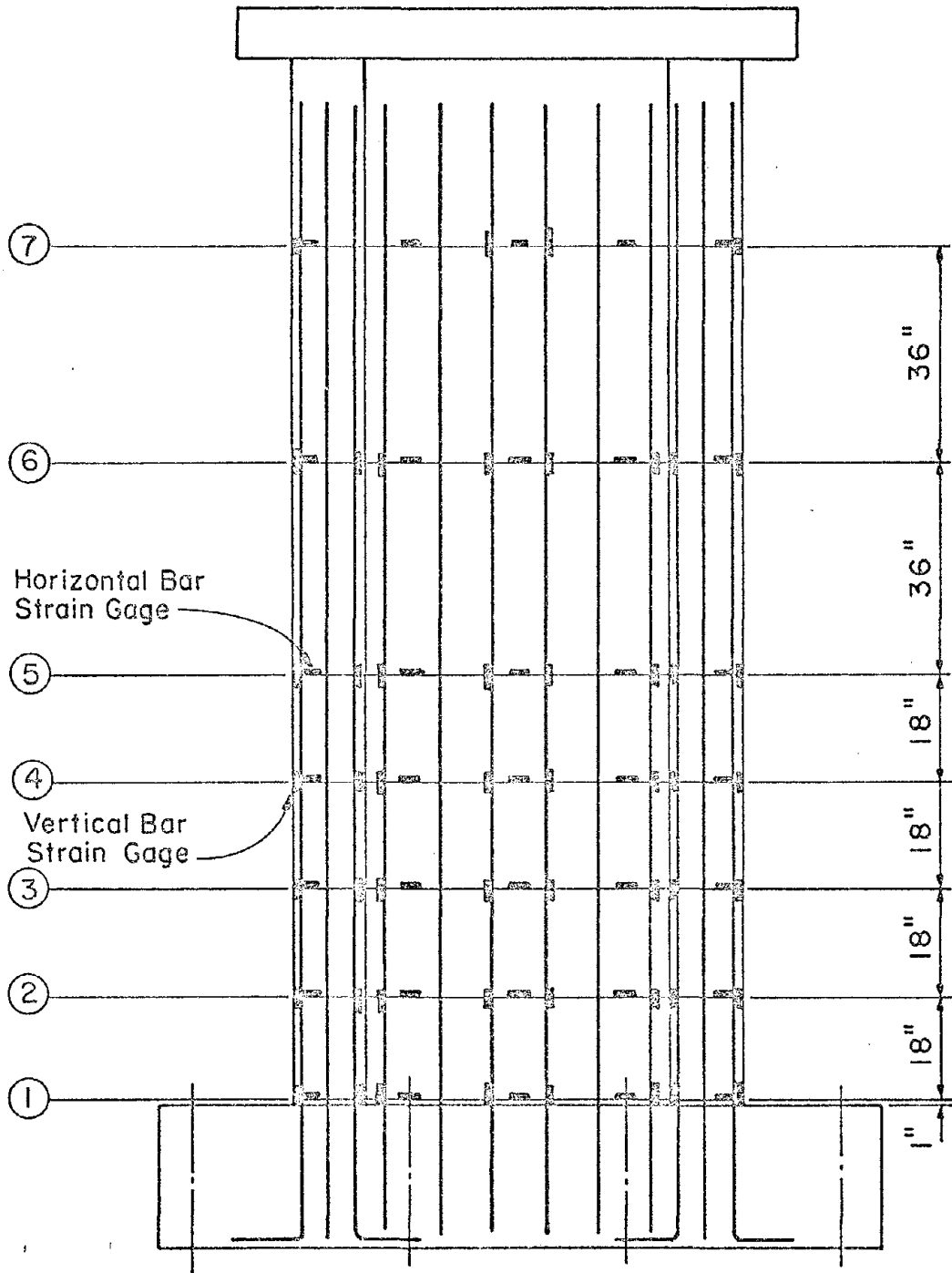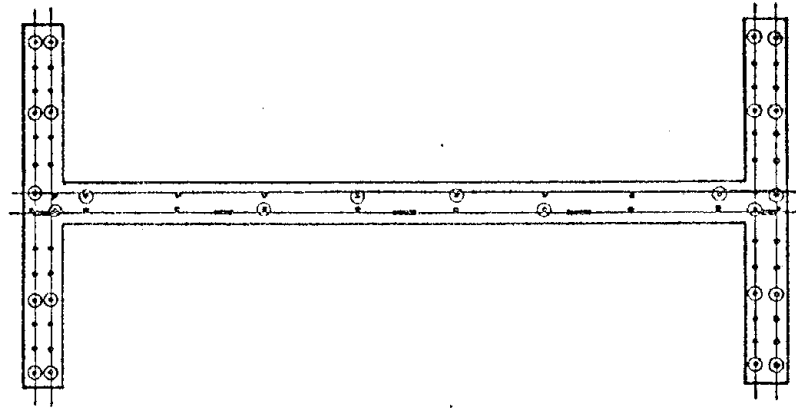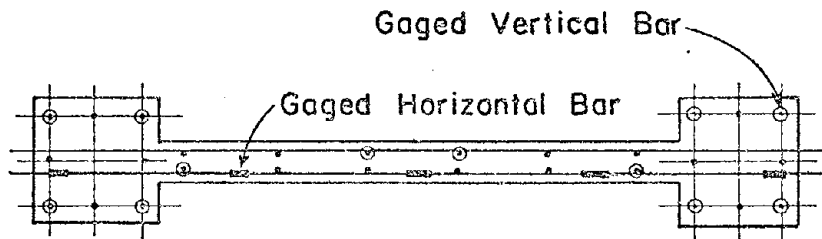
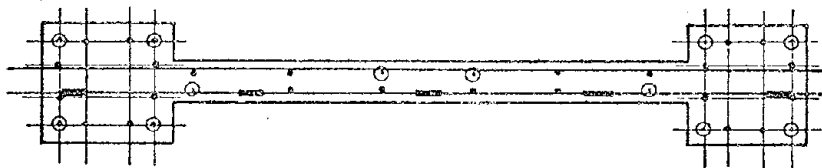Fig. 28   Elevation of Test Specimen Illustrating
Strain Gage Layout
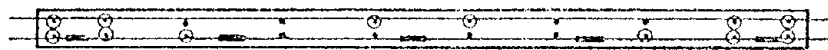
-46-

(a) Specimen FI

Gaged Vertical Bar

Gaged Horizontal Bar

(b) Specimen BI & B3

(c) Specimen B2

(d) Specimen RI

Fig. 29   Cross Sections of Test Specimens Illustrating
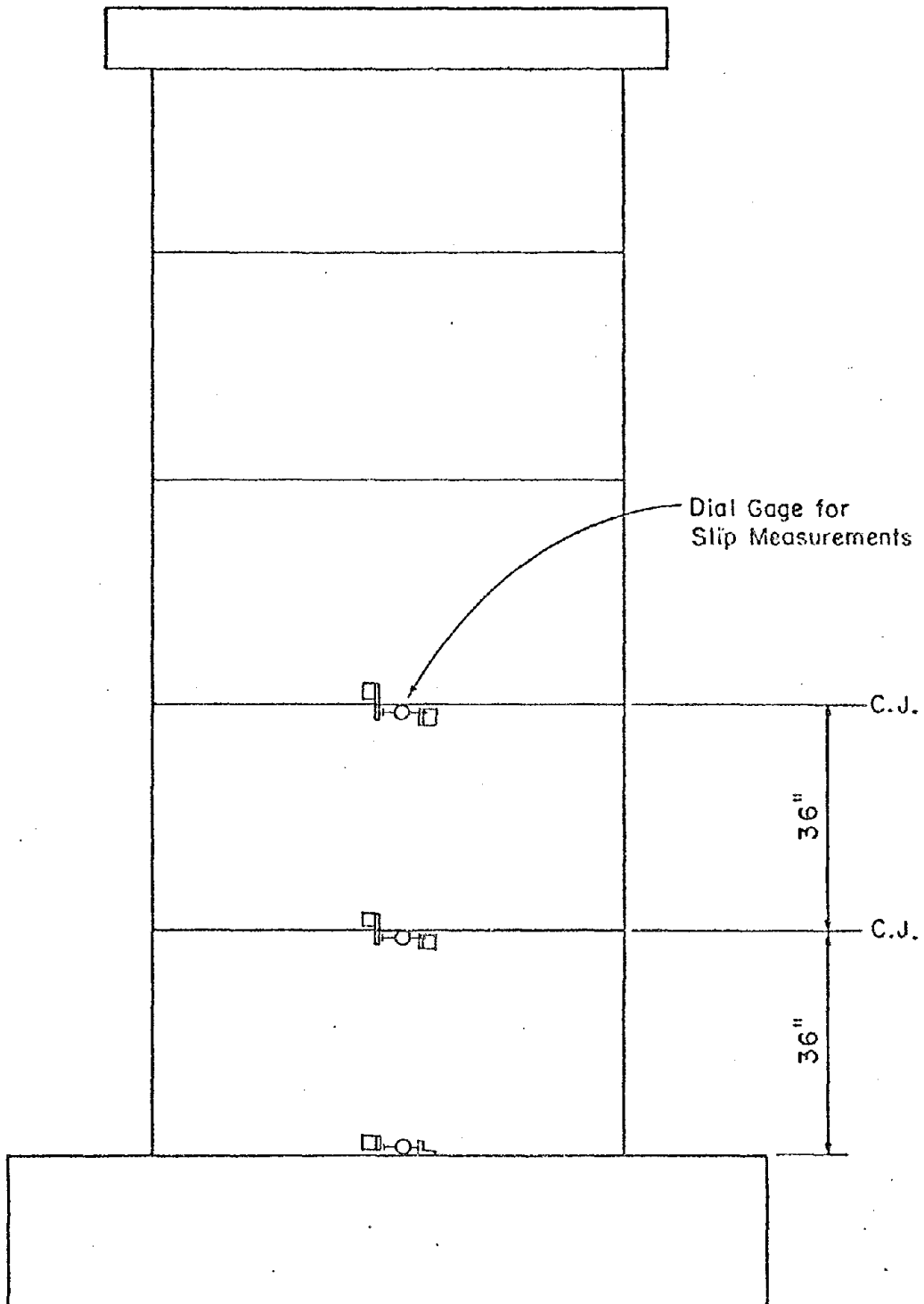Strain Gage Layout

Fig. 30   Location of Dial Gages for Slip Measurements

Test Procedure. Each of the first five test specimens were loaded in increasing increments until yielding occurred. About three increments were required to reach yield. At each increment, three complete cycles were applied. Subsequent to yielding, loading was controlled by deflections in 1-in. increments. Three complete cycles were run at each increment.

The loading history for each specimen is given with the individual test results.

Free Vibration Tests. Free vibration characteristics of the specimens were measured at several stages throughout the lateral load tests. The tests were performed with the specimen disconnected from the hydraulic rams. A 1/4-in. diameter prestressing wire was attached to a bracket on the top slab of the wall. The wire was pulled to a predetermined force. The prestressing wire was then cut and the top displacement of the specimen was monitored and plotted versus time.

Displacement-time curves were used to calculate the frequency and damping characteristics of the walls.

Test Results

Introduction. Data obtained from the first five tests are presented in this section. Sections describing the loading history, load-deflection relationships, moment-curvature relationships, and load-strain relationships for each specimen are included. In addition, the modes of failure, free vibration characteristics, and construction joint behavior are discussed.

Loading History. Loads and deflections applied to

the first five specimens are shown in Fig. 31 through Fig. 35. The yield load and yield deflection obtained from the tests are also indicated on the figures. Yielding was defined as first yield of the main flexural reinforcement and was determined from strains measured on the reinforcement.

Behavior and Modes of Failure. In this section a description of the behavior of each specimen observed during testing is presented.

Specimen F1. Specimen F1 had a flanged cross section with 3.89% reinforcement in each flange. Initial cracking was observed in the first cycle of loading at a load of 36.8 kips. This load corresponds to a nominal shear stress $v_{cr} = 2.0\sqrt{f'_c}$ based on a web thickness of 4 in. and an effective depth of 0.8 ℓ_w where ℓ_w is the horizontal length of the wall.

Specimen F1 yielded at a load of 150.6 kips and a deflection of 1.00 in. in the positive direction of load. At yield, crack widths were on the order of 0.02 in. As the loading progressed beyond yield, visual observations indicated horizontal movement of the web that tended to bow the compression flange near the base of the wall.

The pattern of cracking that developed over the bottom 6 ft. of Specimen F1 is indicated in Fig. 36 and Fig. 37. These photographs were taken when the top deflections were +3 in. and -3 in., respectively. The black lines show a grid pattern of 12x12-in. squares drawn on the specimen.
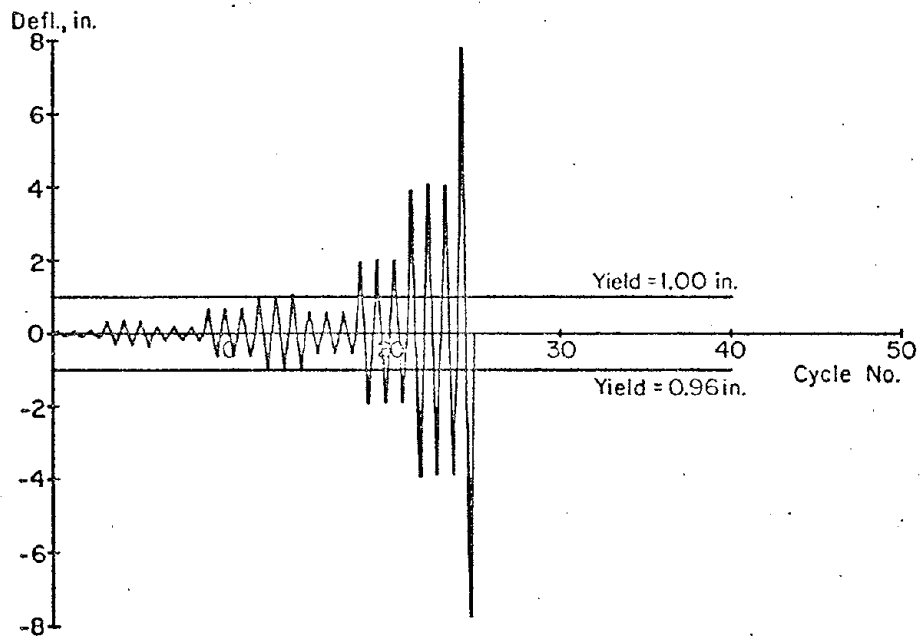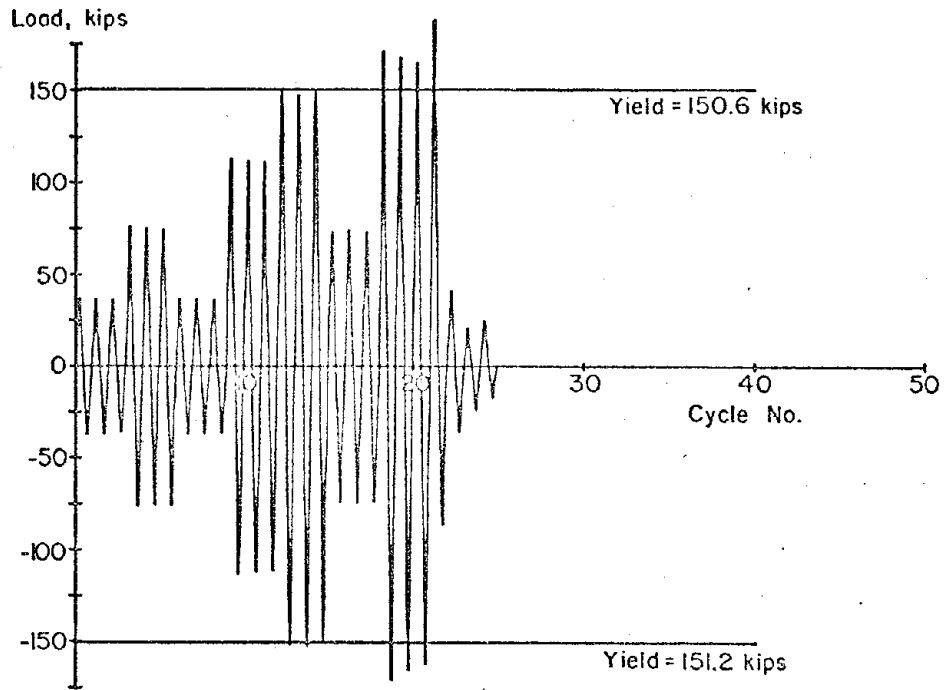
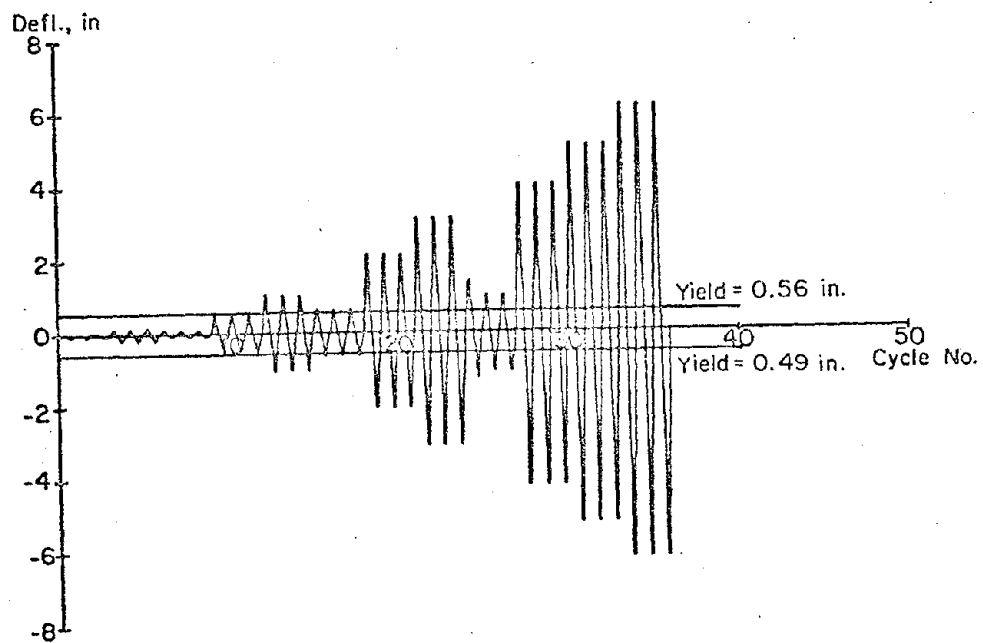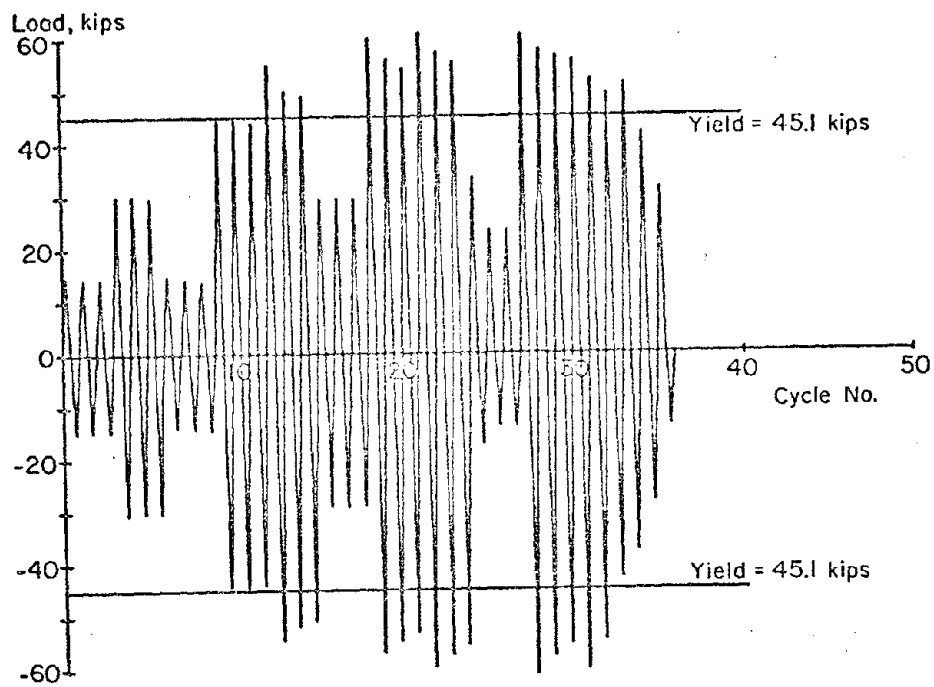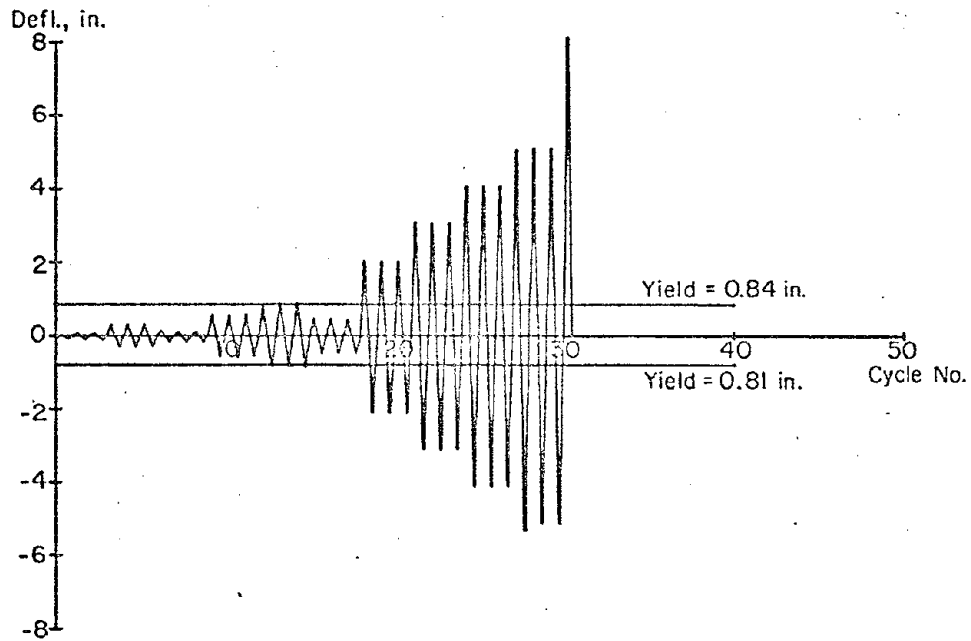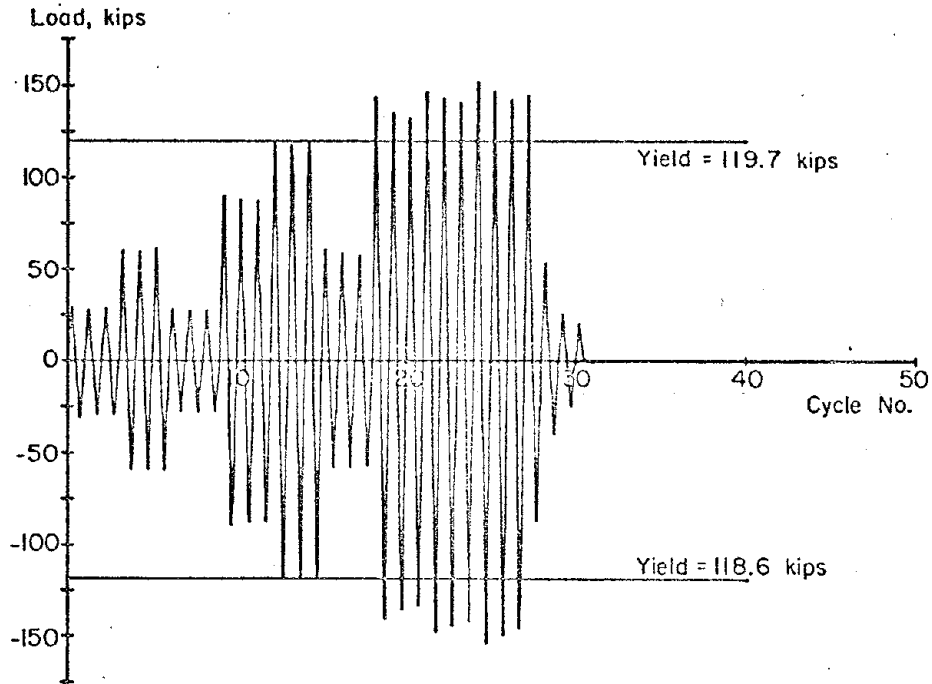Fig. 31 Loading History for Specimen F1

Fig. 32   Loading History for Specimen Bl

Fig. 33   Loading History for Specimen B2

Load, kips.

Yield = 20.1 kips

Yield = 19.4 kips

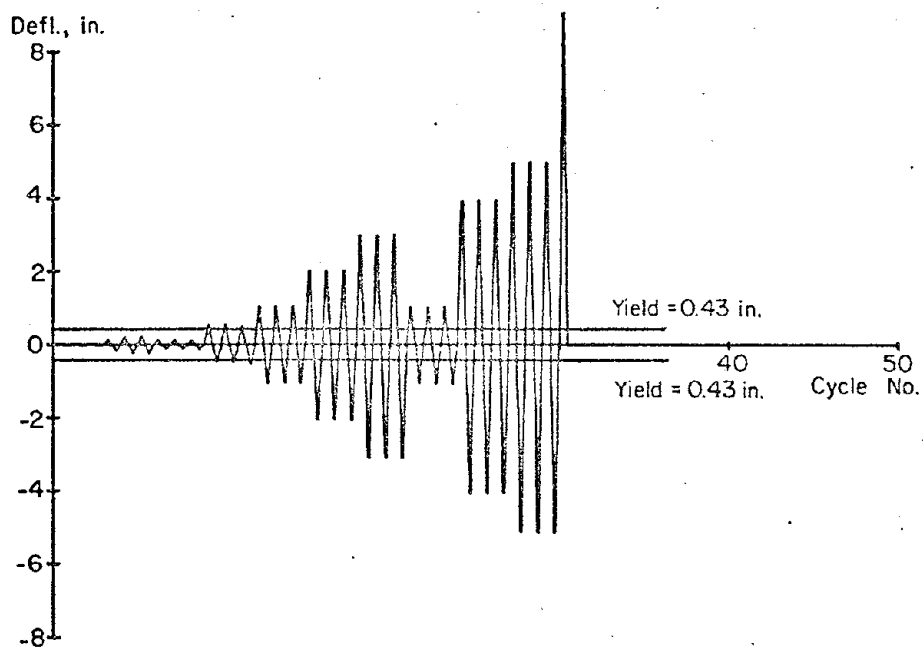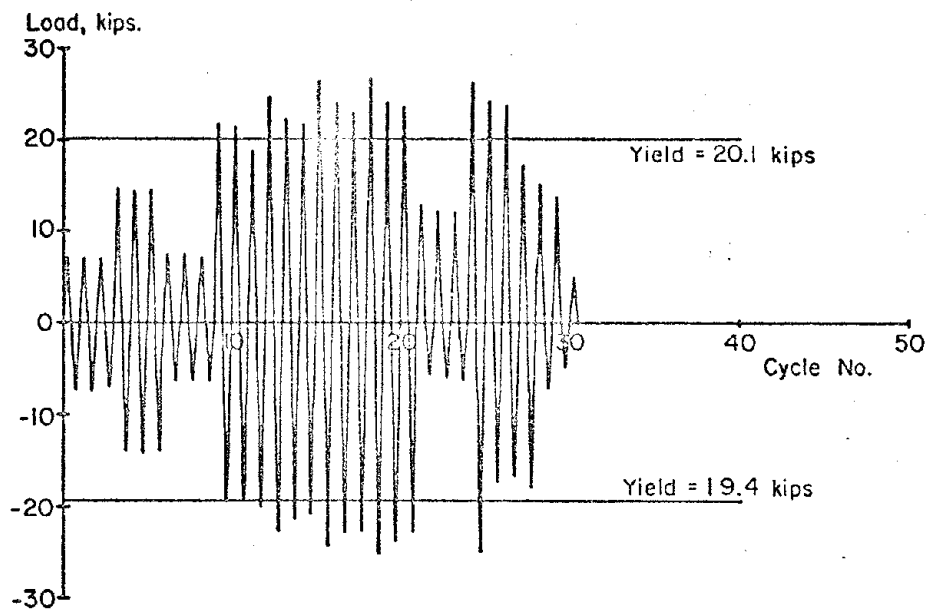Cycle No.

Defl., in.

Yield = 0.43 in.

Yield = 0.43 in.

Cycle No.
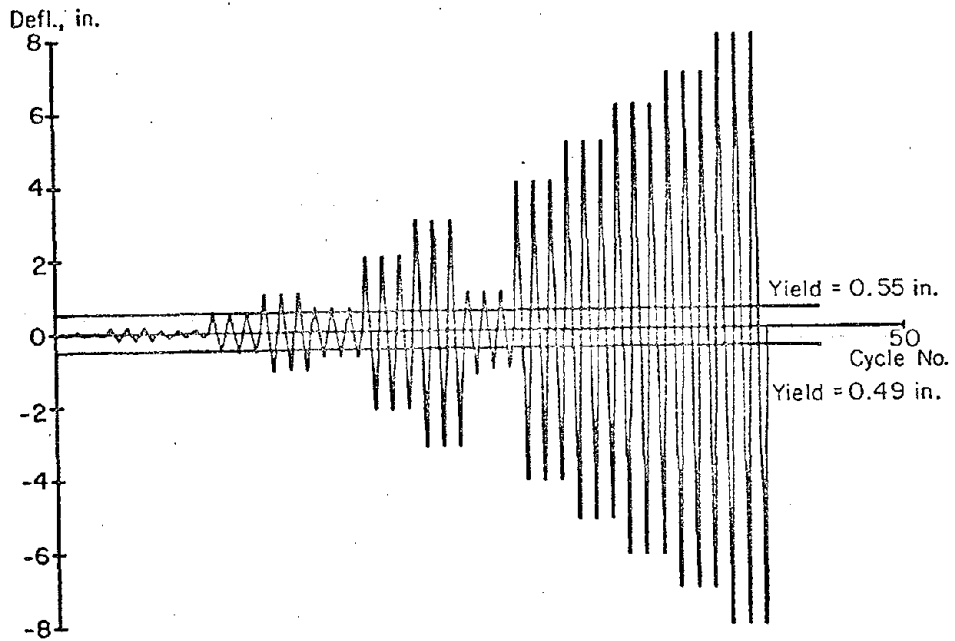
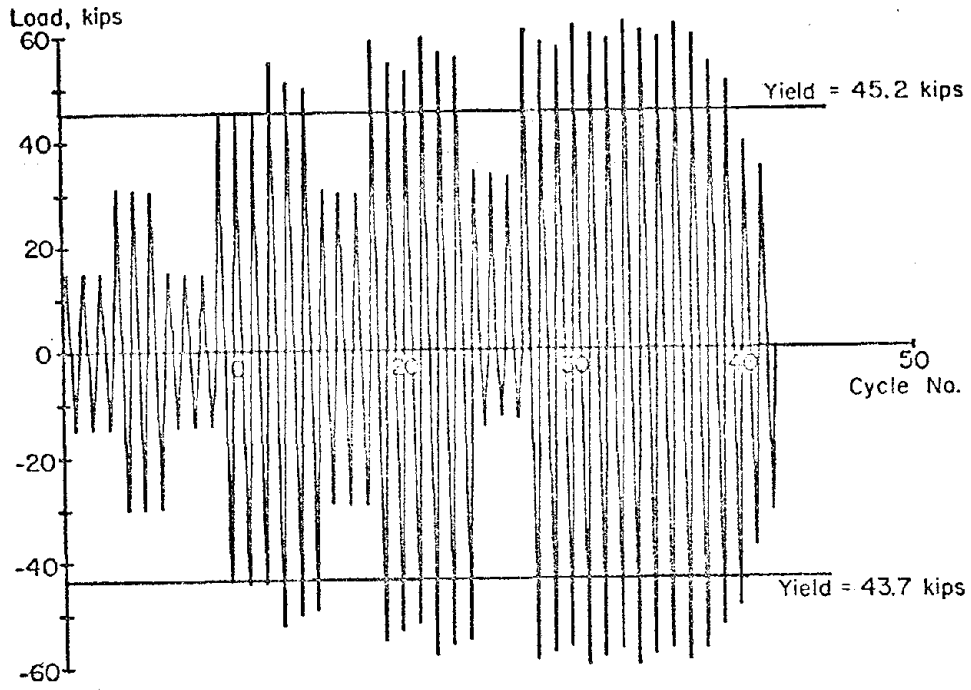Fig. 34 Loading History for Specimen R1

-54-
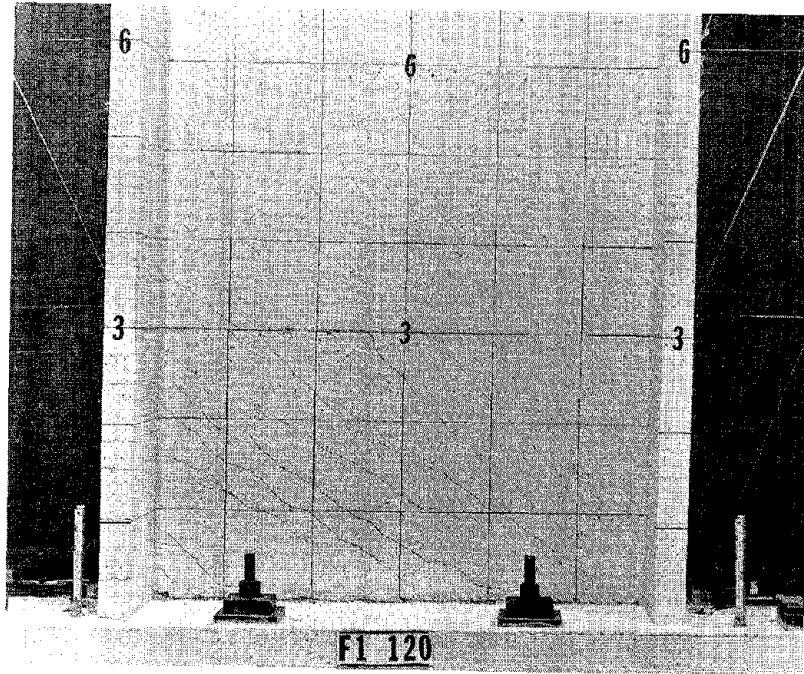
Fig. 35   Loading History for Specimen B3

-55-

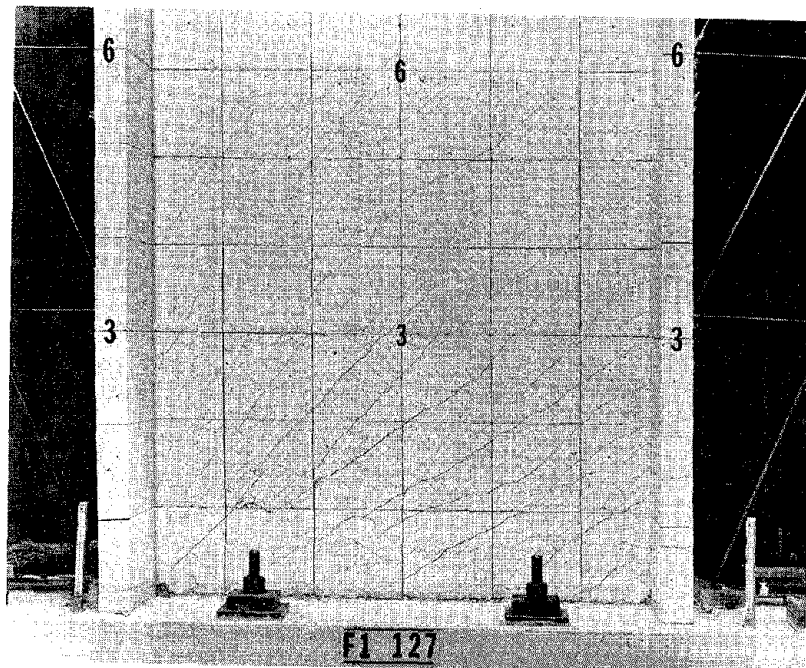Fig. 36   Specimen F1 With Top Deflection of +3 in.

Fig. 37   Specimen F1 with Top Deflection of -3 in.

Diagonal cracking predominates and the cracks fan out from the lower corner of the compression face of the wall to form a system of inclined struts.

As the specimen was being loaded to a top deflection of -4 in. a sudden load drop-off occurred as severe web crushing near the compression flange at the base of the wall was observed. The maximum load obtained corresponded to a nominal shear stress $v_{max} = 10.4\sqrt{f'_c}$. The load observed after the web crushing was 50% of that observed prior to crushing. Six complete inelastic cycles were applied to the specimen prior to web crushing.

Following loss of load, the specimen was pushed to a maximum top deflection of 8 in. The appearance of the specimen at this stage is shown in Fig. 38. Once the web was lost the wall rested on the end flanges which behaved as individual flexural elements. The flexural distortion of the flanges is evident in Fig. 38.

Specimen B1. Specimen B1 had column boundary elements with 1.11% reinforcement in each column. Ties in the columns were spaced on 8-in. centers. Initial cracking was observed in this specimen at a load of 26 kips ($v_{cr} = 1.2\sqrt{f'_c}$). The cracks were flexural and propagated rapidly through the cross section, as would be expected for a lightly reinforced member.

Yielding in Specimen B1 occurred at a load of 45.1 kips and a top deflection of 0.56 in. Measured crack widths
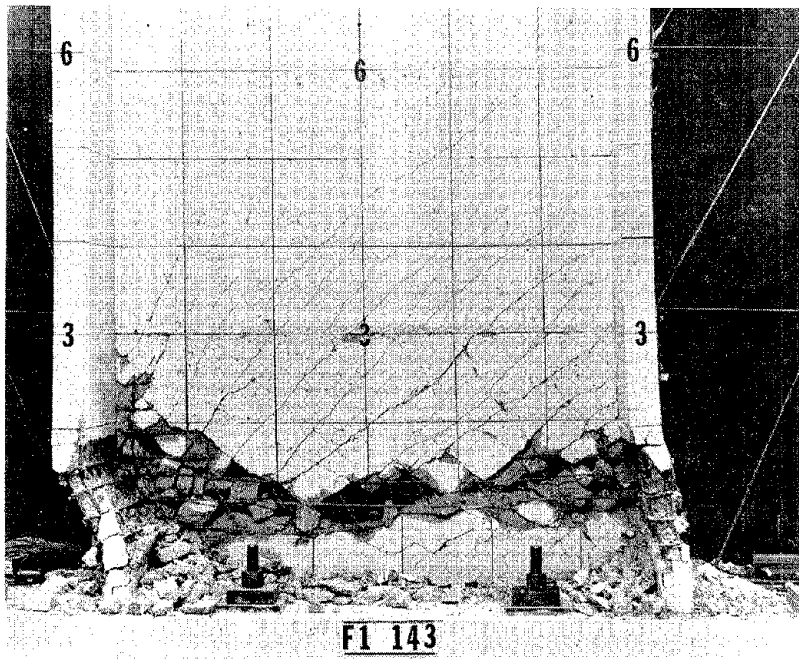
Fig. 38   Specimen F1 After Testing to Destruction

at this load ranged from 0.01 in. to 0.015 in.

Photographs of the wall at top deflections of +3 in.
and -3 in. are shown in Fig. 39 and Fig. 40, respectively.
Buckling of the vertical column reinforcement had occurred by
the end of the 3-in. cycles.

As a result of alternate bar buckling and tensile
yielding the concrete in the columns was severely damaged.
Since the specimen was lightly reinforced, the damage to the
column concrete did not immediately affect the load capacity.
However, as loading progressed, bars that had previously
buckled began to fracture. As bars fractured and as pieces
of concrete fell out of the columns, the load carried by the
specimen decreased. Finally, the concrete in one of the col-
umns was completely destroyed and the web of the wall was
crushed by the compressive forces transferred from the column.

Figure 41 shows the specimen after testing was com-
pleted. The maximum load carried by the wall was 61.0 kips
$(v_{max} = 2.9\sqrt{f_c'})$.

Specimen B2. Specimen B2 had column boundary ele-
ments with 3.67% reinforcement in each column. Column ties
were provided on 8-in. centers. Initial cracking was observed
at a load of 30 kips $(v_{cr} = 1.4\sqrt{f_c'})$. The cracks were a flexure-
shear type.

Yielding occurred at a load of 119.7 kips and a de-
flection of 0.84 in. Crack widths observed at yield ranged
from 0.01 in. to 0.02 in.
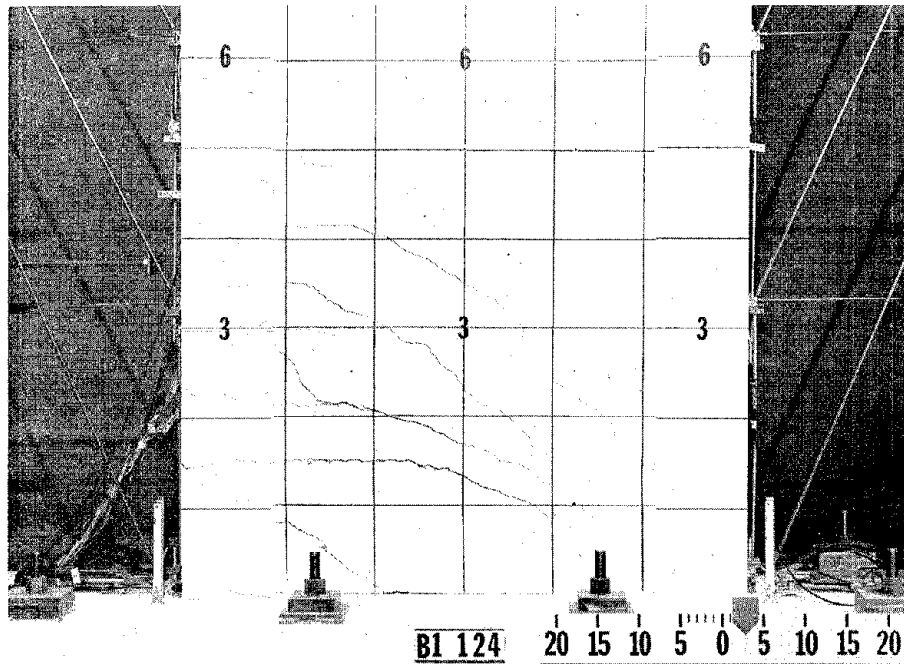
-59-

Fig. 39   Specimen B1 With Top Deflection of +3 in.
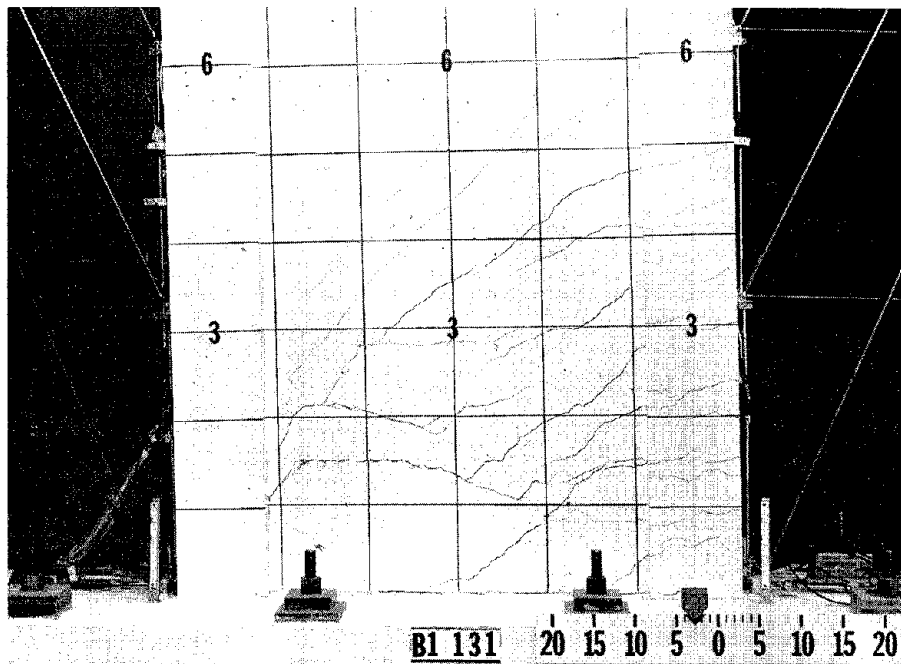

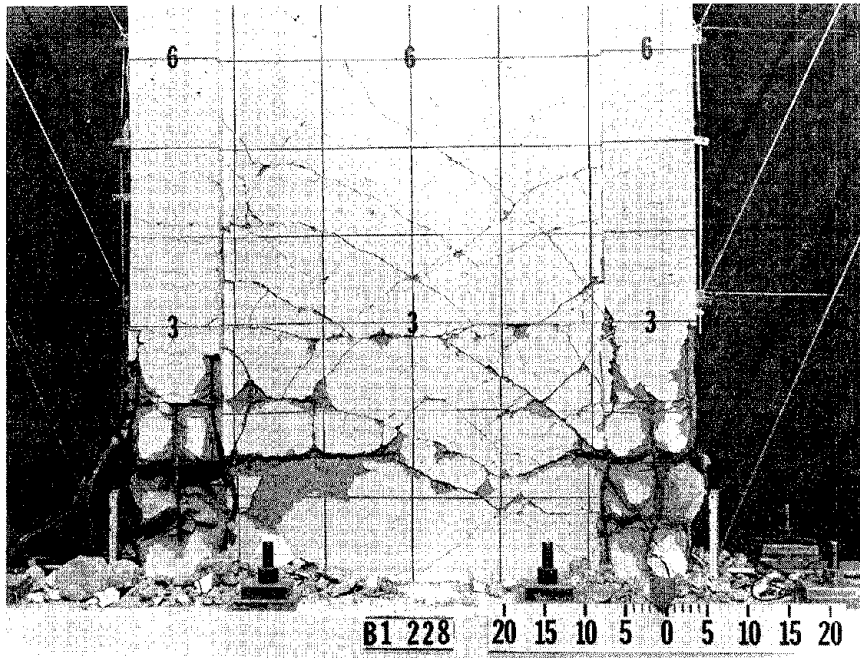Fig. 40   Specimen B1 with Top Deflection of -3 in.

Fig. 41   Specimen B1 After Testing to Destruction

The cracking pattern at top deflections of +3 in. and -3 in. can be seen in Fig. 42 and Fig. 43, respectively.

As the 4-in. cycles were applied, spalling of the web concrete was observed. Buckling of the vertical column reinforcement was also observed.

During the second half of the first 5-in. cycle, when the top deflection was 4.8 in., a sudden loss of load occurred as crushing of the concrete in the web and in the compression column was observed. The capacity of the specimen dropped by about 40% at this point. Following this sudden load loss, the two remaining 5-in. cycles were run and resulted in additional damage to the specimen and additional loss of load capacity. Figure 44 shows the specimen after termination of the test. The maximum load carried by Specimen B2 was 152.8 kips ($v_m = 7.2\sqrt{f_c'}$).

Specimen R1. Specimen R1 had a rectangular cross section with 1.47% vertical reinforcement concentrated within a distance of 7.5 in. (0.1 ℓ_w) from each end.

Flexural cracking of the wall was first observed at a load of 12 kips ($v_{cr} = 0.6\sqrt{f_c'}$). Yielding occurred at a load of 20.1 kips and a deflection of 0.43 in. The maximum crack width observed at this load was 0.02 in. The cracking pattern that developed over the lower 6 ft. of the wall is shown in Fig. 45 and Fig. 46. The photographs were taken at top deflections of +3 in. and -3 in., respectively.

During the 3-in. loading cycles, buckling was observed in bars at both ends of the wall. Following buckling,
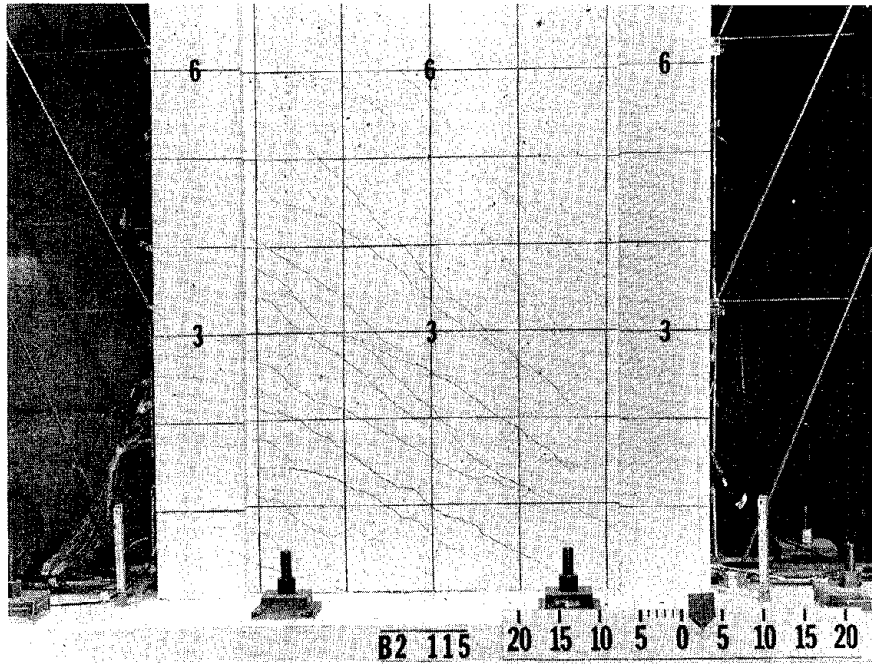
-62-

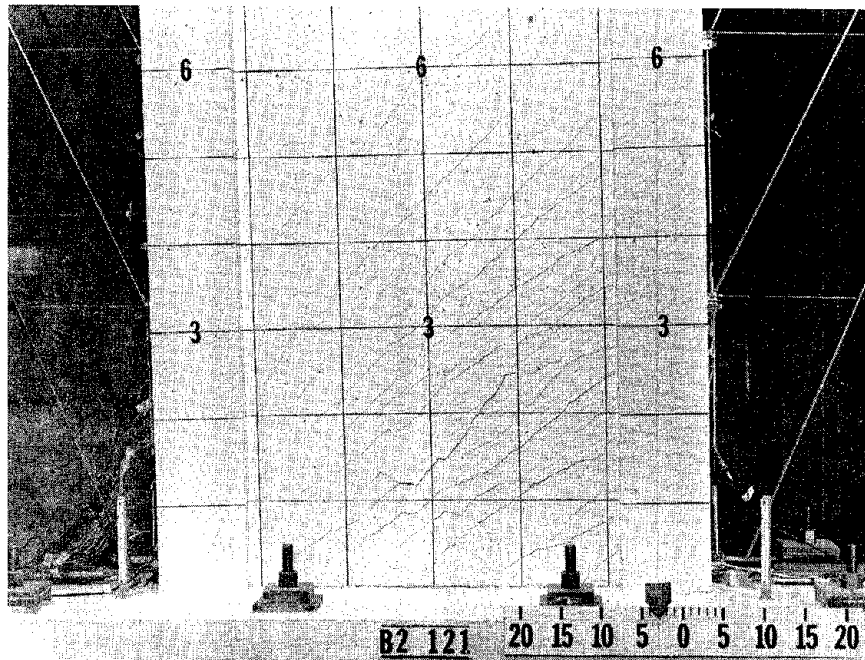Fig. 42   Specimen B2 With Top Deflection of +3 in.

Fig. 43   Specimen B2 With Top Deflection of -3 in.
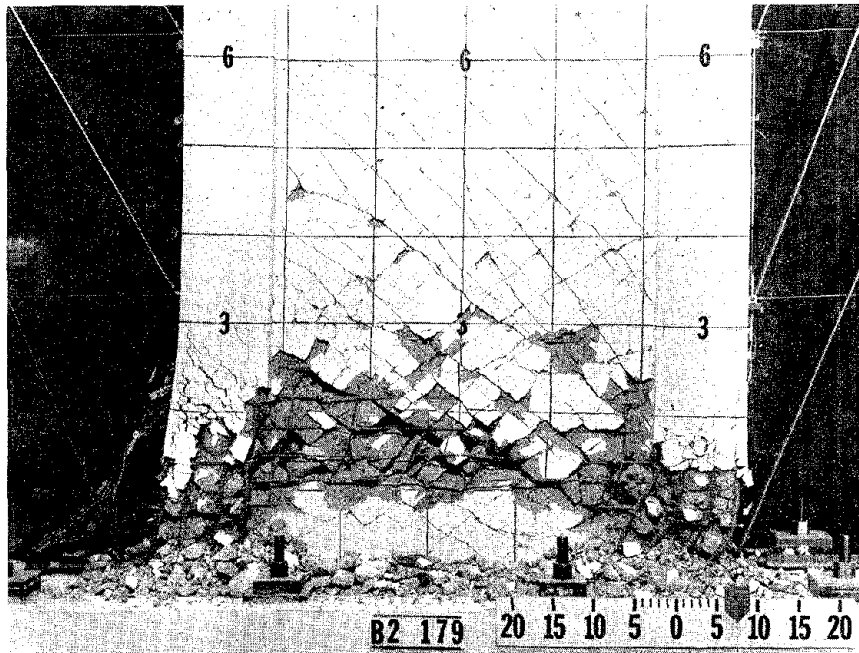
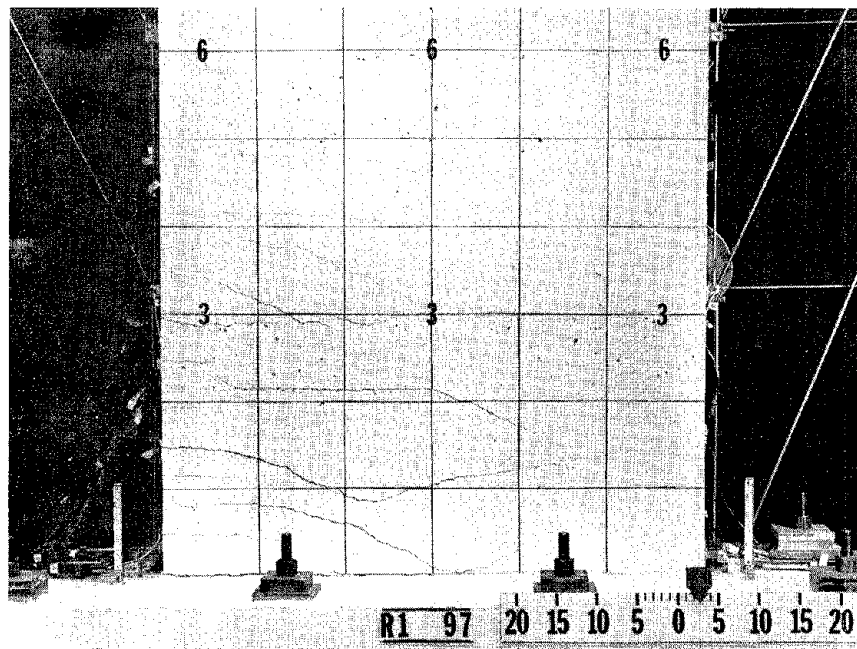Fig. 44   Specimen B2 After Testing to Destruction

-64-

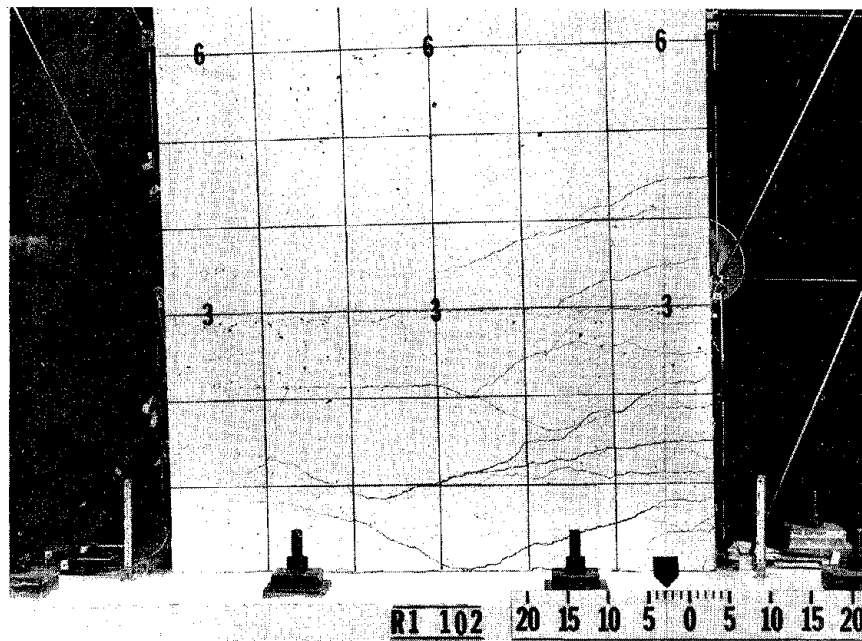Fig. 45   Specimen R1 With Top Deflection of +3 in.

Fig. 46   Specimen R1 With Top Deflection of -3 in.

during the second 4-in. loading cycle, two bars at one end of the wall fractured. Because the specimen was lightly reinforced in flexure, the concrete in the wall was not crushed prior to bar fracture. During the 5-in. cycles, four additional main vertical bars fractured; two at each end of the wall. Each bar fracture was associated with a drop in the load resisted by the specimen.

A photograph of the wall after the test is shown in Fig. 47. The specimen carried a maximum load of 26.6 kips $(v_{max} = 1.4\sqrt{f'_c})$.

Specimen B3. Specimen B3 had column boundary elements with 1.11% vertical reinforcement in each column. This specimen was nominally identical to Specimen B1 except that confinement reinforcement was provided in the lower 6 ft. of each column. The confinement hoops were designed according to Appendix A of the 1971 ACI Code.[1] The volume of hoop steel obtained by the design was 1.28%. Specimen B3 was subjected to the same loading sequence as Specimen B1.

Initial cracking of Specimen B3 was observed at a load of 28 kips $(v_{cr} = 1.4\sqrt{f'_c})$. The cracking load and the cracking pattern were very similar to those for Specimen B1.

The yield load for B3 was 45.2 kips and the yield deflection was 0.55 in. These values are similar to those for Specimen B1. At yield, the maximum crack width measured on Specimen B3 was 0.025 in.

The cracking pattern that developed in Specimen B3 is shown in Fig. 48 and Fig. 49 at top deflections of +3 in.
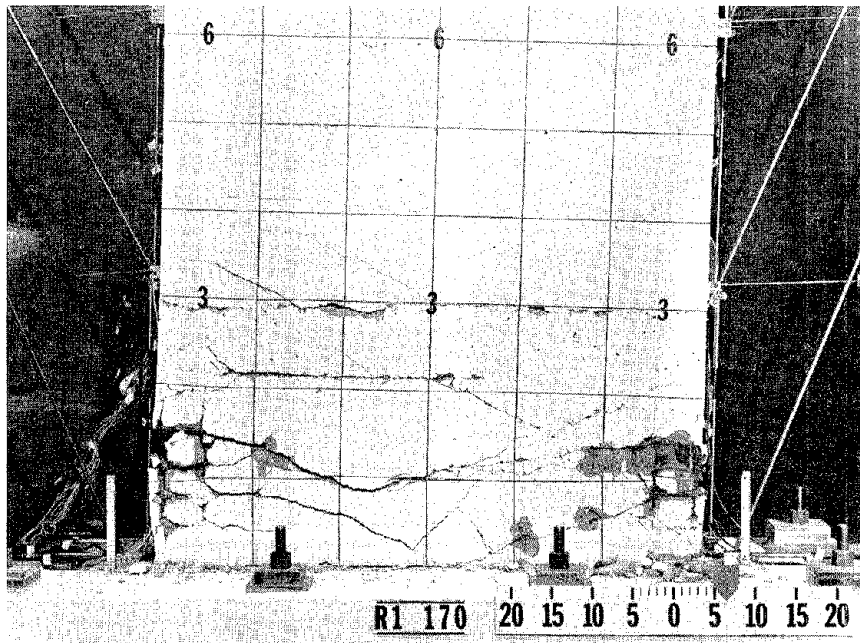
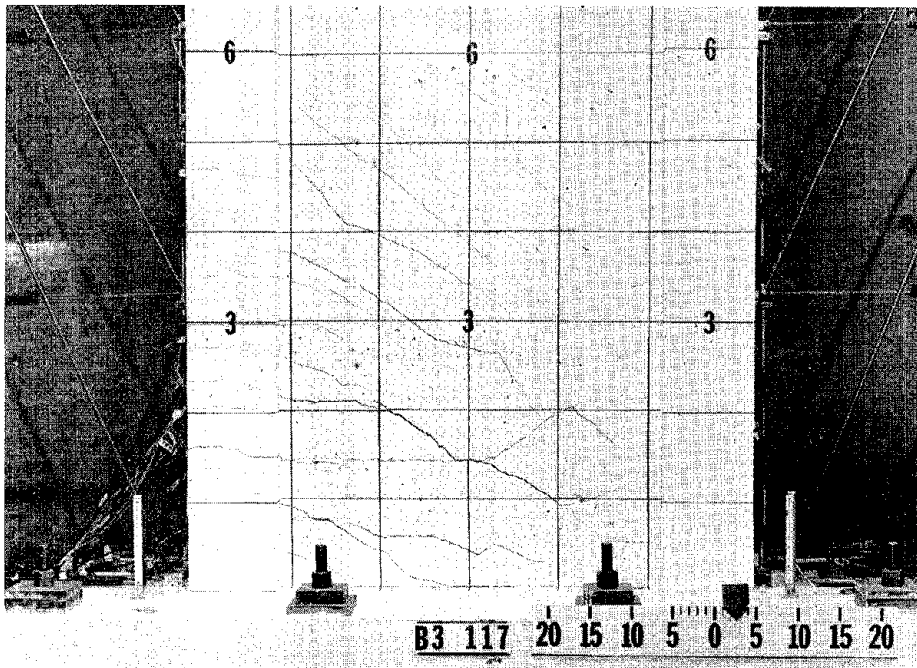Fig. 47 Specimen R1 After Testing to Destruction

-67-

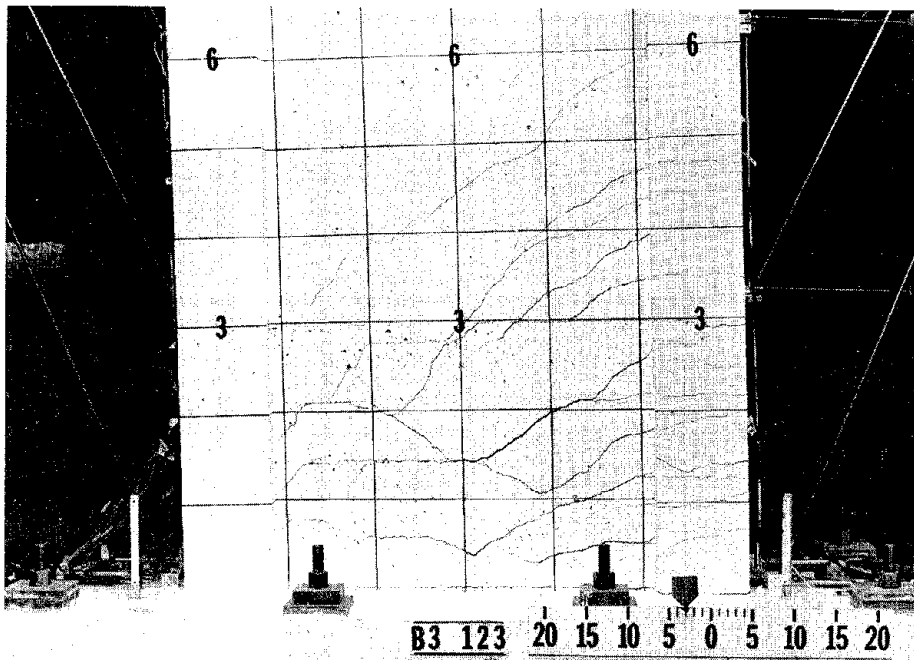Fig. 48   Specimen B3 With Top Deflection of +3 in.

Fig. 49   Specimen B3 With Top Deflection of -3 in.

and -3 in., respectively. Comparison of these two figures

with Fig. 39 and Fig. 40 show the similarity of the crack

patterns of Specimens B3 and B1.

Because of the confinement reinforcement, the con-

crete in the core of the columns of Specimen B3 was contained.

In addition, the confinement hoops helped to limit bar buckling.

First buckling was observed during the 7-in. loading cycles.

The buckling was associated with a shearing displacement of the

compression column.

During the last 7-in. cycle, one of the main vertical

bars fractured at the base of the wall. As the 8-in. loading

cycles were applied, five additional bars fractured.

Specimen B3 carried a maximum load of 62.0 kips

$(v_{max} = 3.1\sqrt{f'_c})$, as compared with a maximum load of 61.0 kips

for Specimen B1. The photograph in Fig. 50 shows the extent

of damage to B3 after testing was completed. Web concrete

in Specimen B3 was more extensively damaged than that in

Specimen B1. However, the primary zone of damage did not

extend above the 6-ft. level where the confinement hoops

were terminated.

Load-Deflection Relationships. Load-deflection re-

lationships for the five specimens are shown in Fig. 51 through

Fig. 55. The curves are given for only the first cycle of each

load or deflection increment, and only new maximum increments

are plotted. The numbers on the figures refer to the number

of the load cycle. A similar format is used for all curves
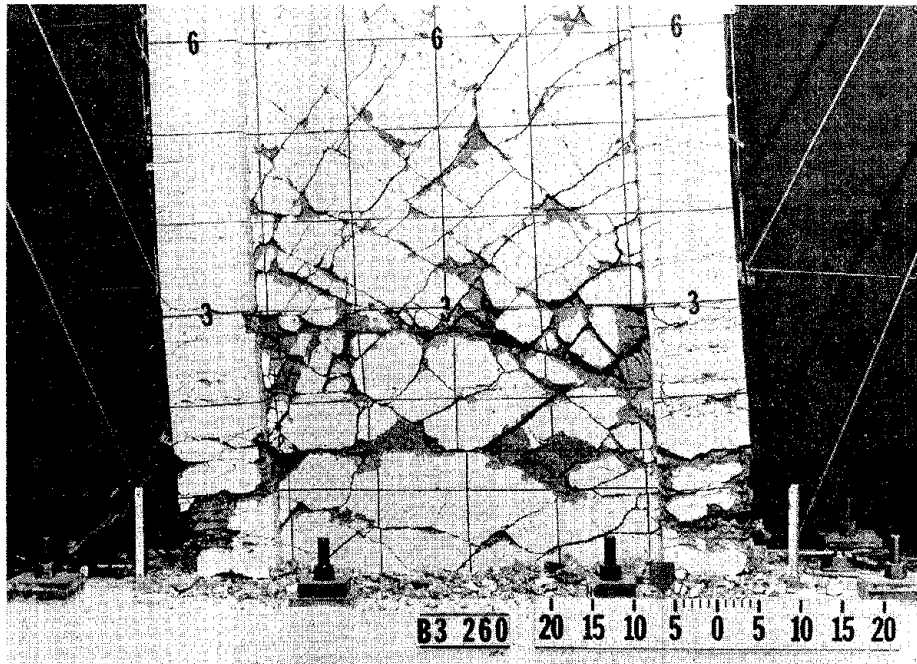
presented in Part I.

Fig. 50   Specimen B3 After Testing to Destruction
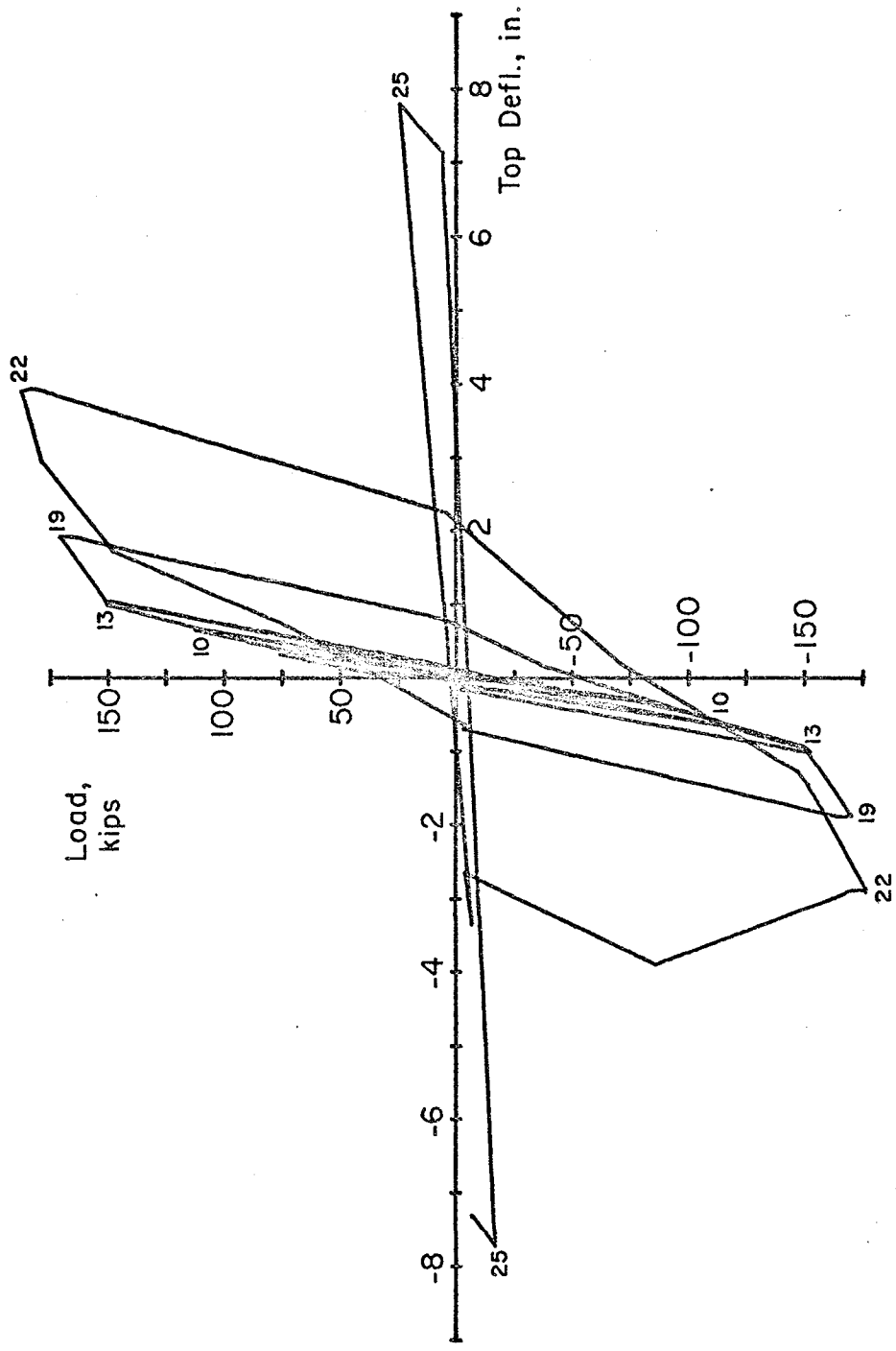
-70-

Fig. 51   Load Versus Top Deflection for Specimen F1
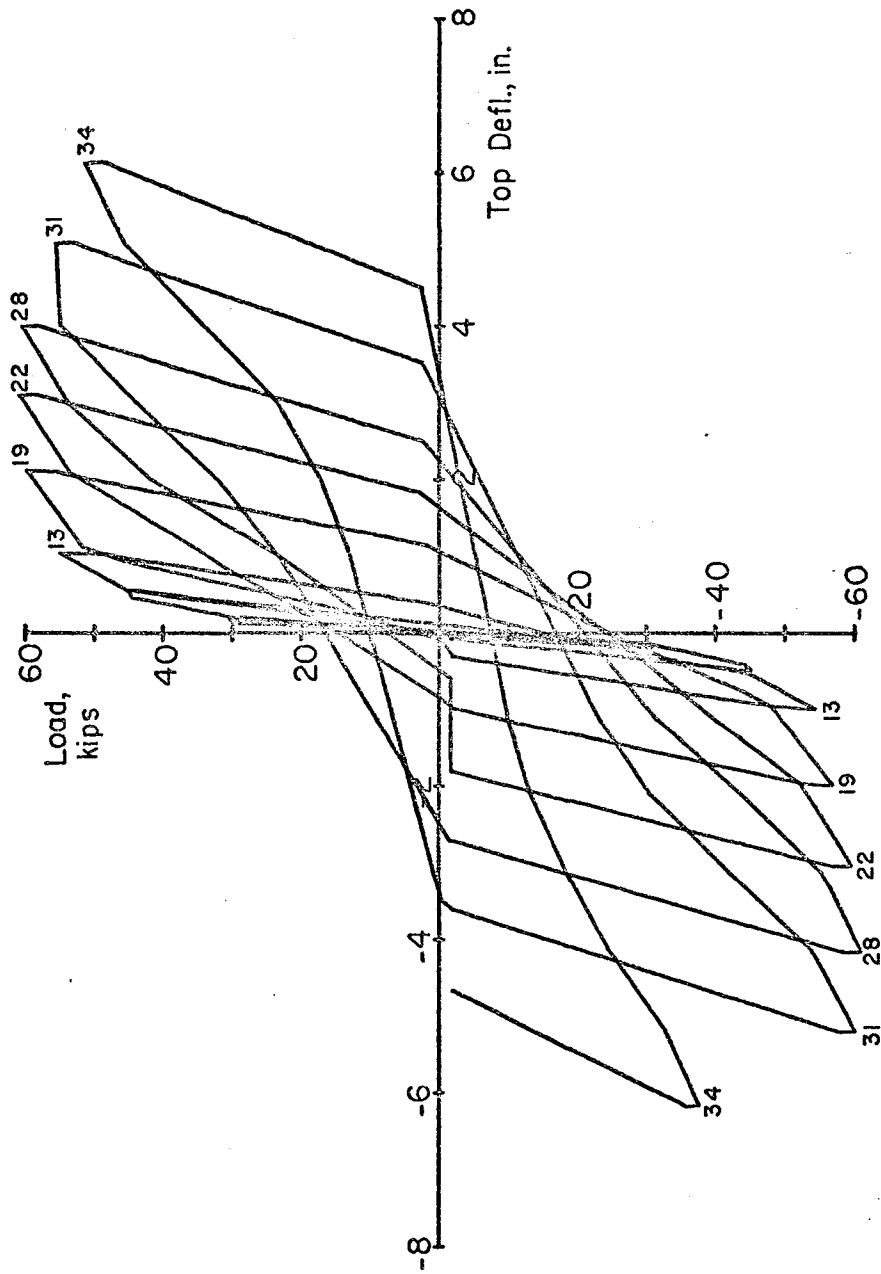
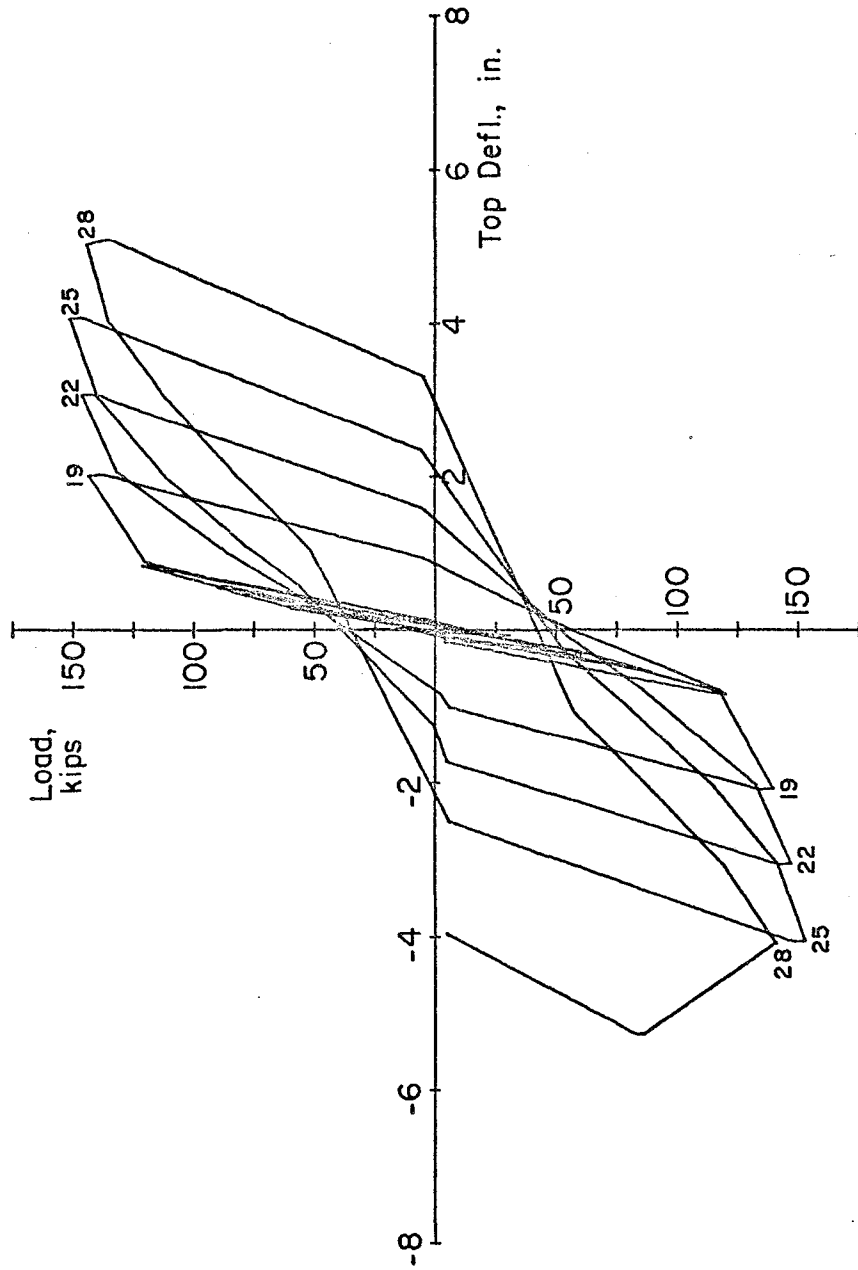Fig. 52 Load Versus Top Deflection for Specimen B1

-72-

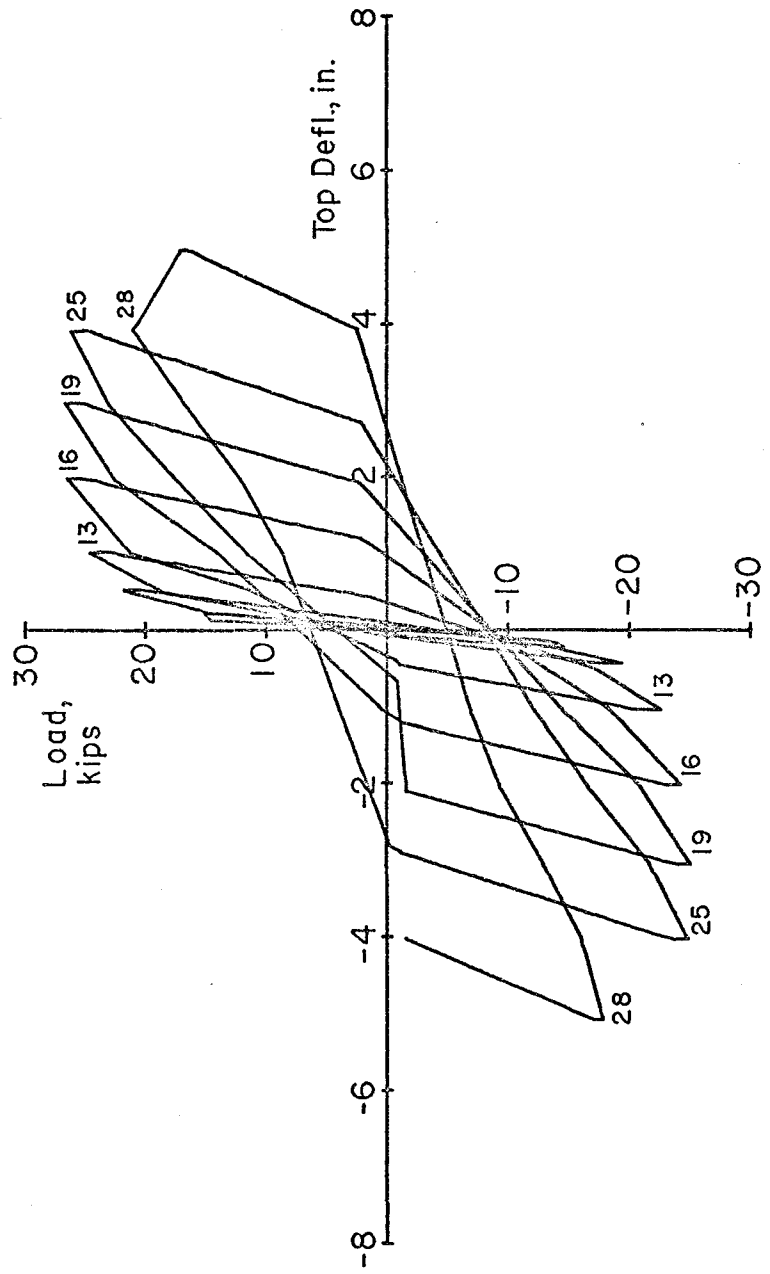Fig. 53   Load Versus Top Deflection for Specimen B2

-73-

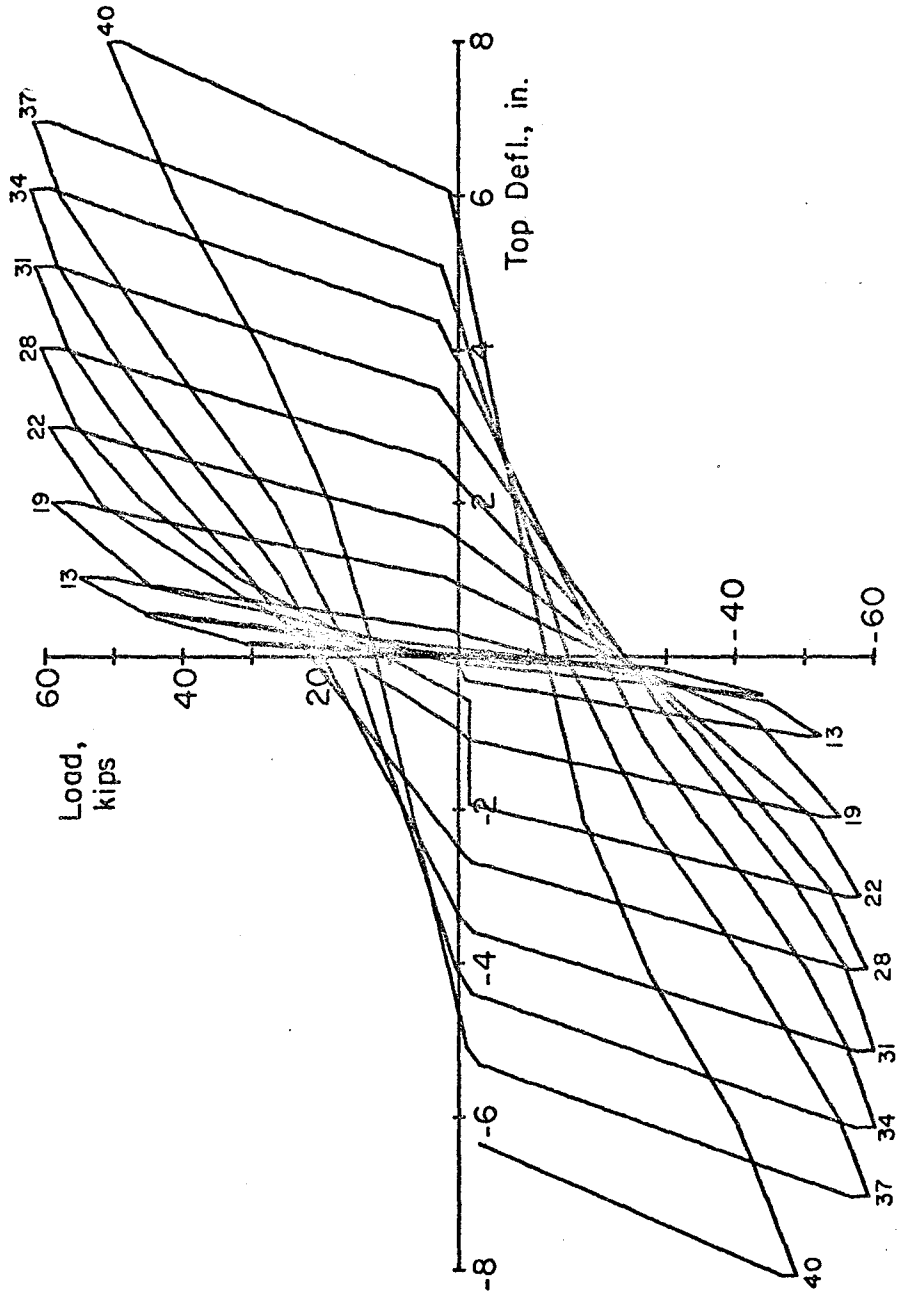Fig. 54 Load Versus Top Deflection for Specimen R1

Fig. 55 Load Versus Top Deflection for Specimen B3

Two features should be noted regarding the figures presented. First, in plotting the results a straight line between successive load stages was assumed. Second, discontinuities in the curves at zero load levels occur because only the first cycle of each set of cylces is plotted.

Moment-Curvature Relationships. Moment-curvature relationships, given in Fig. 56 through 60, were derived from measured deformations along each end of the wall over a gage length of about 3 in. above the top of the base block. Moments are calculated for a section at the top of the base block.

Load-Strain Relationships. Strains were measured on both the vertical and the horizontal reinforcement. Figures 61 through 65 show results obtained from the gages on the main vertical steel at the base of the wall for each specimen. The gages selected are at opposite ends of the wall.

Data from gages on the horizontal reinforcement are shown in Fig. 66 through Fig. 70.

Free Vibration Characteristics. The free vibration characteristics of the specimens were measured at several stages as the tests progressed. The first vibration test was run prior to the application of lateral loading. The second vibration test was run after the lateral loading cycles closest to the yield level had been applied. Additional vibration tests were run at later loading stages depending on the physical condition of the test specimen.

An example of the time-displacement relationships obtained from the tests is shown in Fig. 71. The curves show
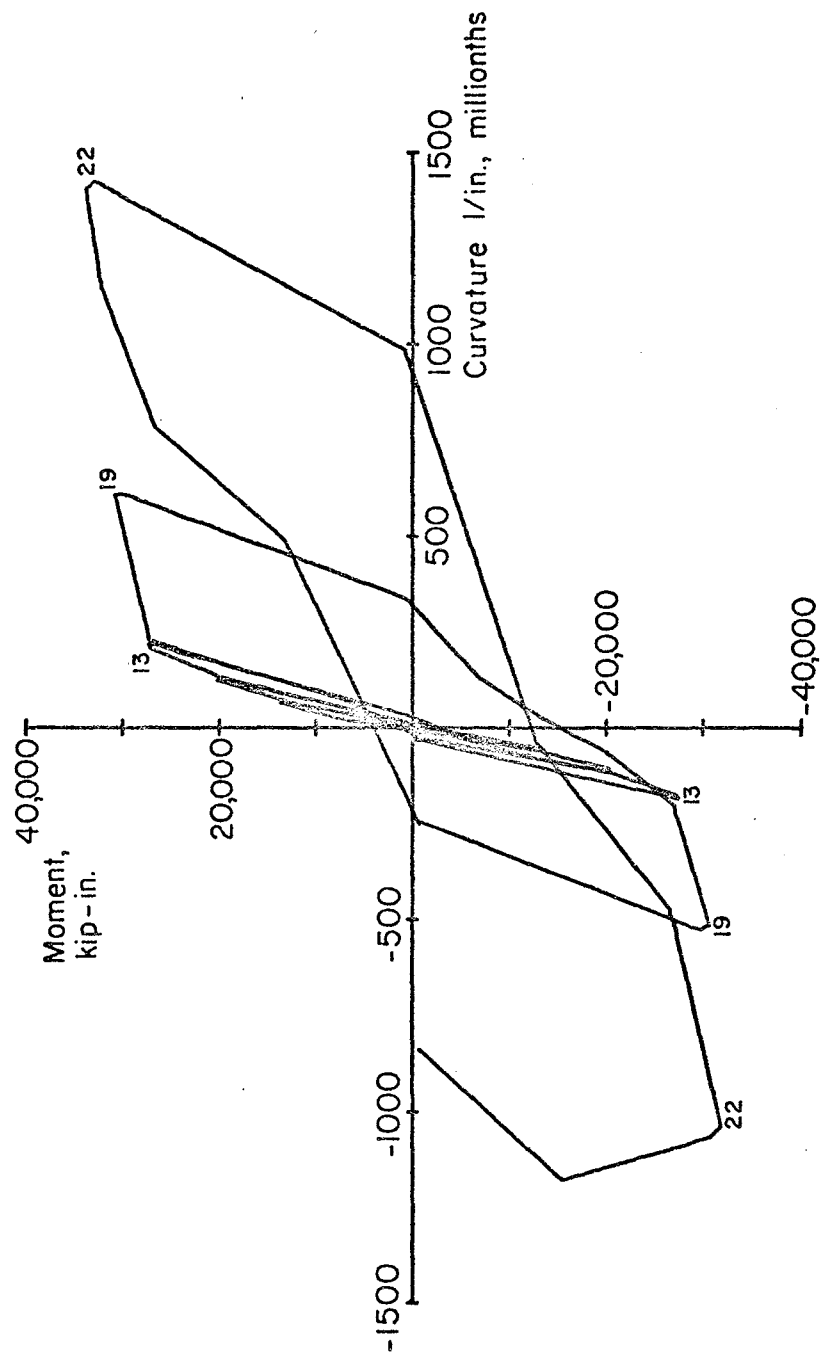
Fig. 56 Moment Versus Curvature at Base of Specimen F1
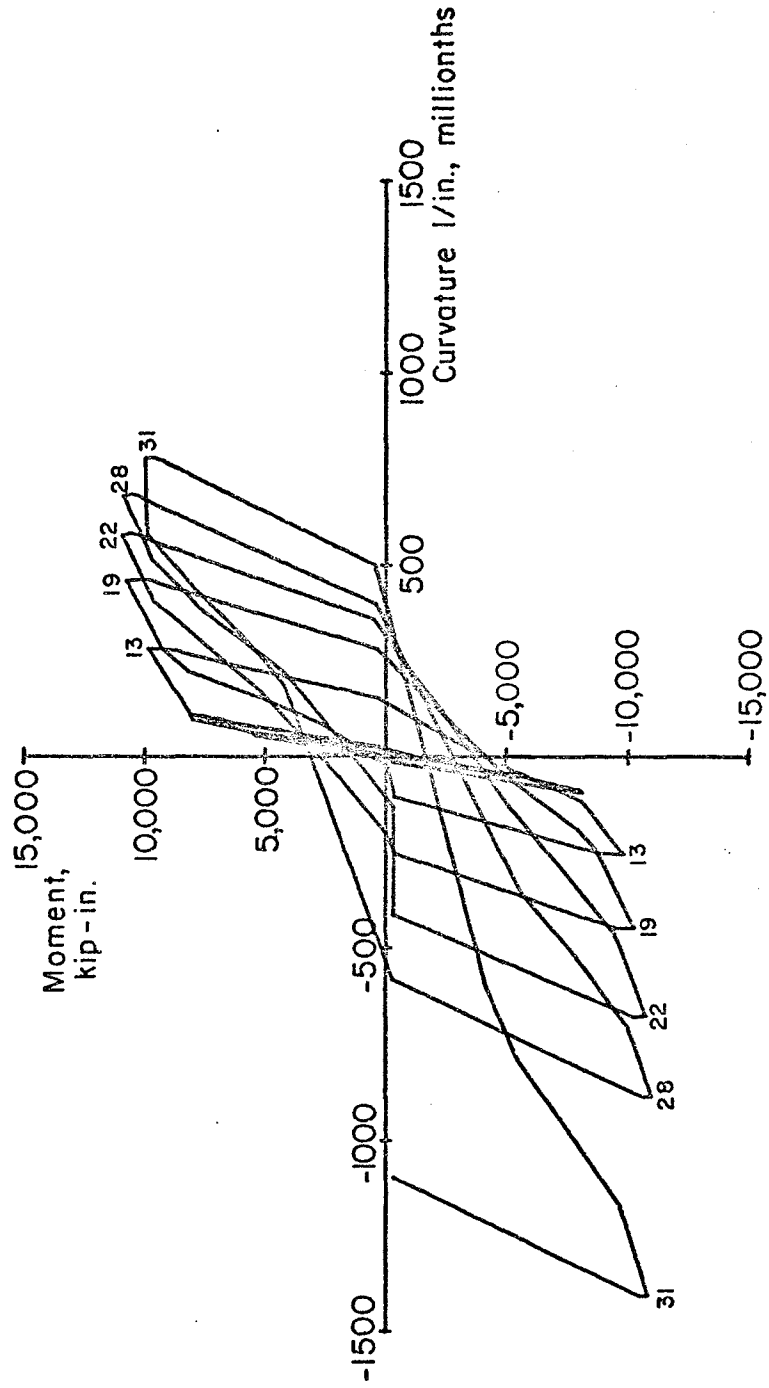
Fig. 57 Moment Versus Curvature at Base of Specimen B1
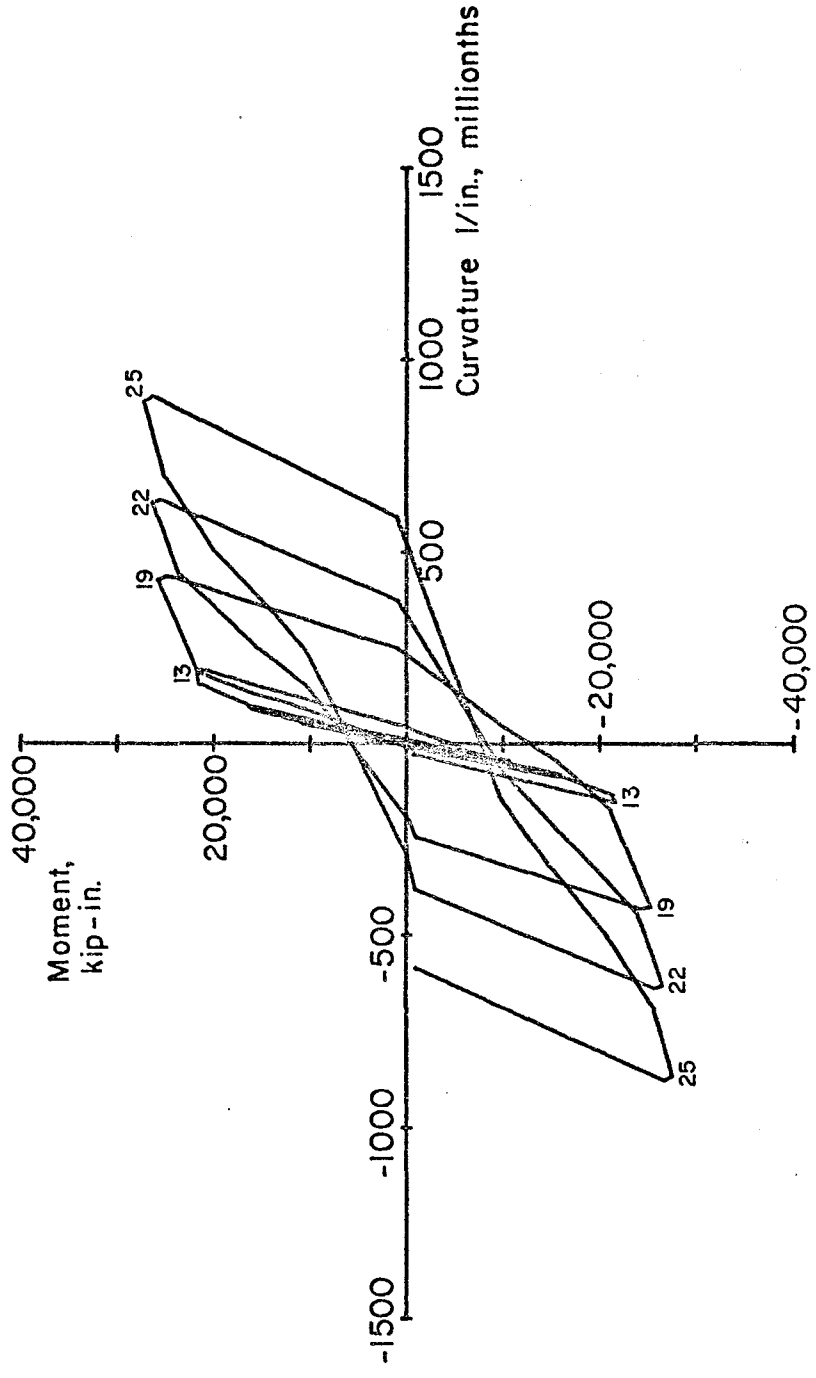
Fig. 58 Moment Versus Curvature at Base of Specimen B2
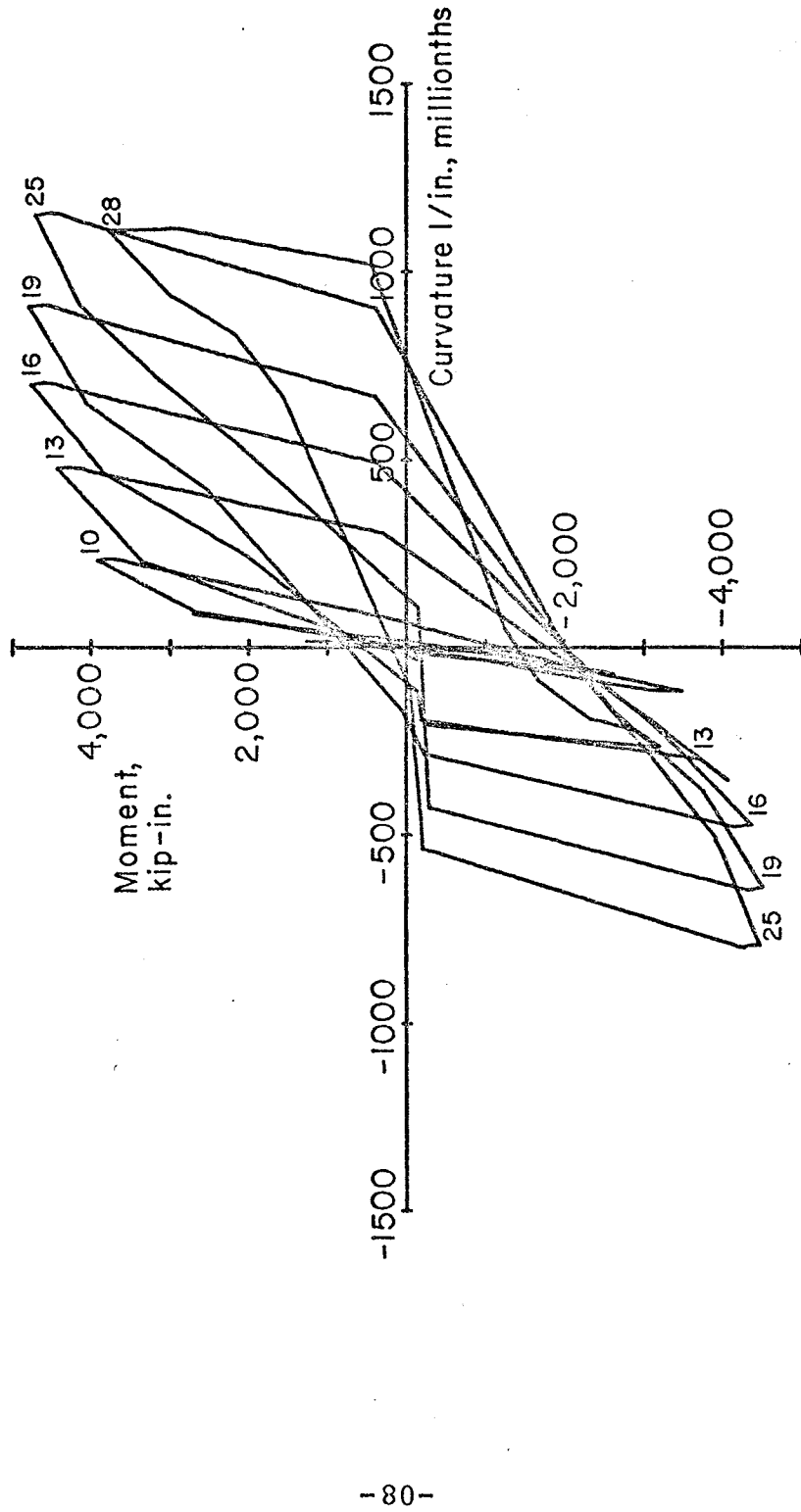
Fig. 59   Moment Versus Curvature at Base of Specimen R1

Fig. 60 Moment Versus Curvature at Base of Specimen B3

Load,
kips

Strain Gage VJT1

150

100

50

-20,000   -10,000   10,000   20,000
                                         Strain, millionths

-50

-100

-150

13

19

13

19

VJT1

VAT1

22

Load,
kips

Strain Gage VAT1

150

100

50

25

-20,000   -10,000   10,000   20,000
                                         Strain, millionths

-50

-100

-150

19

22
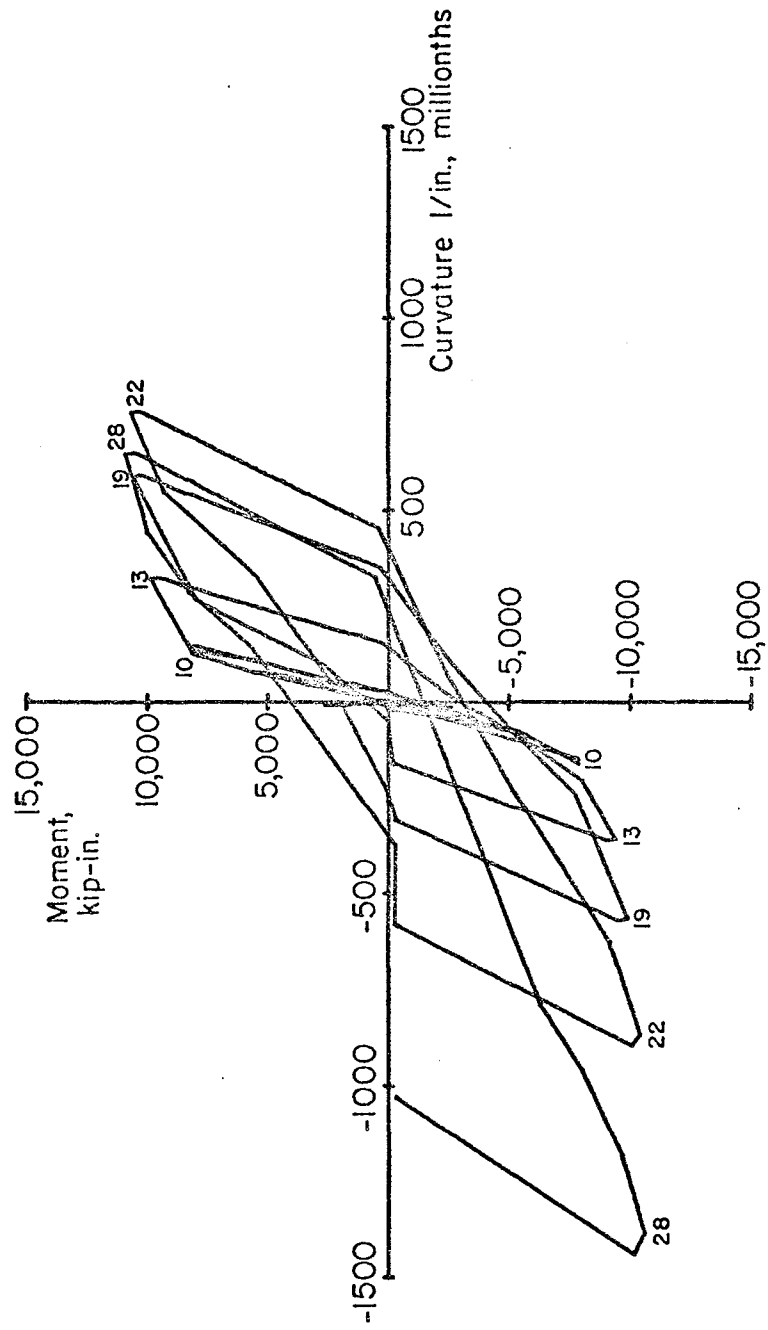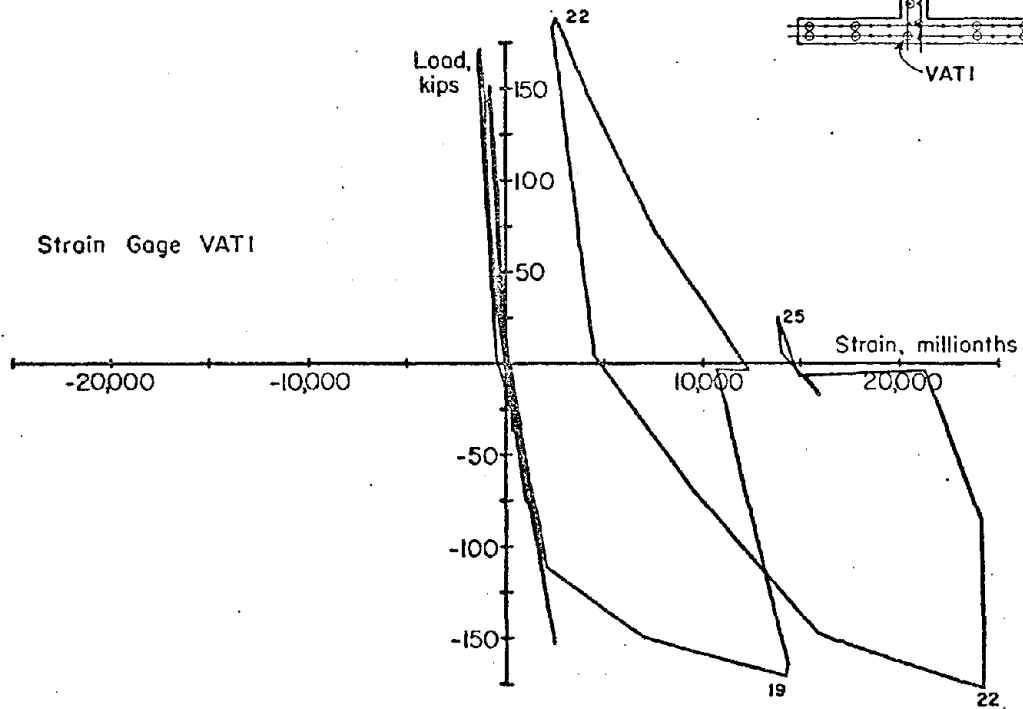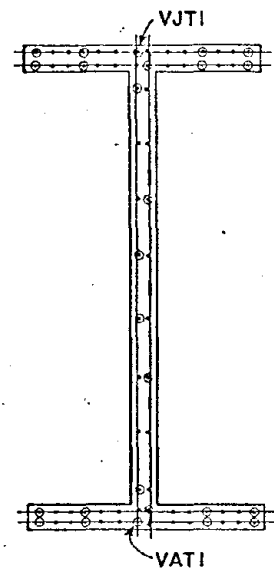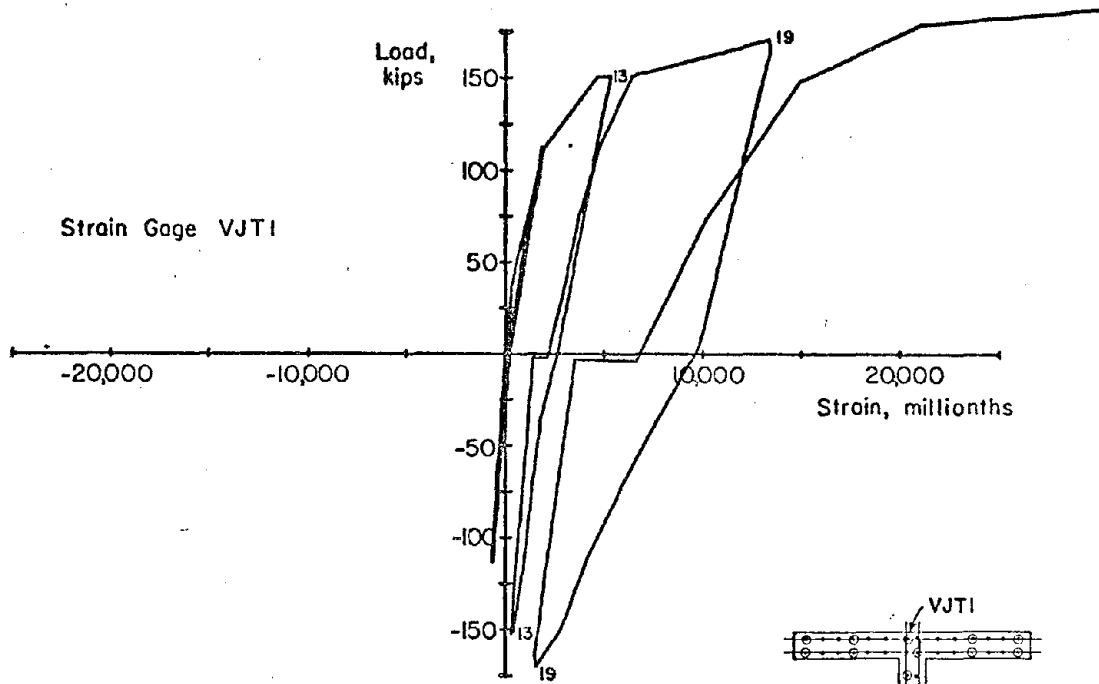
Fig. 61   Measured Strains on Vertical Reinforcement at
          Base of Specimen F1
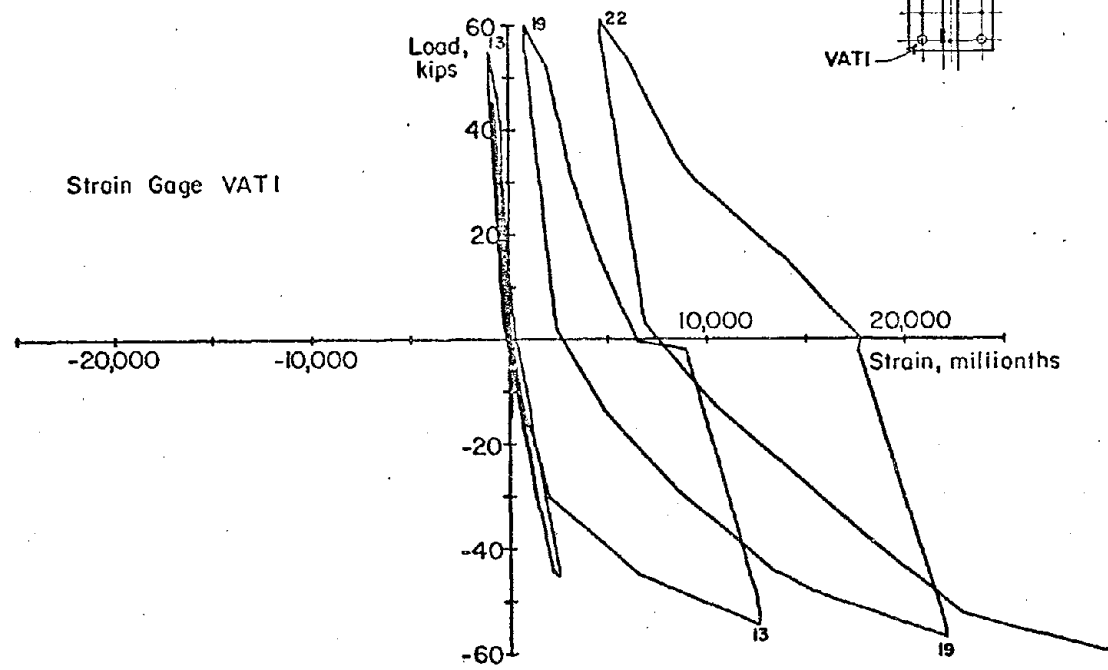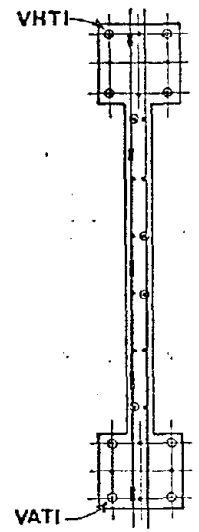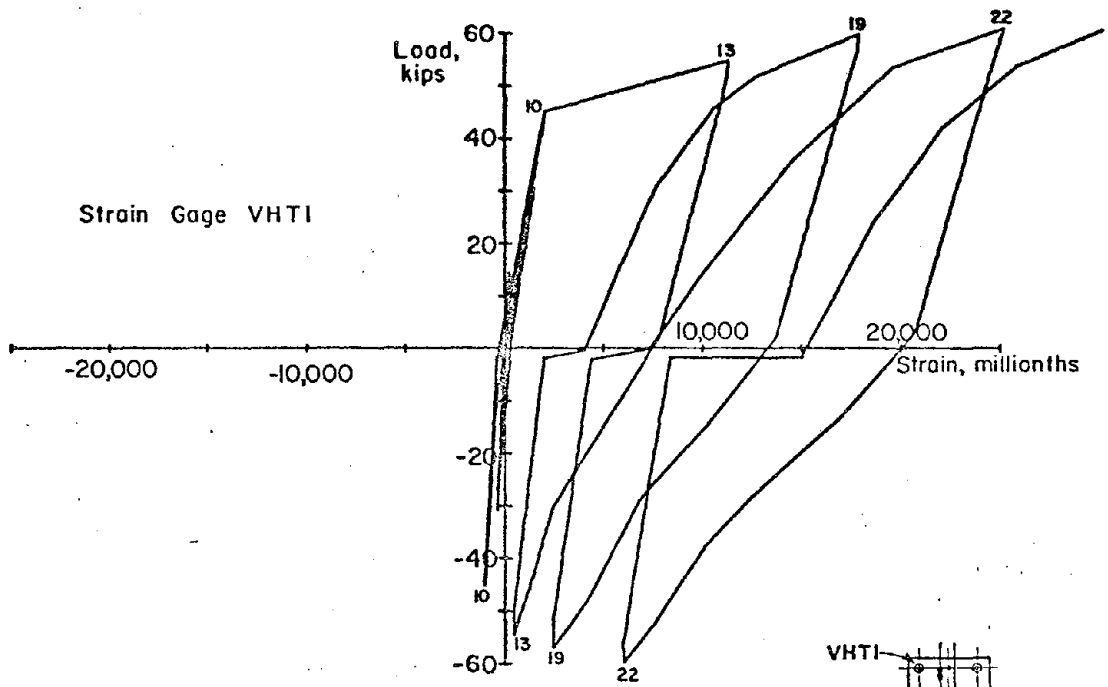
Fig. 62   Measured Strains on Vertical Reinforcement at
          Base of Specimen B1
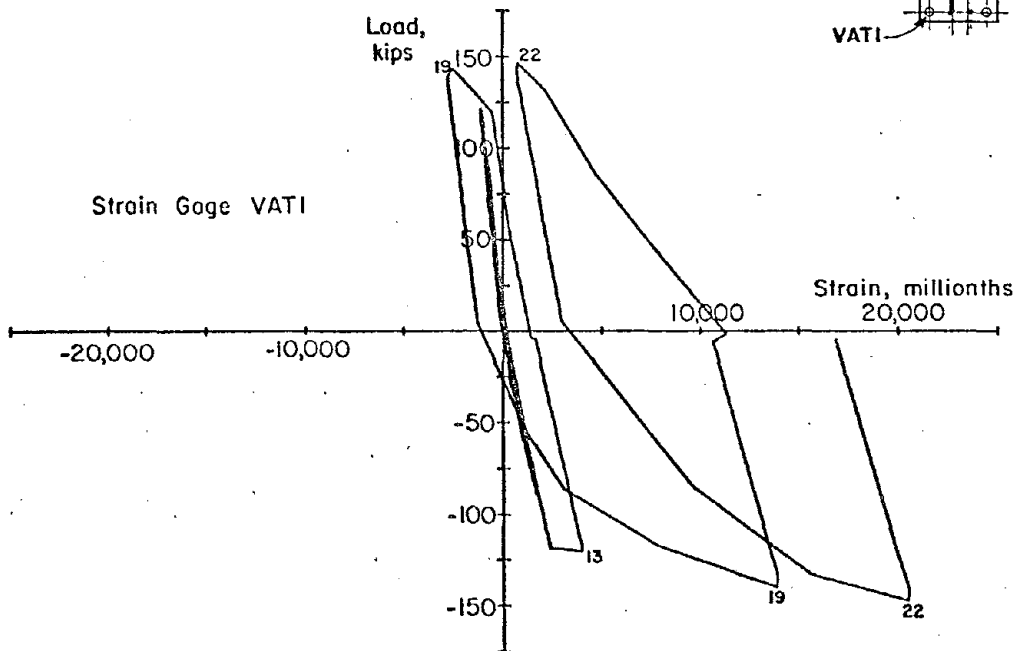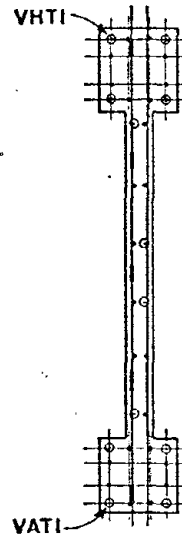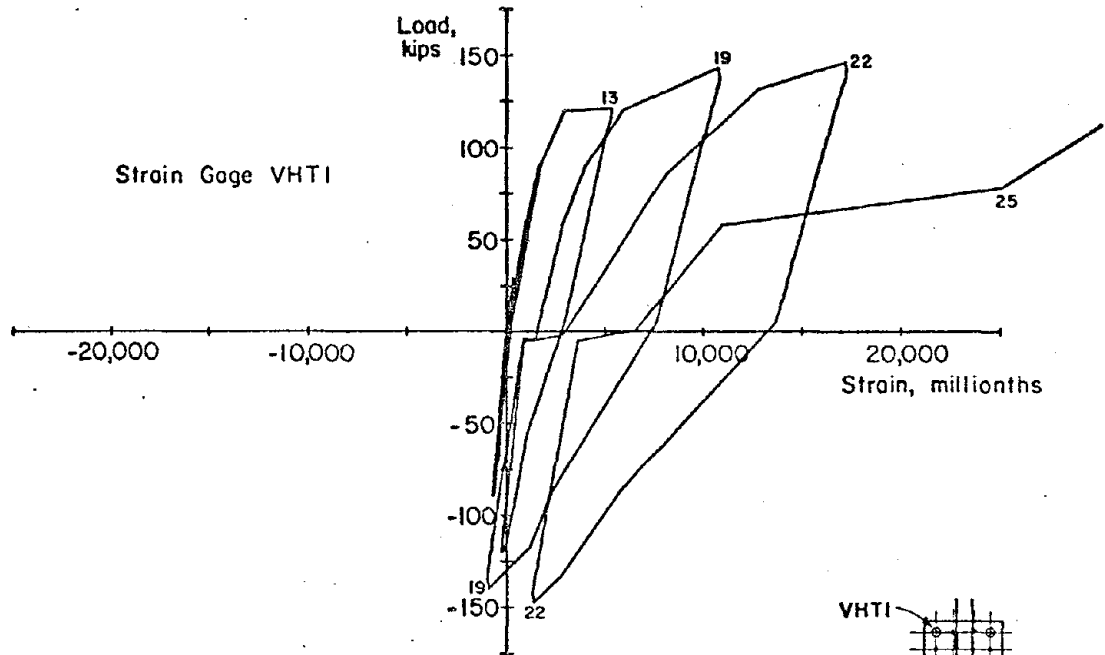
Fig. 63 Measured Strains on Vertical Reinforcement at
Base of Specimen B2
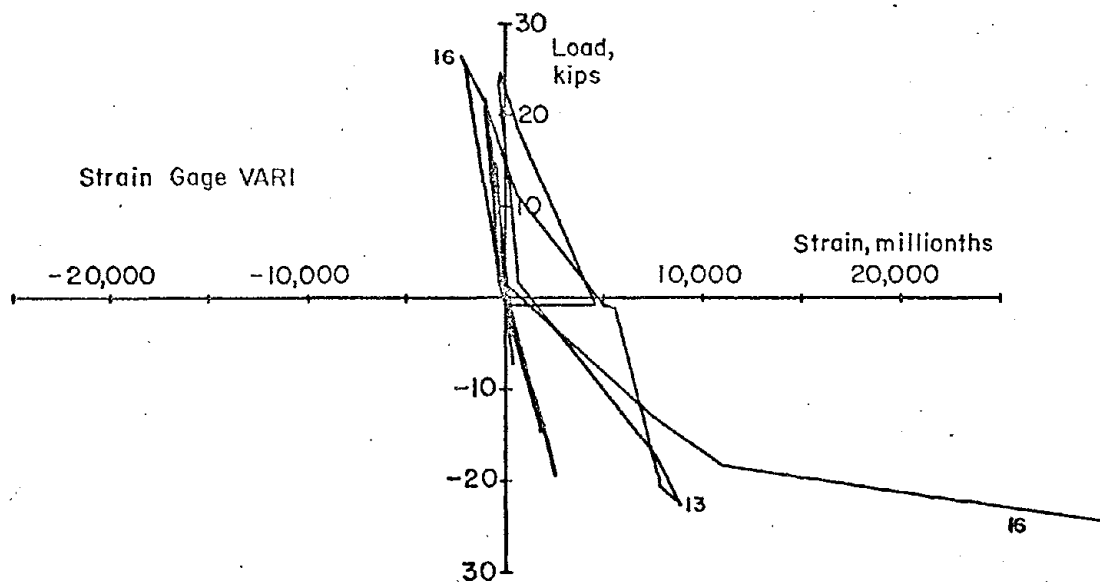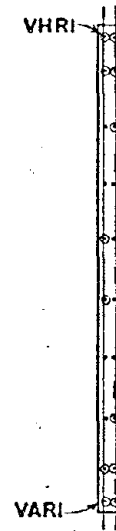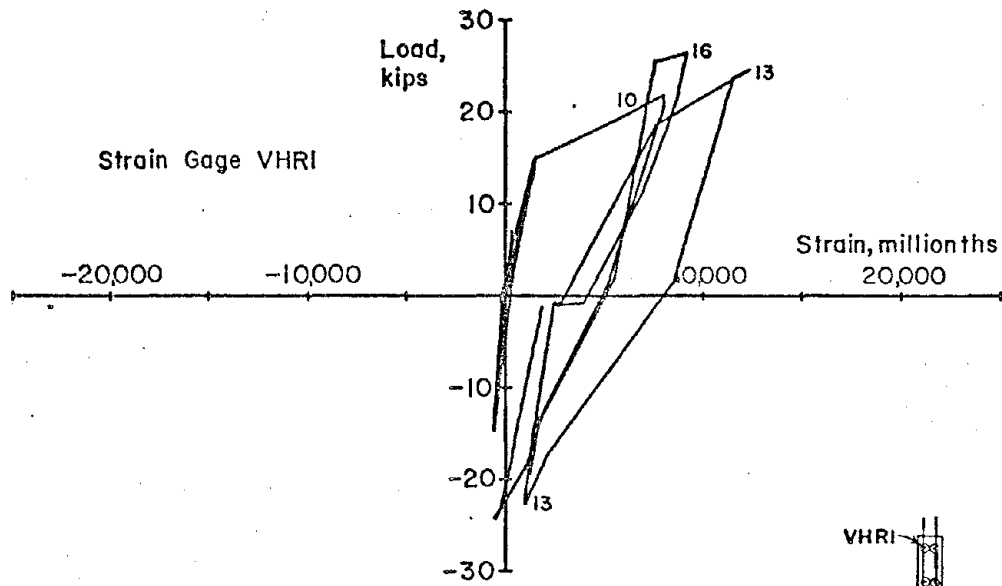
Fig. 64   Measured Strains on Vertical Reinforcement at
          Base of Specimen R1
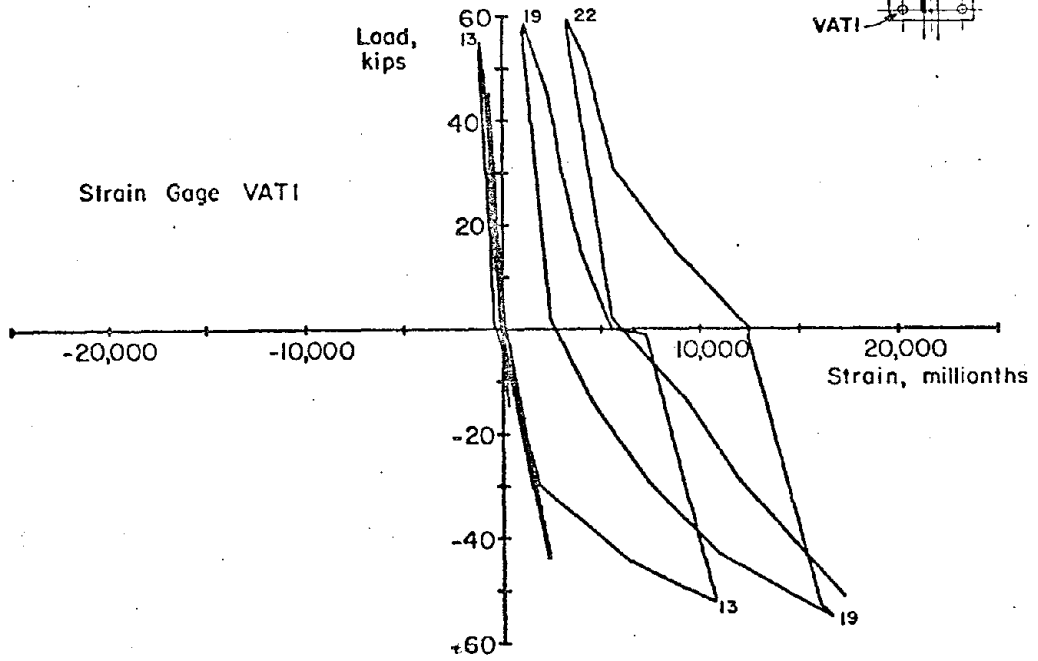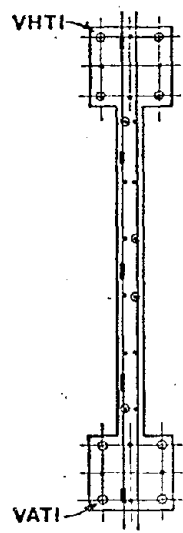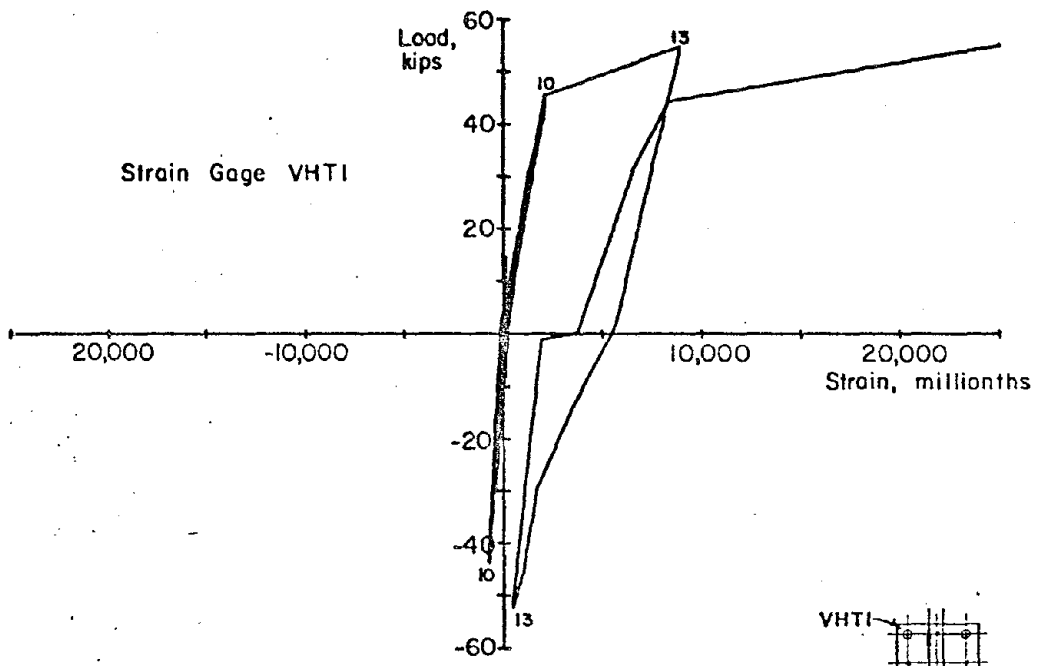
Fig. 65   Measured Strains on Vertical Reinforcement at
Base of Specimen B3

-86-

Strain Gage HE2

Load, kips

150

100

50

-8000   -4000   4000   8000
                                    Strain, millionths

-50

-100

-150

25

13

19

22

13

19

22

③

②

①

18"

18"

1"

HE2

HEI

22

19

150

13

Load, kips

Strain Gage HEI

100

50

25

-8000   -4000   4000   8000
                                    Strain, millionths

-50

-100

-150

19

22
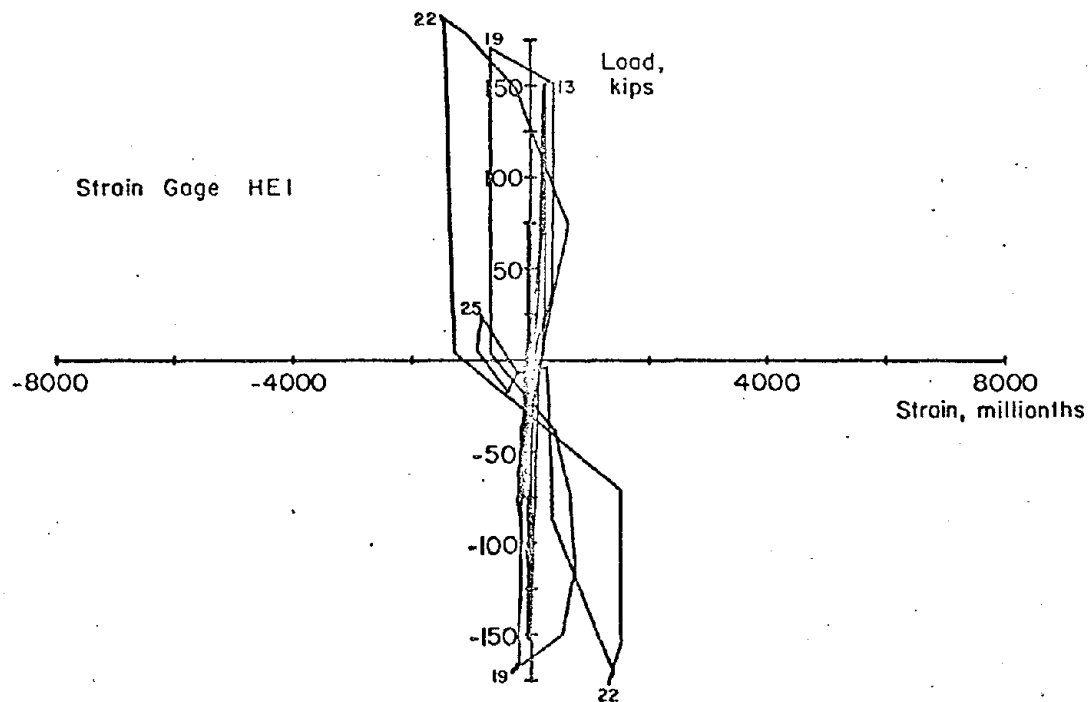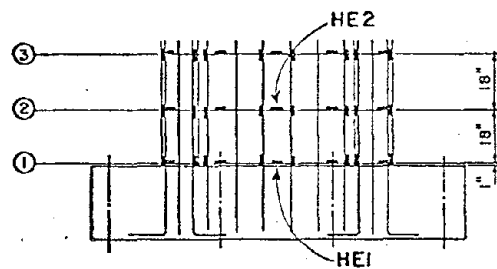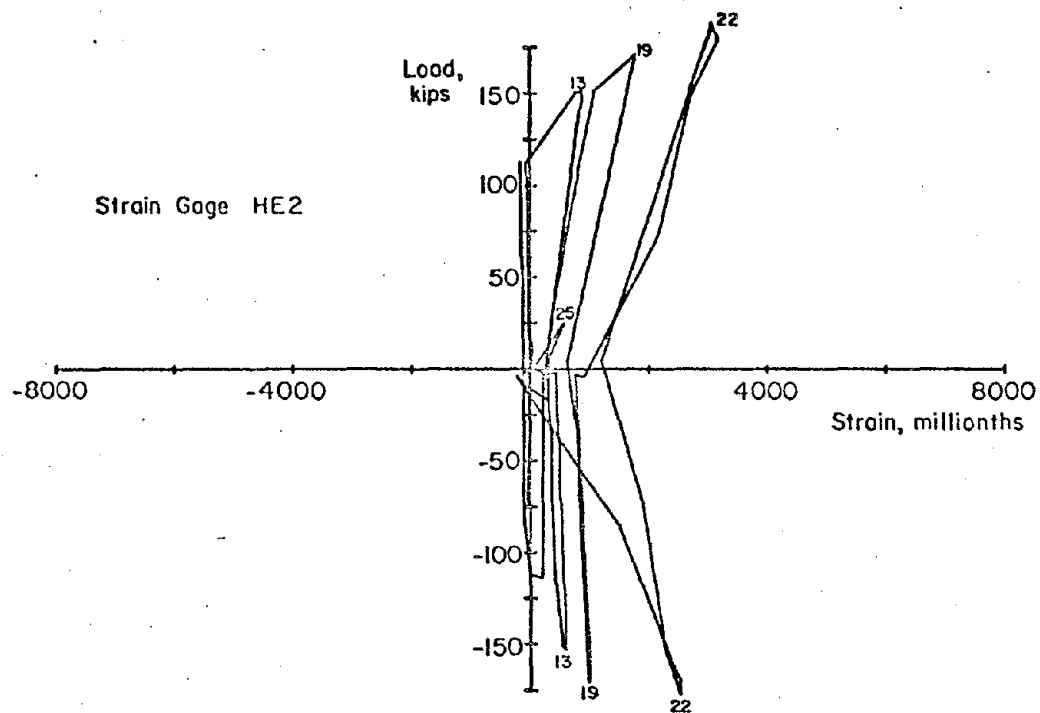
Fig. 66   Measured Strains on Horizontal Reinforcement
          in Specimen F1

-87-
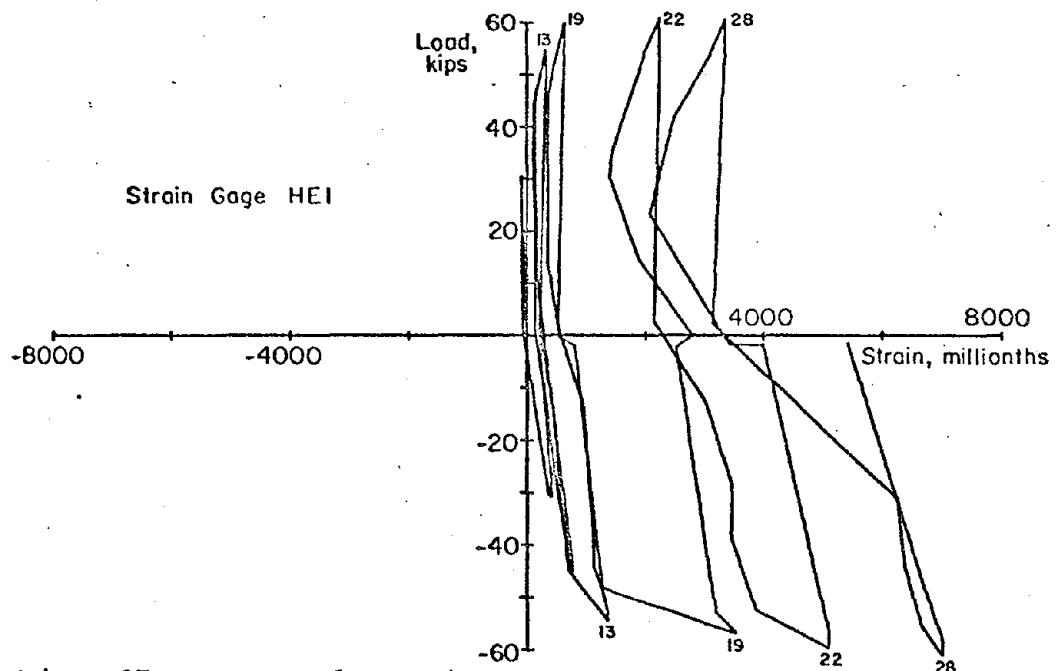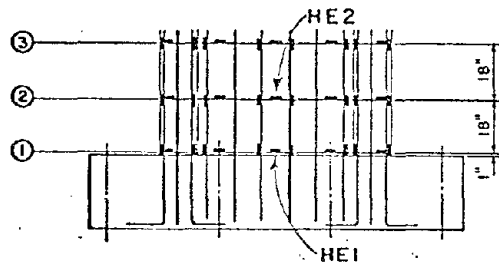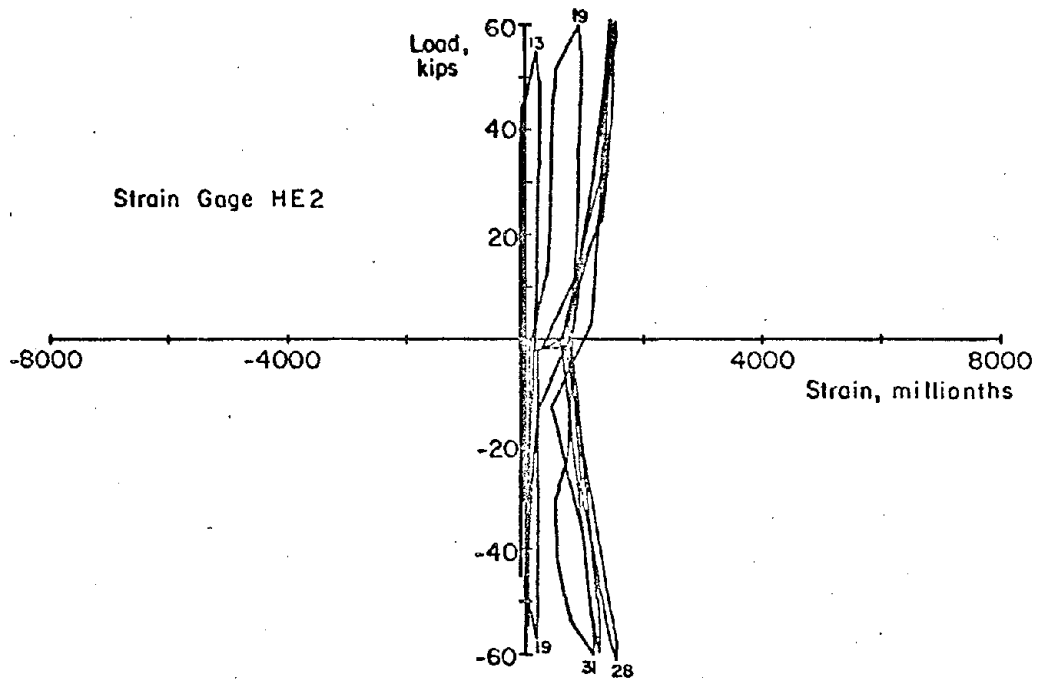
Fig. 67 Measured Strains on Horizontal Reinforcement
in Specimen B1
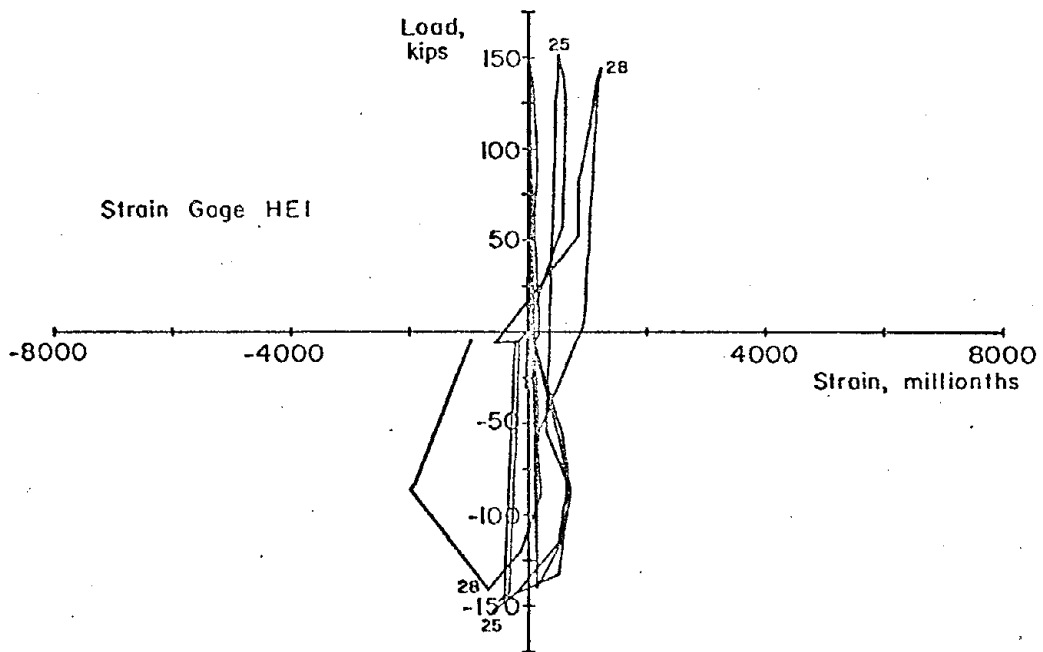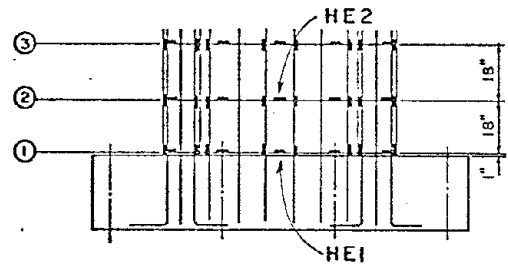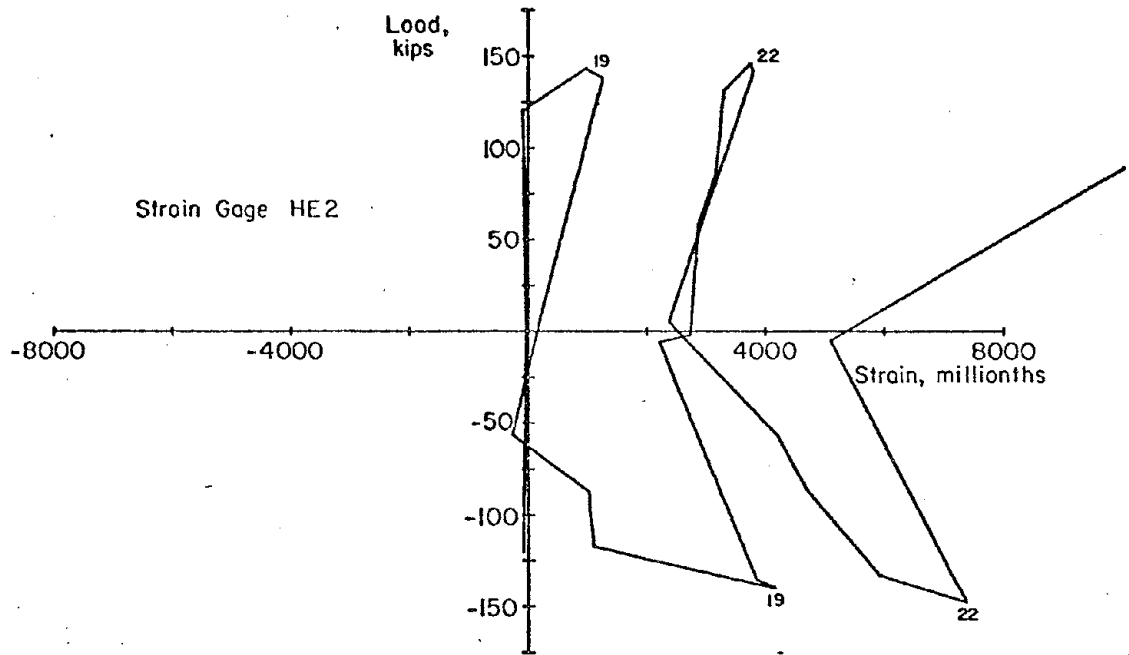
Fig. 68   Measured Strains on Horizontal Reinforcement
           in Specimen B2

-89-

Strain Gage HE2

Load,
kips

30

20

10

Strain, millionths

-8000   -4000   4000   8000

-10

-20   28

-30

HE2

③

②

①

18"

18"

1"

HE1

Strain Gage HE1

Load,
kips

30

13   16

20

10

Strain, millionths

-8000   -4000   4000   8000

-10

-20

13

16

-30
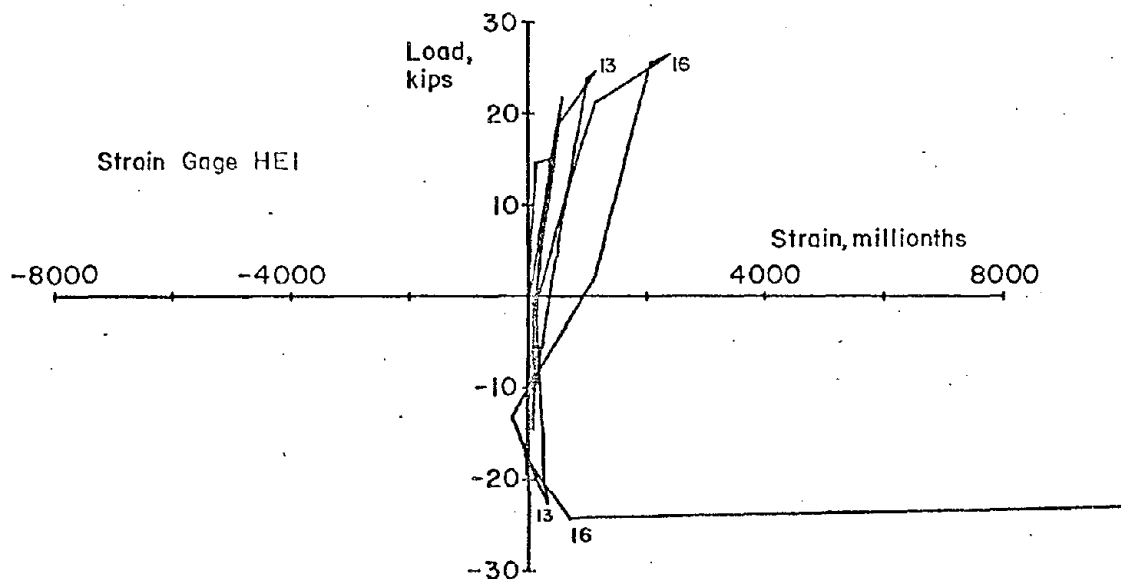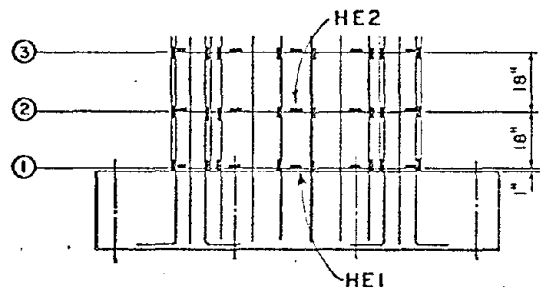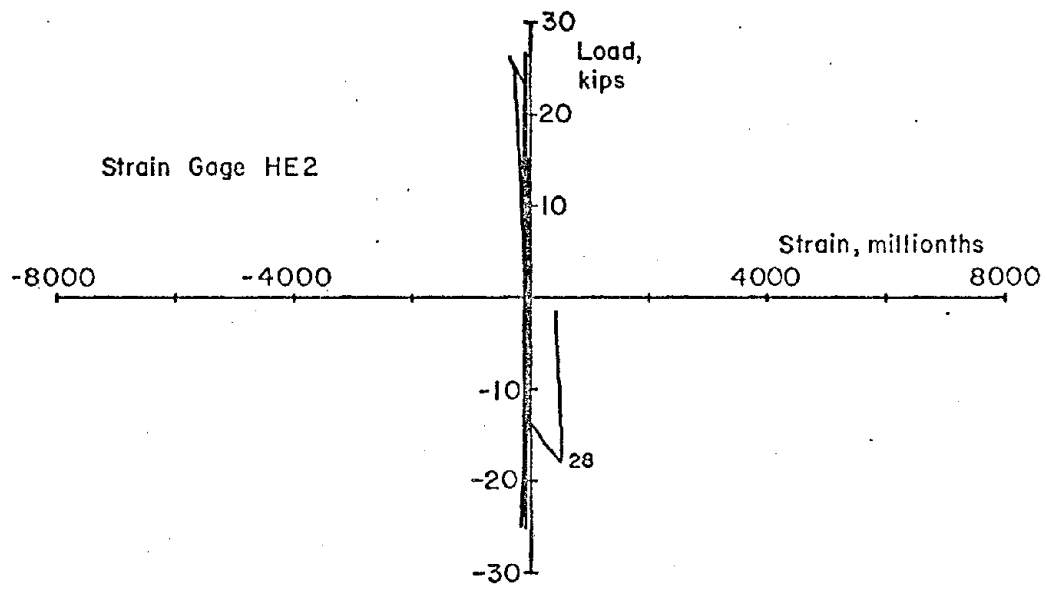
Fig. 69   Measured Strains on Horizontal Reinforcement
in Specimen R1
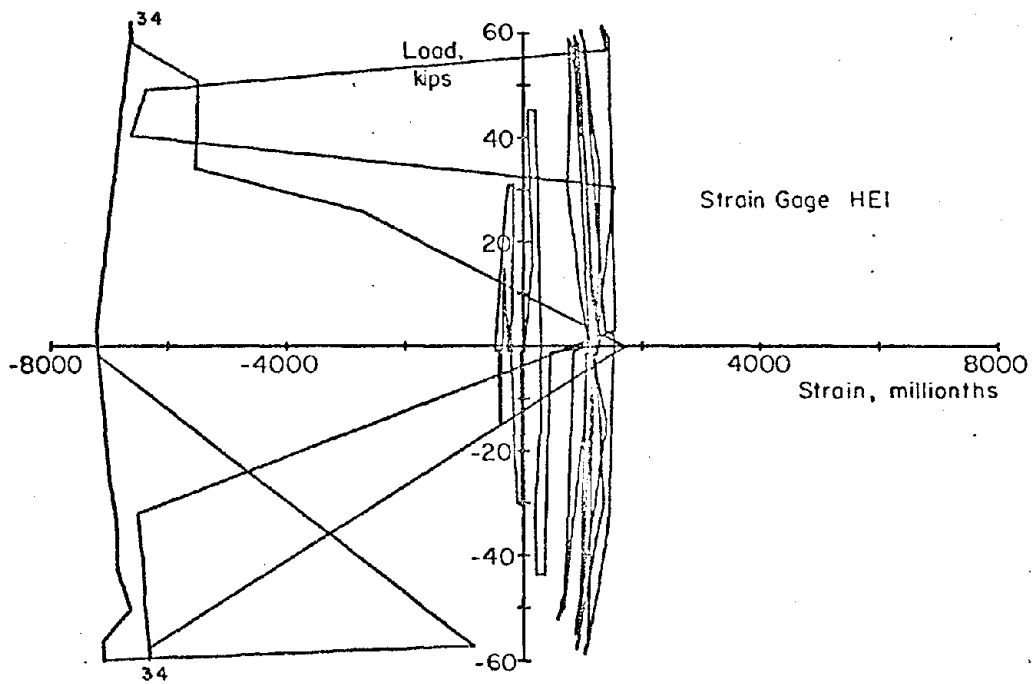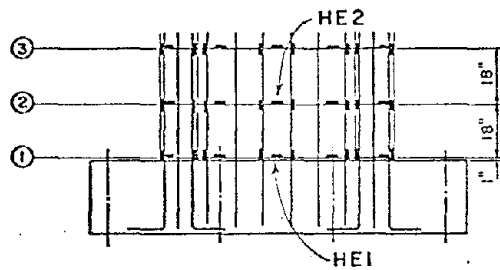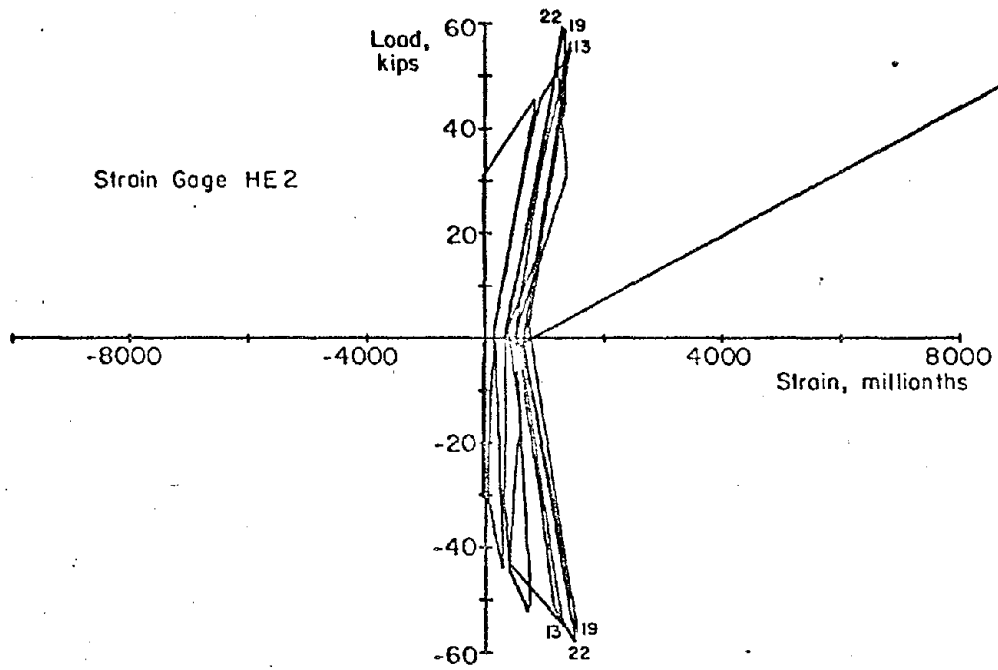
Fig. 70 Measured Strains on Horizontal Reinforcement
in Specimen B3 -91-
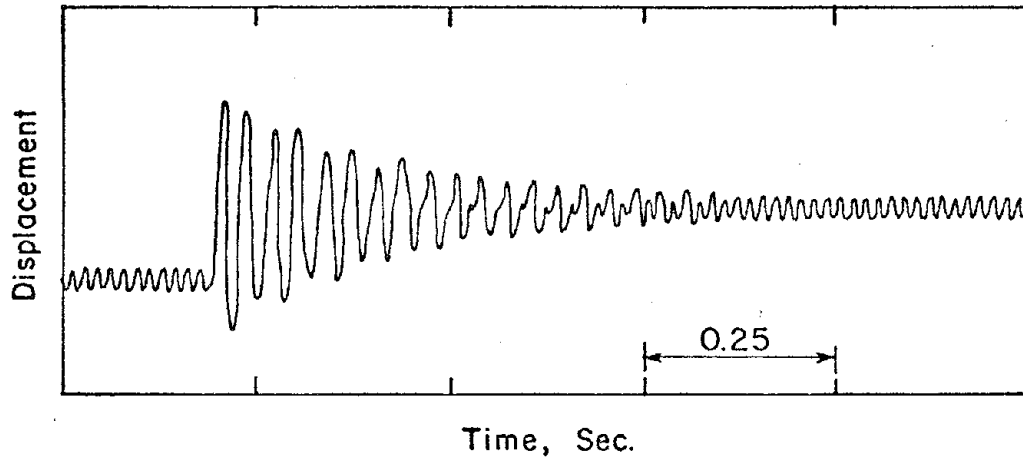
a) Uncracked Section
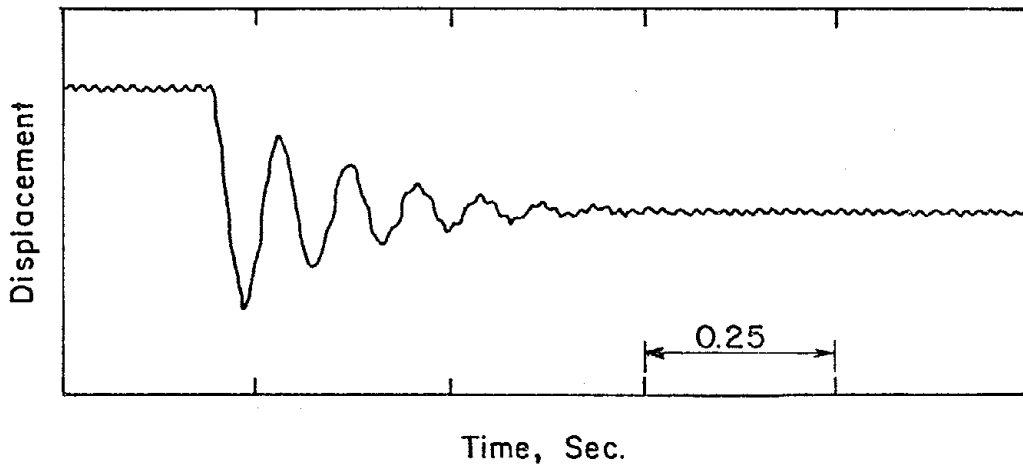
b) Cracked Section (Previously Cycled at Yield Point)
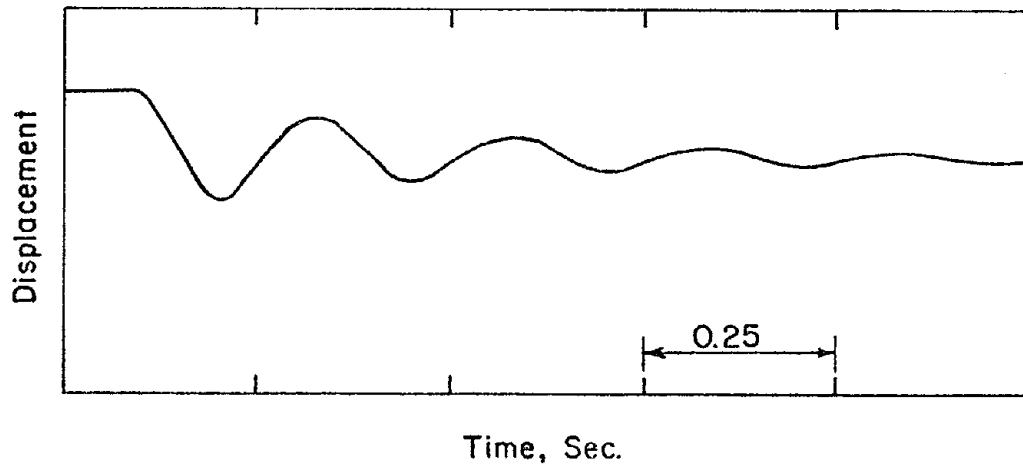
c) Cracked Section (Previously Cycled at 3" Deflection)

Fig. 71   Displacement Versus Time Relationships From
Free Vibration Tests of Specimen B1

a very significant change in free vibration characteristics as the specimen becomes more extensively cracked.

Using the displacement-time curves, the damped natural frequency and the logarithmic decrement were computed. The damping coefficient was then calculated from the logarithmic decrement. Values obtained for the measured frequency and damping are summarized in Table 4.

Generally, the frequency decreased by a factor of about three from the uncracked state to the yield state. For the same condition, the damping coefficient changed from about 2% to about 10% of critical.

Subsequent to yielding, the frequency continued to decrease by another factor of about three. However, the damping did not change significantly.

Construction Joint Behavior. Dial gages were used to monitor the relative displacement or slip across the lower three construction joints.

The results of measurements for the construction joint at the base of each wall are shown in Fig. 72 through Fig. 76. Maximum values of slip ranged to 0.3 in. While this slip adds a component to the lateral displacement of the walls, the slip did not appear to affect the overall behavior of the walls. No specimen failures could be attributed to the performance of the construction joints.

Analysis of Test Results

Introduction. The results described in this section

TABLE 4   Summary of Free Vibration Test Results

Specimen	Description	Measured Frequency (cps)	Measured Damping (% of Critical)	No. of Prior Load Cycles
F1	Uncracked	33.8	2.0	0
	Cycled at 85% of yield	13.0	9.8	12
	Uncracked	30.0	2.2	0
B1	Cycled at yield	11.1	8.5	12
	Cycled at 3-in. deflection	3.9	9.0	24
	Uncracked	29.4	4.0	0
B2	Cycled at yield	13.0	10.0	15
	Cycled at 3-in. deflection	3.9	15.0	24
R1	Uncracked	21.8	3.0	0
	Cycled at 75% of yield	10.5	7.0	6
	Uncracked	29.7	2.7	0
	Cycled at yield	10.9	10.0	12
B3	Cycled at 3-in. deflection	4.3	8.0	24
	Cycled at 6-in. deflection	5.2	9.0	36
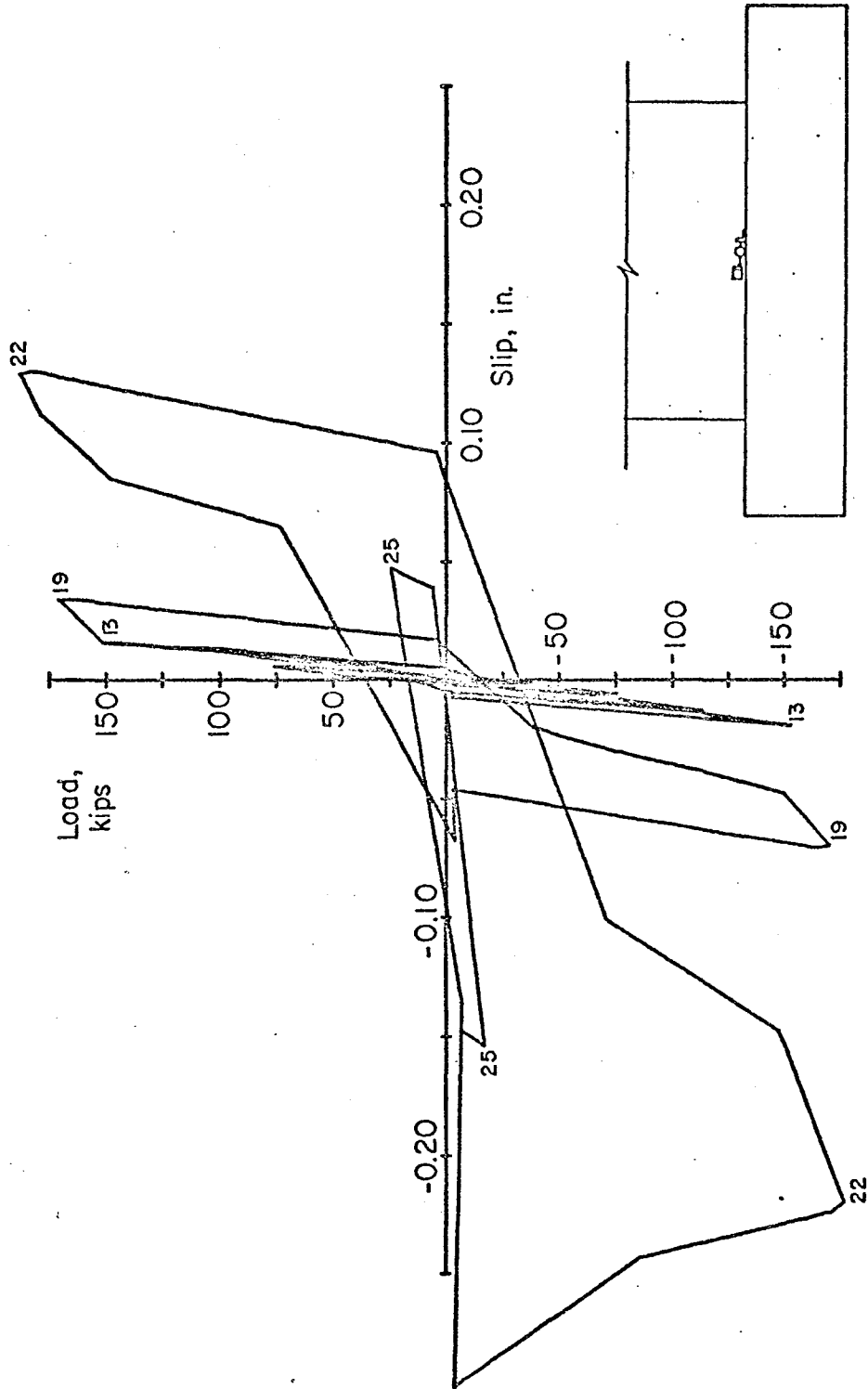
Fig. 72 Load Versus Slip Relationship for Base Construction Joint of Specimen F1
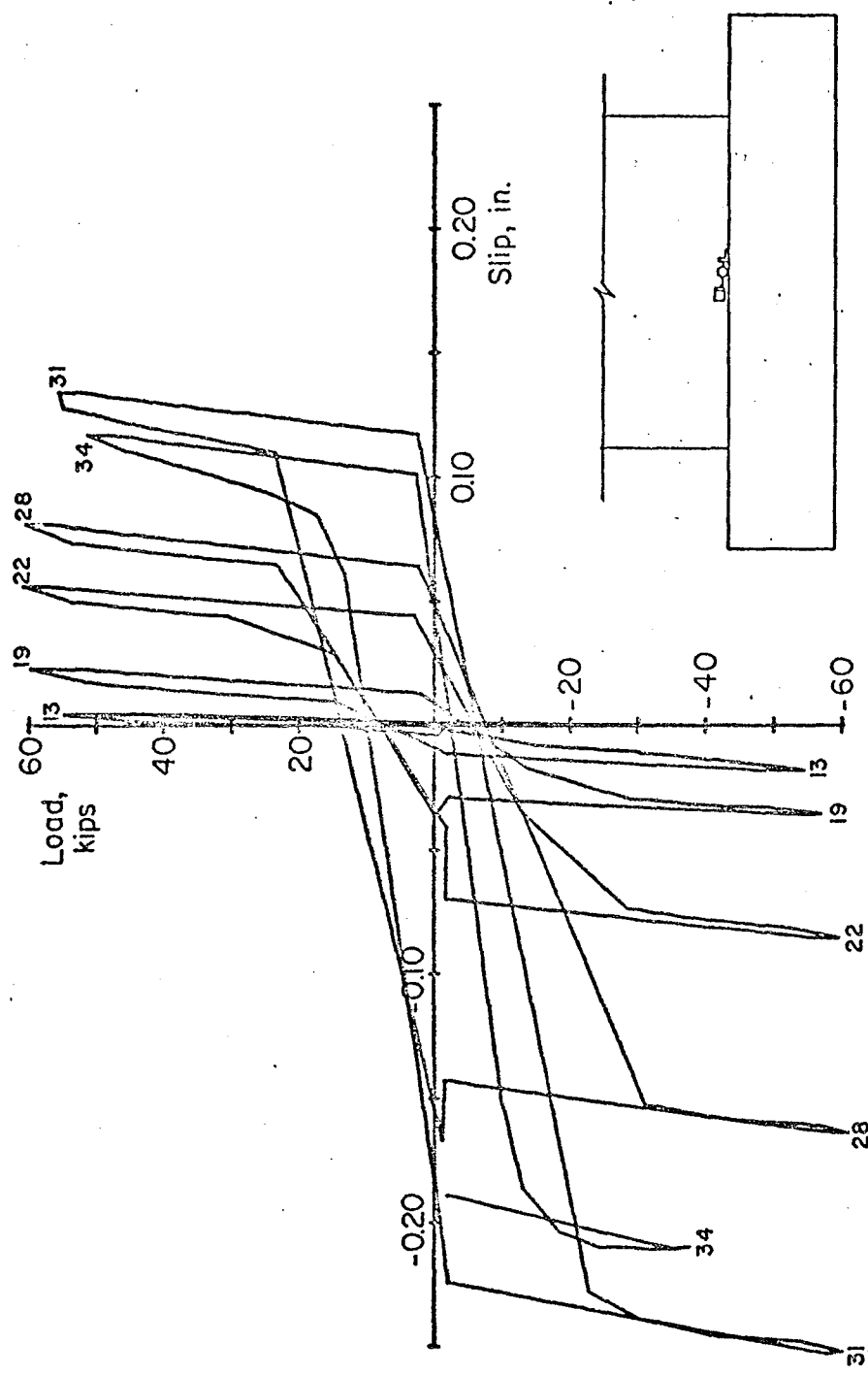
Fig. 73 Load Versus Slip Relationship for Base Construction Joint of Specimen B1
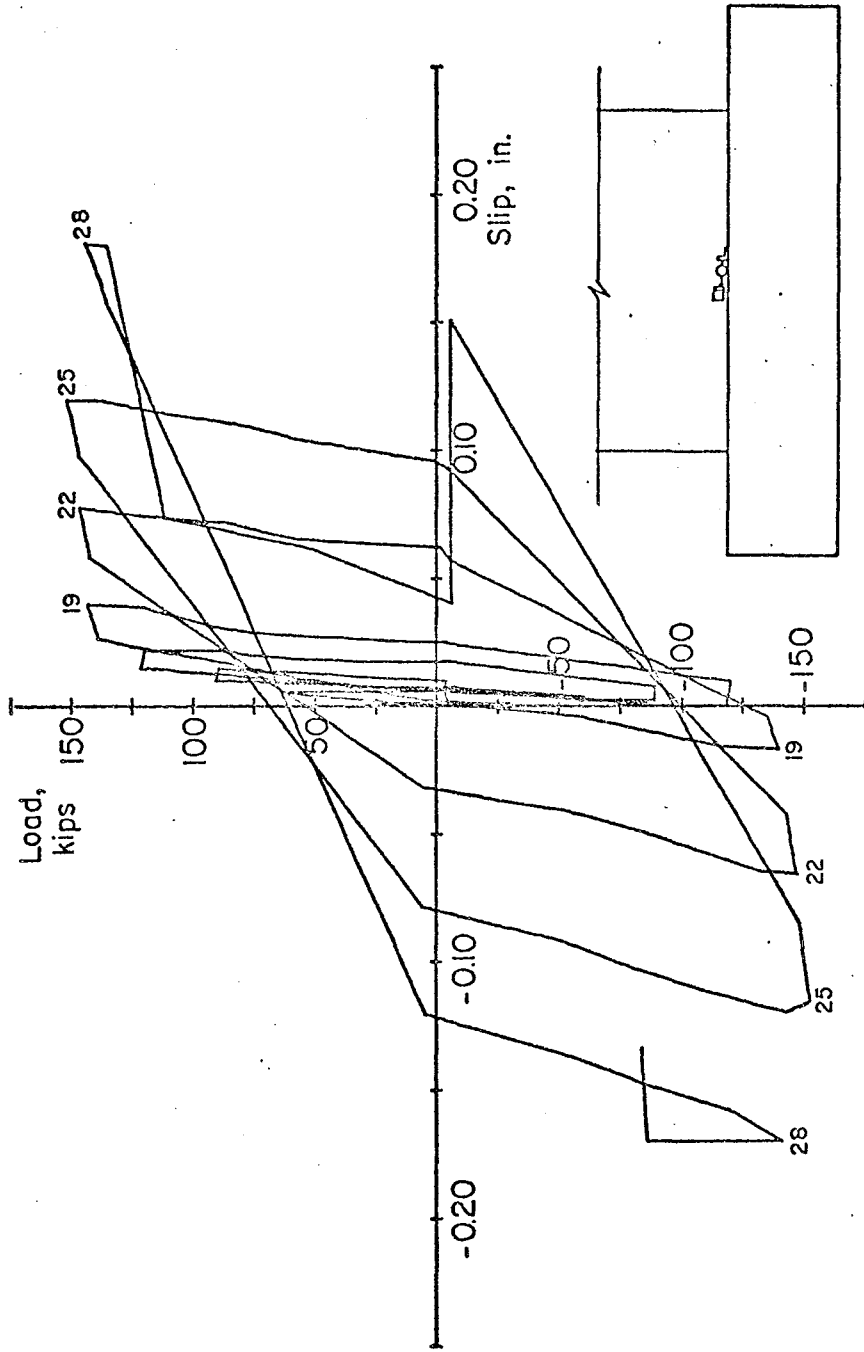
Fig. 74 Load Versus Slip Relationship for Base Construction Joint of
Specimen B2
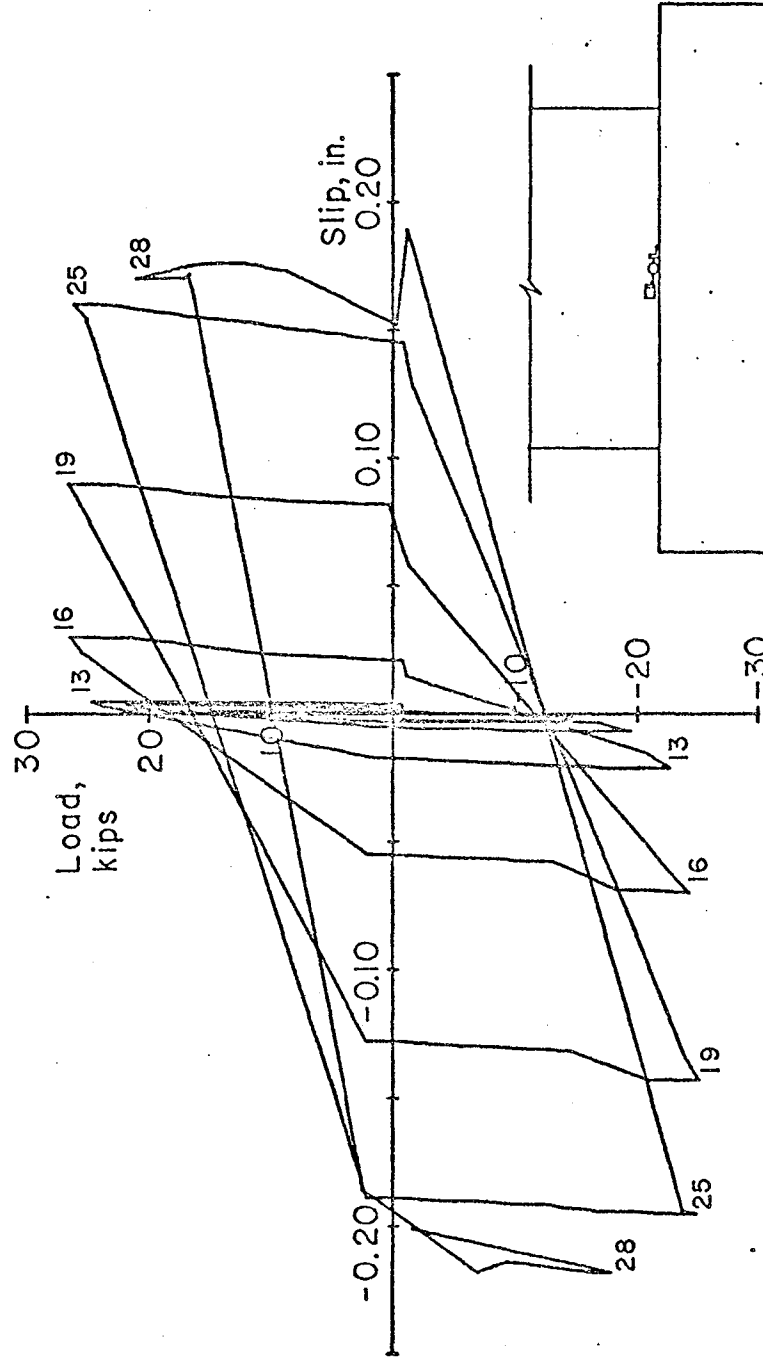
Fig. 75 Load Versus Slip Relationship for Base Construction Joint
of Specimen Rl
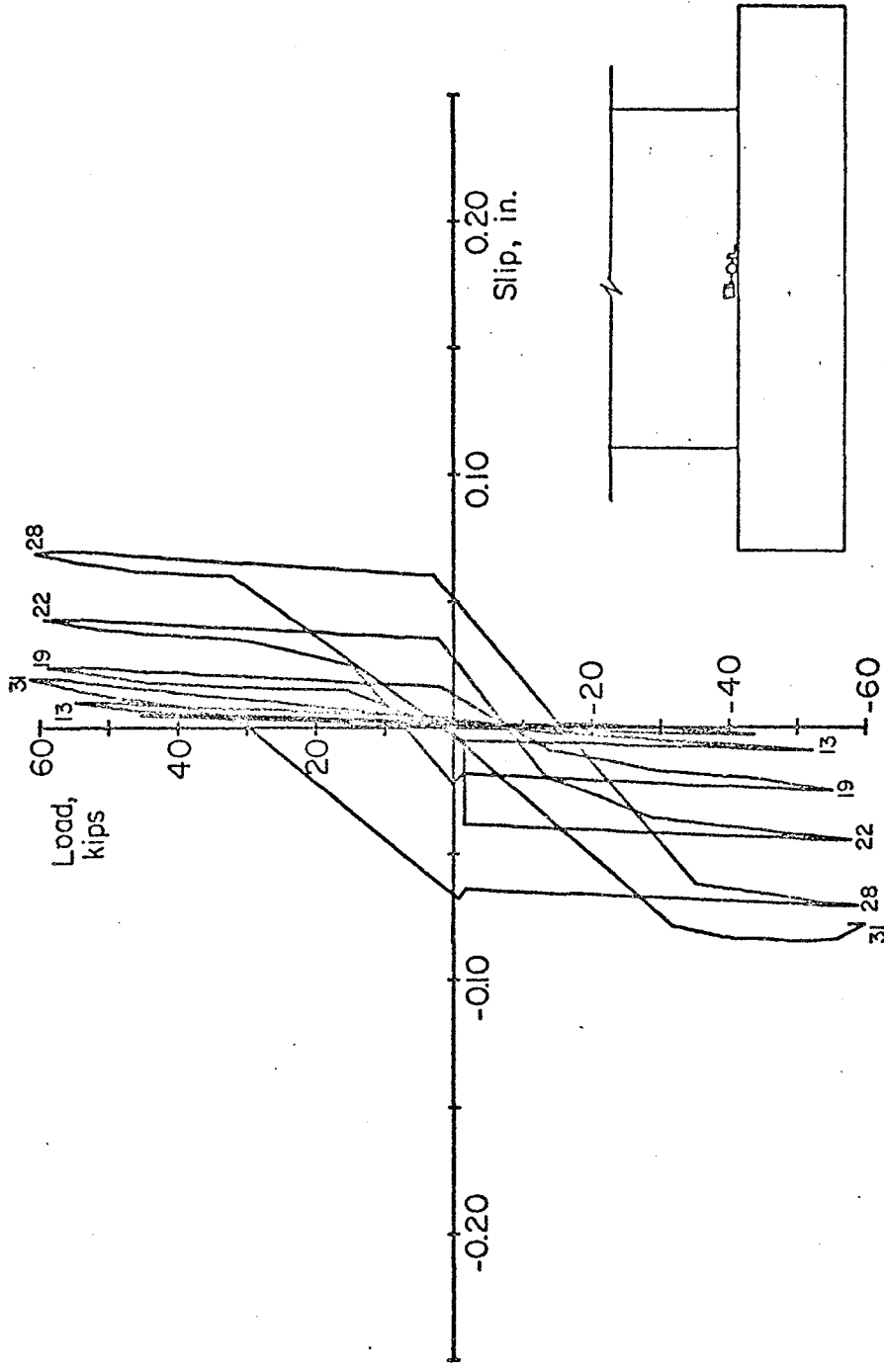
Fig. 76 Load Versus Slip Relationship for Base Construction Joint
of Specimen B3

are based on a preliminary analysis of the data. A more detailed analysis of the test results is in progress.

Strength. The measured yield and maximum loads for each specimen are summarized in Table 5.

Also shown in Table 5 are the calculated yield and maximum loads. These values were obtained from a flexural analysis of each cross section. Analysis of the sections was based on satisfying the applicable conditions of equilibrium and strain compatibility. A linear distribution of strain over the section was assumed. Measured material properties were used. The analysis considered complete stress-strain relationships for concrete and steel, including strain hardening of the reinforcement. A detailed description of the computer program developed for the sectional analysis is given in the analytical part of the Progress Report.

Calculated yield loads are in good agreement with the measured values except for Specimen R1 which yielded at a higher load than expected.

Maximum loads calculated do not account for any variation in strength resulting from load reversals. Except for Specimen F1, all of the walls reached a maximum capacity within 10% of the calculated capacity for a monotonically loaded wall. Specimen F1 apparently reached its shear capacity before developing its full moment capacity.

Design loads calculated according to the 1971 ACI Code[1] are compared with the maximum observed loads in

TABLE 5   TEST RESULTS

Specimen	Yield Load			Maximum Load		
	Observed (kips)	Calculated (kips)	Observed/Calculated	Observed (kips)	Calculated (kips)	Observed/Calculated
F1	150.6	154.5	0.97	187.9	252.6	0.74*
B1	45.1	46.9	0.96	61.0	67.1	0.91
B2	119.7	120.4	0.99	152.8	159.1	0.96
R1	20.1	16.6	1.21	26.6	29.1	0.91
B3	45.2	46.9	0.96	62.0	67.1	0.92

*Web crushing at $v_{max} = 10.4\sqrt{f'_c}$

Table 6. The ACI design does not account for strain harden-
ing of the reinforcement. It should be noted that in three
of the specimens, maximum bar spacing requirements led to a
significant over-design for shear. The intent was to design
the shear reinforcement to allow the development of the flex-
ural capacity. All specimens exceeded the ACI design strength.
It can be seen from Table 6 that Specimen F1 had a capacity
30% greater than the shear design capacity.

Load-Deflection Characteristics. Figures 77 through
80 show the envelope of the load versus deflection relation-
ships for the five specimens. Also shown are calculated load
versus deflection curves. The calculated curves were obtain-
ed by drawing straight lines between three points correspond-
ing to cracking, yield, and maximum.

The points at cracking were calculated using the
measured modulus of rupture and linear elastic beam theory.

The yield and maximum loads were calculated based
on measured material properties as described previously. The
yield and maximum deflections were calculated as the sum of
three components; flexural distortion, shearing distortion,
and rigid body overturning caused by slip of the main flex-
ural reinforcement.

The flexural component was derived by first calcu-
lating the sectional moment versus curvature relationships.
Then, using moment-area expressions, the flexural component
was calculated based on the applied moment diagram and the
moment versus curvature relationships.

TABLE 6   COMPARISON OF TEST AND DESIGN STRENGTHS

Specimen	Flexural Strength			Shear Strength		
	Observed (kips)	ACI Design (kips)	$\dfrac{\text{Observed}}{\text{ACI Design}}$	Observed (kips)	ACI Design (kips)	$\dfrac{\text{Observed}}{\text{ACI Design}}$
F1	187.9	145	1.30	187.9	140	1.34
B1	61.0	46	1.33	61.0	82*	0.74
B2	152.8	129	1.18	152.8	127	1.20
R1	26.6	18	1.48	26.6	82*	0.32
B3	62.0	46	1.35	62.0	82*	0.76

*Shear reinforcement governed by maximum bar spacing requirements.
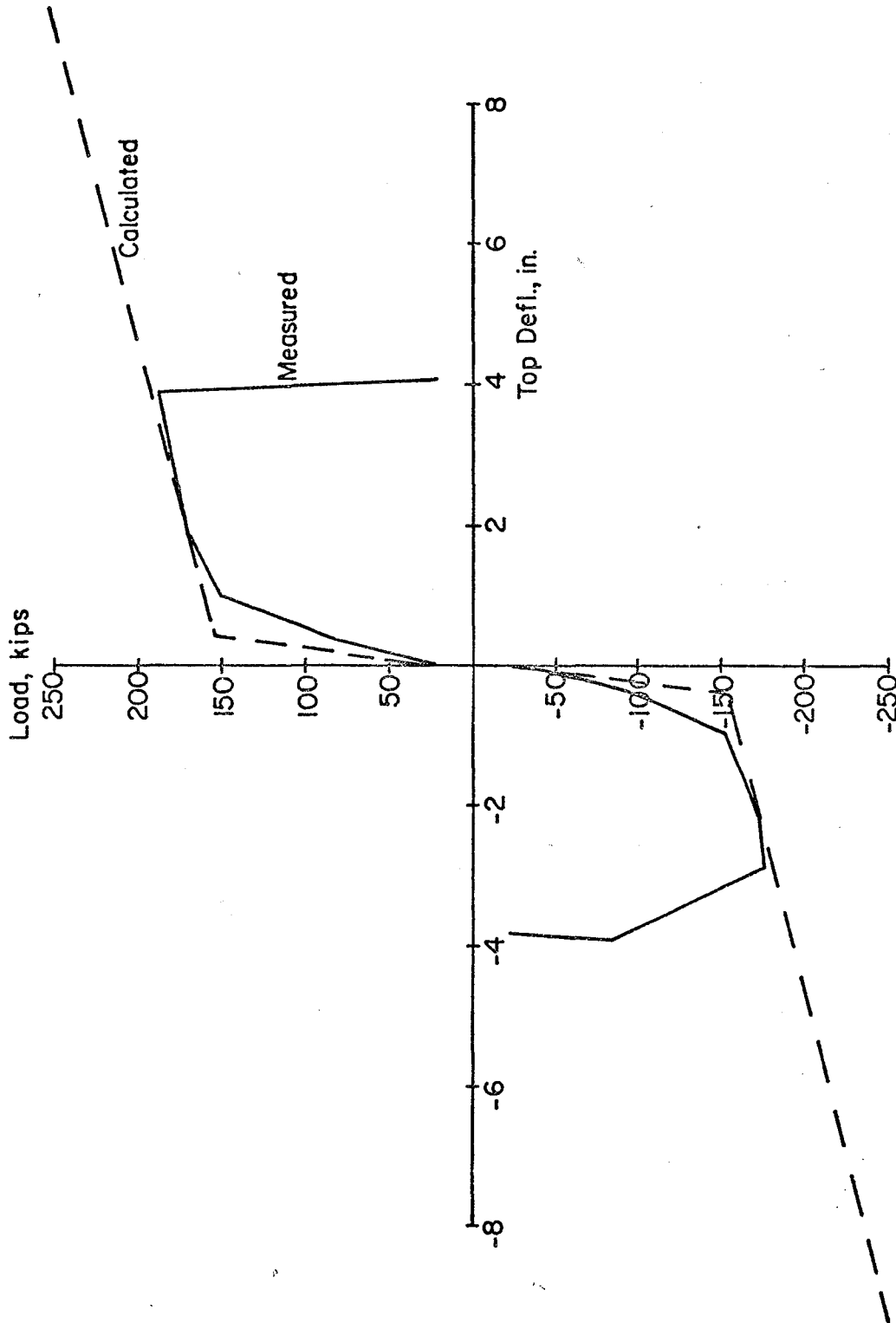
Fig. 77 Measured and Calculated Load Versus Deflection Envelopes for Specimen F1
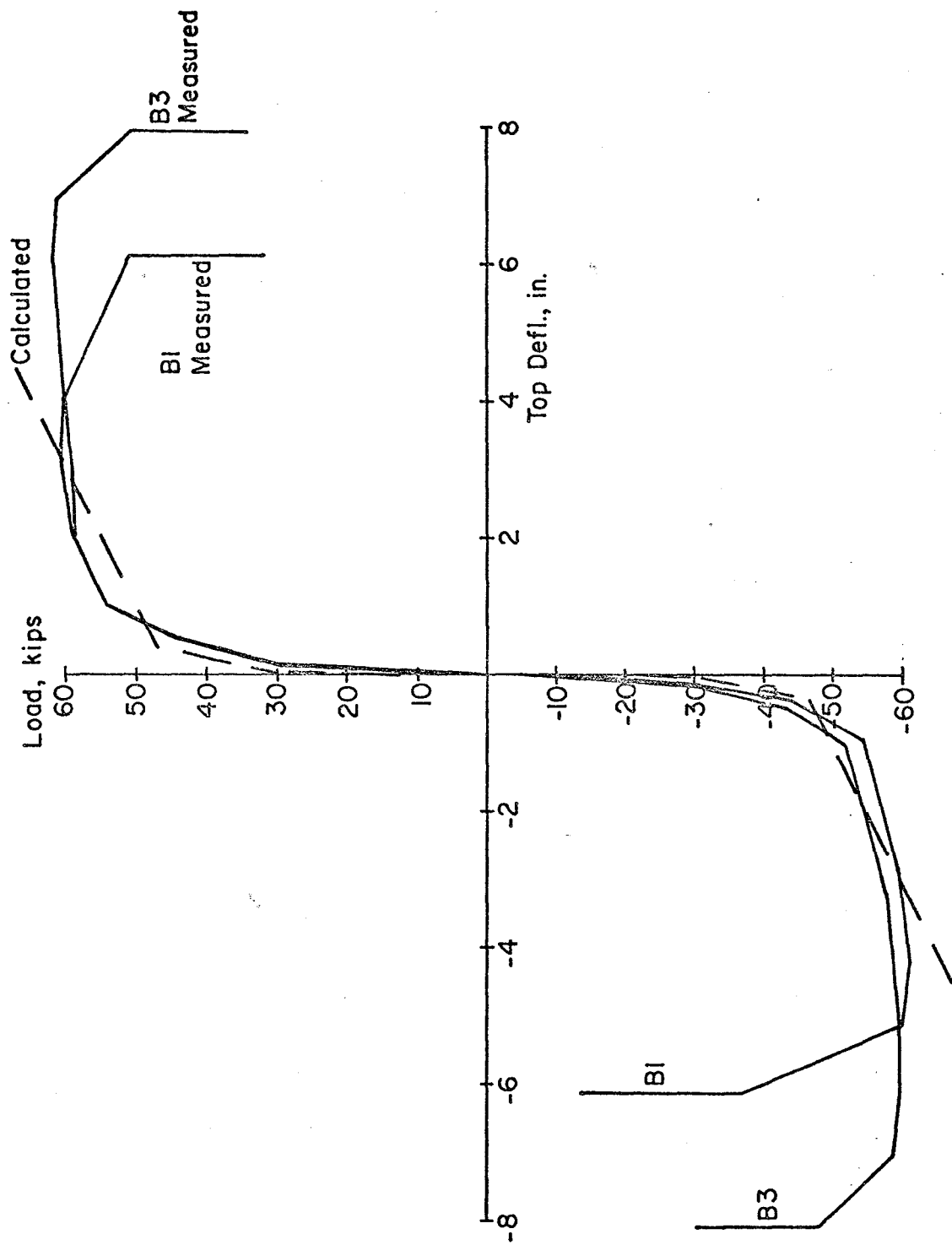
Fig. 78   Measured and Calculated Load Versus Deflection Envelopes
for Specimens B1 and B3
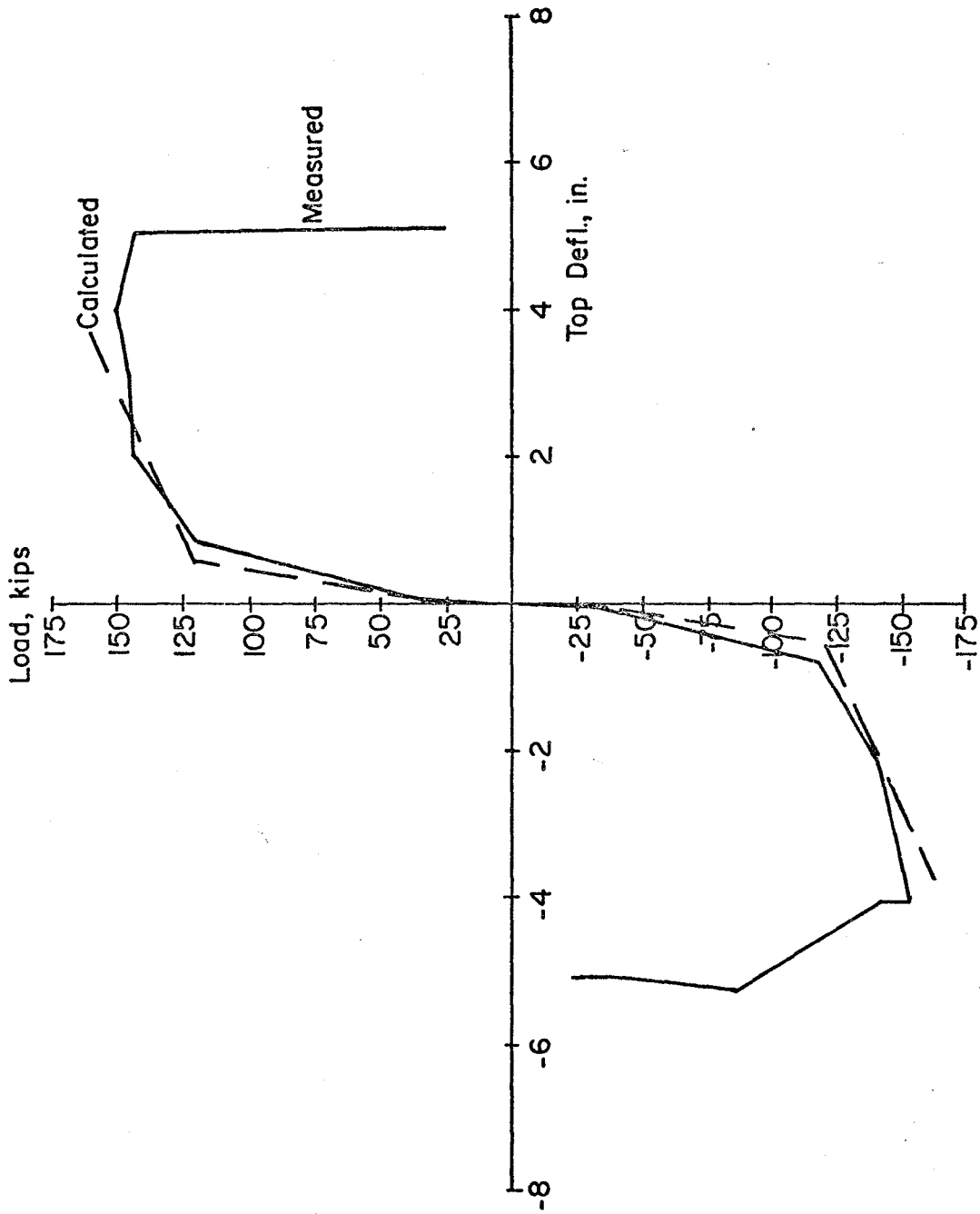
Fig. 79 Measured and Calculated Load Versus Deflection Envelopes
for Specimen B2
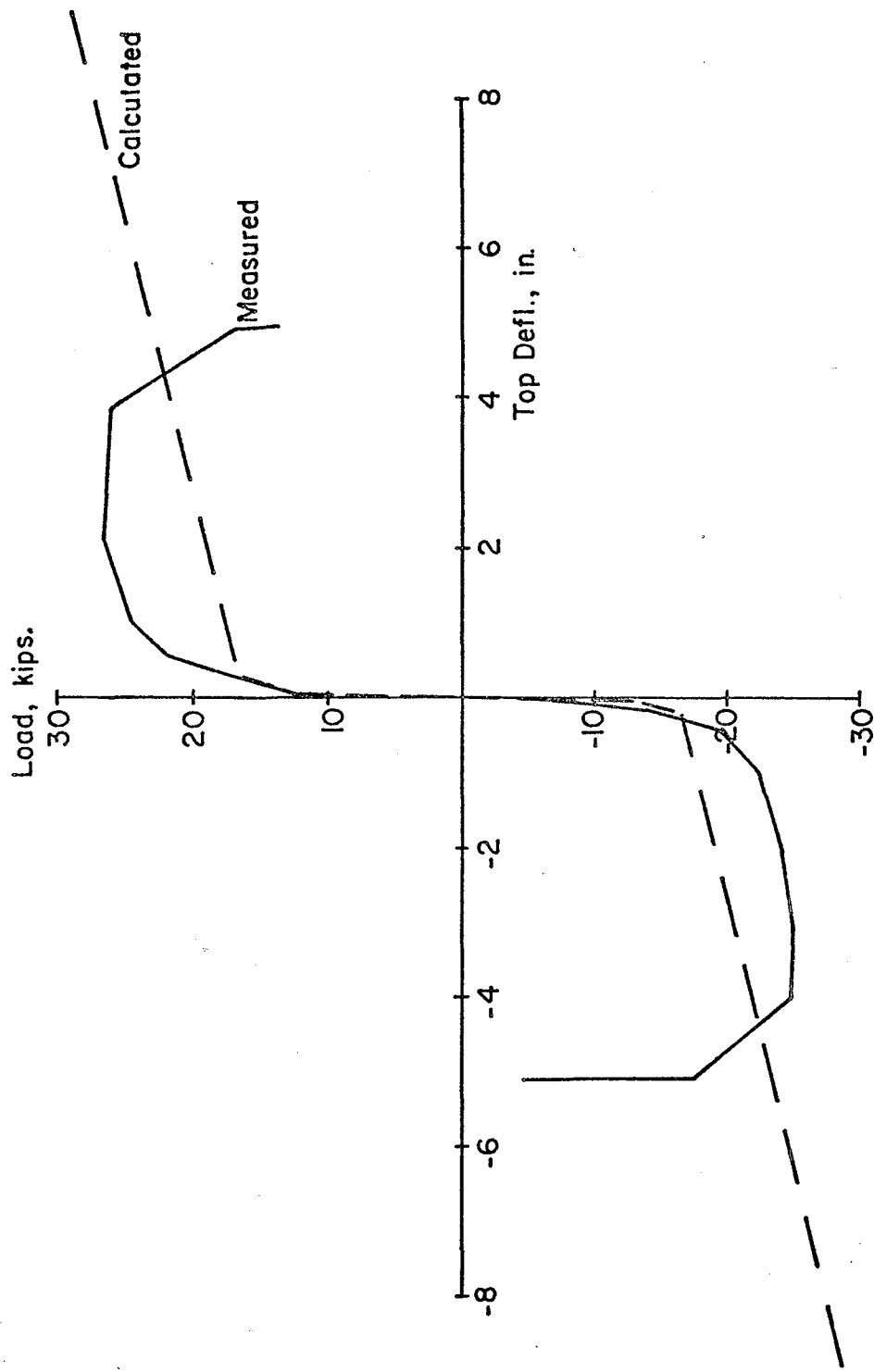
Fig. 80 Measured and Calculated Load Versus Deflection Envelopes
for Specimen R1

For these preliminary calculations, the shearing component was estimated as an elastic shearing deformation. This assumption underestimates the shearing component and needs to be studied in more depth.

Finally, the rigid body component was calculated by estimating the slip of the reinforcing bars in the tension column. The slip was estimated by assuming a linear bond stress distribution in the bars and integrating the yield strain over the development length of the bar. This component was generally quite small. Rotation was assumed to occur about the extreme compression fiber of the wall.

It is emphasized that the calculated curves do not account for any effects of loading reversals. In addition, the assumption used in calculating the shearing distortion cannot be considered adequate.

Comparison of the calculated and measured curves in Fig. 77 through Fig. 80 indicates reasonable agreement considering the limitations discussed previously.

Summary and Interim Conclusions

Behavior of Isolated Walls. In general, two types of behavior were observed in the walls. These types were distinguished by the magnitude of the applied shear. Load versus deflection envelopes for the specimens are compared in Fig. 81.

The two specimens subjected to high shears were F1 and B2. Maximum nominal shear stresses $v_{max} > 7\sqrt{f'_c}$ were applied. In these specimens the cracking patterns and failure

-108-
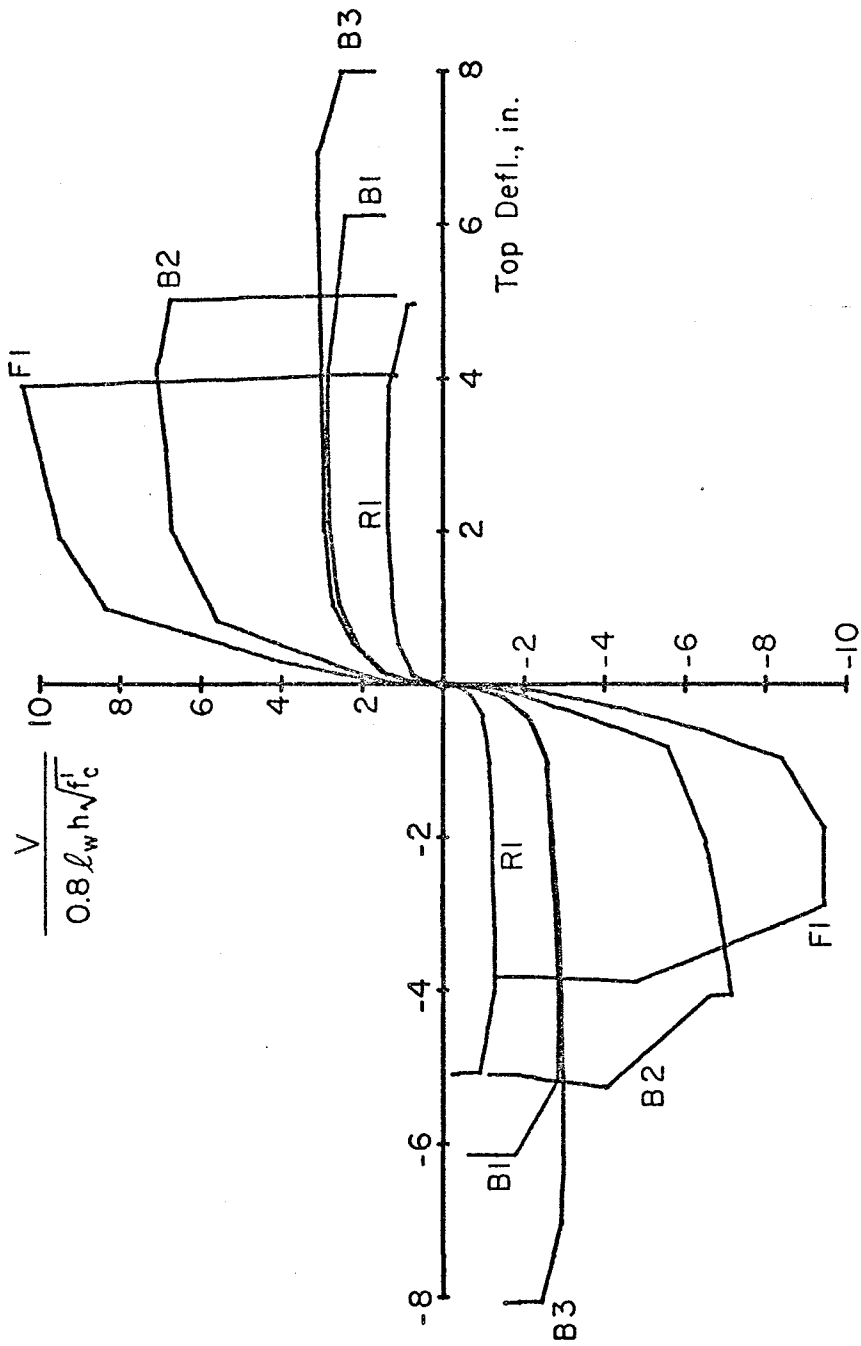
Fig. 81 Load Versus Deflection Envelopes for the Test Specimens

modes indicated that the effects of shear predominated. The
test of Specimen F1 was terminated by web crushing. The test
of Specimen B2 was terminated by a shear-compression failure.
Both failures occurred suddenly.

The three specimens subject to low shear were B1,
R1, and B3. Maximum nominal shear stresses $v_{max} < 3.1\sqrt{f_c'}$
were applied. In these specimens the cracking patterns and
failure modes indicated the predominate effects of flexure.
The failure mode for these specimens consisted of deteriora-
tion of the boundary elements by alternate tensile yielding
and compressive buckling of the main tensile reinforcement.
Eventually fractures of the main reinforcing bars occurred.
The fractures were undoubtedly influenced by prior bar buckl-
ing. However, loss of load capacity in these specimens was
gradual.

Specimen B3 had confinement hoops in the columns
over a height of 6 ft. The confinement resulted in a speci-
men with greater ductility than for the equivalent unconfined
specimen.

Summary of Test Results. The following observa-
tions are based on the data from the tests of the first five
specimens.

1. All specimens had a load capacity greater than
that predicted by the 1971 ACI Code[1] for both
flexure and shear design.

2. All specimens had post-yield deflection capabilities under reversing load.

3. Two specimens were loaded relatively lightly in shear ($v_{max} < 3\sqrt{f_c'}$) and had ordinary column ties. Capacities of these specimens were governed by damage to the boundary elements as alternate tensile yielding and compressive buckling of the main flexural reinforcement occurred. Buckling of a bar was followed, within one to three loading cycles, by fracture of the bar. Strength loss in these specimens was associated with bar fractures and with the loss of broken concrete pieces not contained by the reinforcing cage.

4. Two specimens were loaded relatively heavily in shear ($v_{max} > 7\sqrt{f_c'}$). The failure mode for these specimens was associated with web shear distress. In one of these specimens, the test ended with severe web crushing at a nominal shear stress $v_{max} = 10.4\sqrt{f_c'}$. Six inelastic cycles were applied to the specimen prior to web crushing.

5. Lateral confinement reinforcement added around the main flexural reinforcement in the boundary elements of one specimen helped to limit bar buckling. These hoops also contained the broken pieces of concrete within the core of the boundary elements. Even with the confinement, buckling of the main flexural reinforcement occurred.

-111-

However, the length of the buckled portion of
the bar was shorter in the confined specimen.
Buckling was followed by bar fracture within
one or two loading cycles. The specimen with
confinement underwent 29 inelastic cycles prior
to bar fractures. In comparison, the specimen
without confinement underwent 21 inelastic
cycles.

6. The load capacity of the confined specimen was
   approximately the same as that for a companion
   specimen without confinement.

7. The confined specimen had an overall top de-
   flection ductility factor of about 50% greater
   than that for the companion specimen without
   confinement.

8. For all specimens, the primary area of distress
   was within a height equal to the horizontal
   length of the wall.

9. The construction joint at the base of each speci-
   men showed maximum slips in the range of 0.2 in.
   to 0.3 in. No specimen failures could be at-
   tributed to construction joint performance.

10. Free vibration measurements taken at intervals
    throughout the test of each wall showed that
    the frequency decreased by a factor of about
    three from the uncracked state to the state

where yielding had occurred. For the same conditions, damping increased from about 2% to about 10% of critical. After yielding, no significant change in damping was observed.

PART II - SYSTEMS

Objective and Scope

Description of the Systems. The purpose of Part II of the experimental investigation is to study the behavior of wall systems subjected to loadings representing forces generated during earthquakes. A wall system is defined as a group of interacting structural elements, at least one of which is a wall. Four such systems have been selected for testing. As shown in Figs. 82 through 85, these systems have been selected to represent a full range of prototype wall systems that might be used in buildings.

System 1, shown in Fig. 82, consists of two identical wall elements connected by relatively deep coupling beams. An overall length-to-depth ratio of 2.5 was selected for these beam elements. This ratio places them outside the range of those in systems tested by Santhakumar and Paulay.[5] Shear and flexure are expected to have approximately equal influence on the behavior of these members. Shear reinforcement will be provided to assure that their strength is governed by flexure. The wall elements are rectangular in cross section and have an overall height-to-depth ratio of approximately three.

System 2, shown in Fig. 83, is similar to System 1 except for the length of the coupling beams. An overall length-to-depth ratio of five has been selected for the coupling beams in this system. The behavior of these slender connecting beams is expected to be governed by flexure.
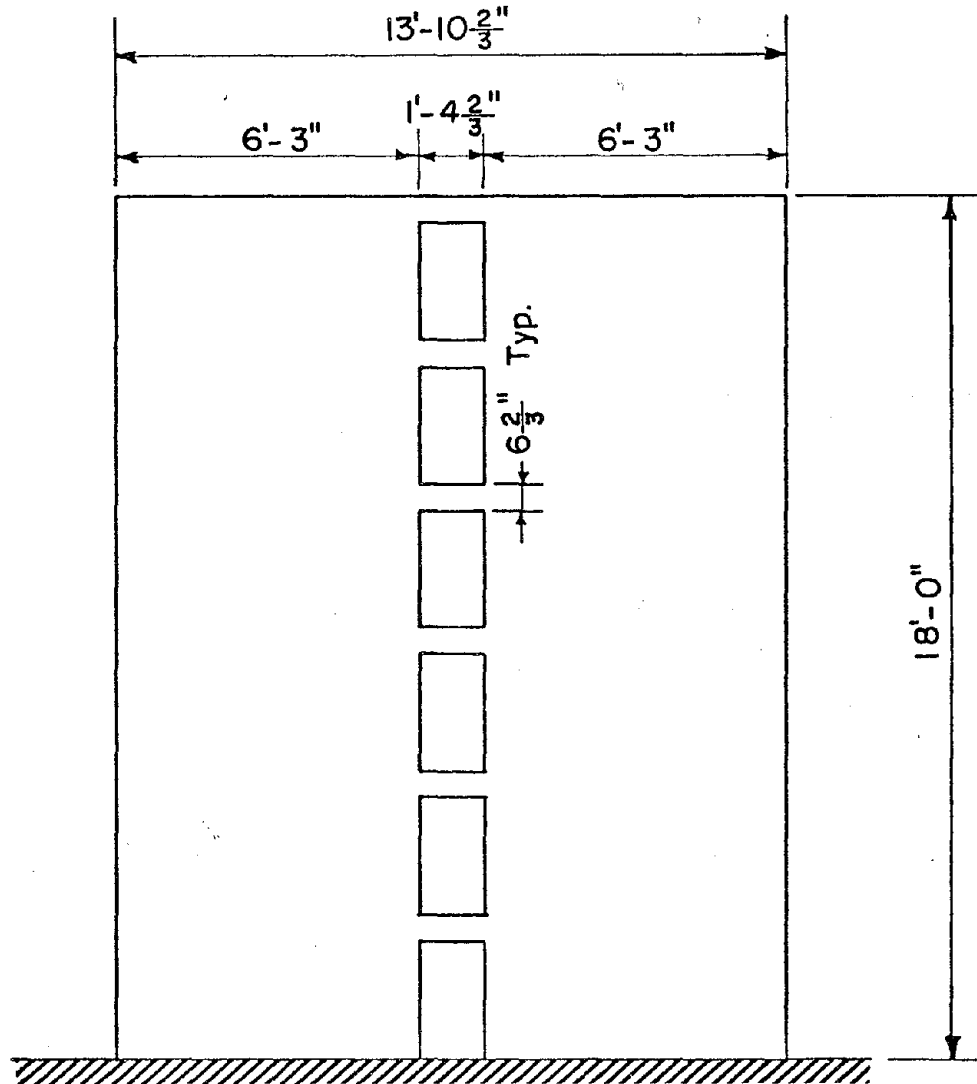
Fig. 82 System 1 - Walls Coupled by Deep Beams
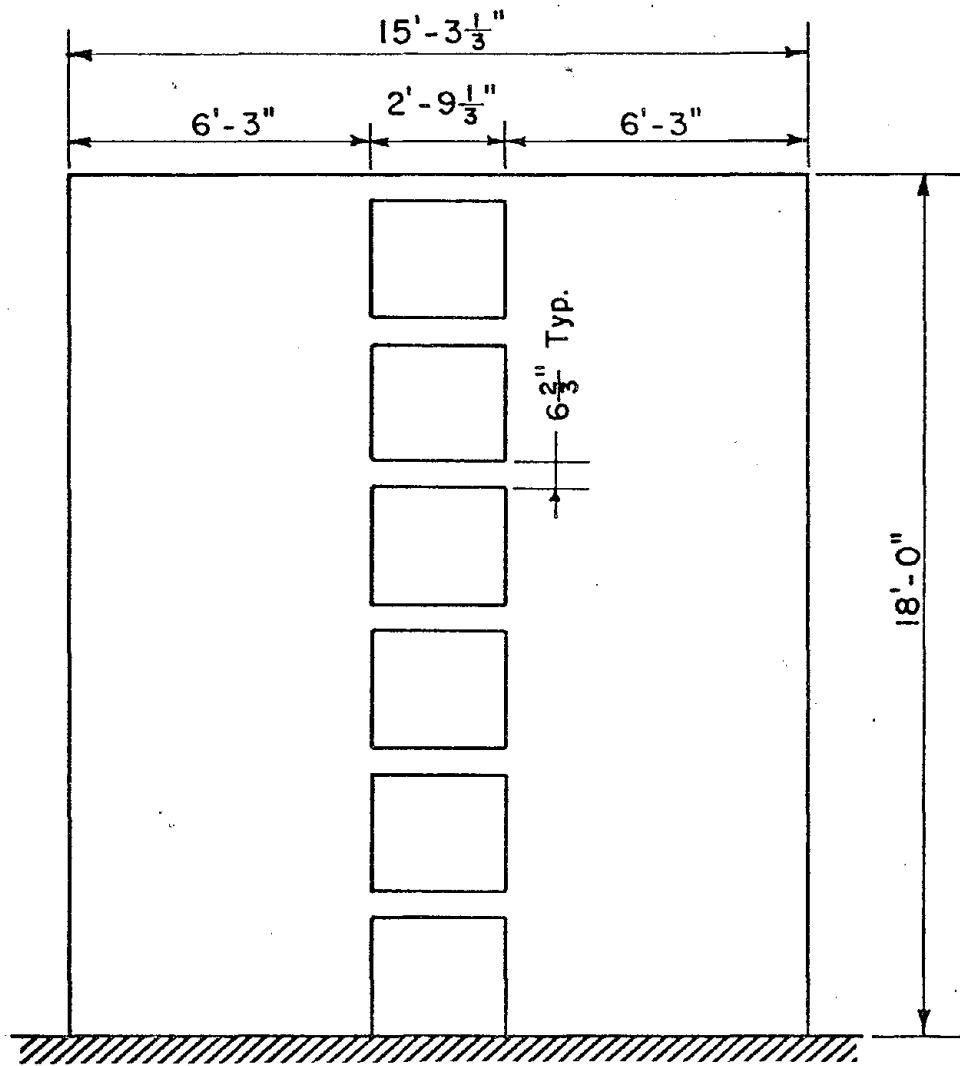
Fig. 83   System 2 - Walls Coupled by Slender Beams
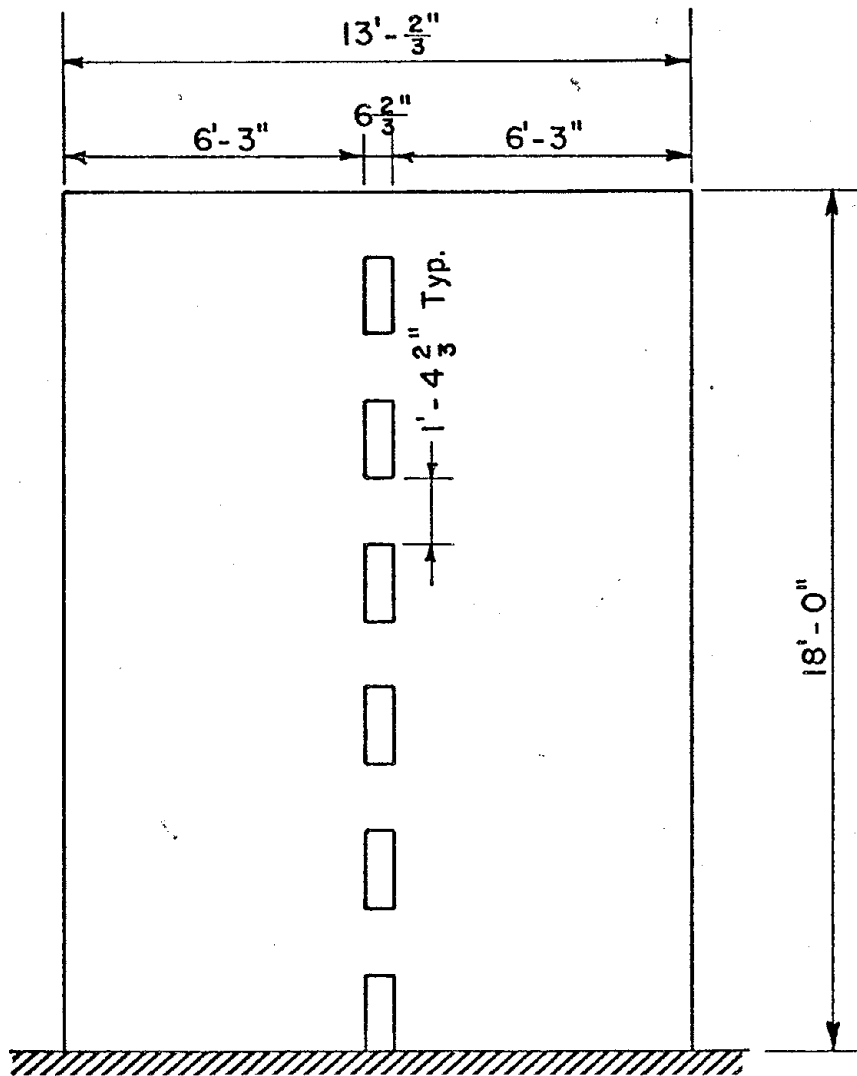
Fig. 84   System 3 - Wall with Central Openings

-117-
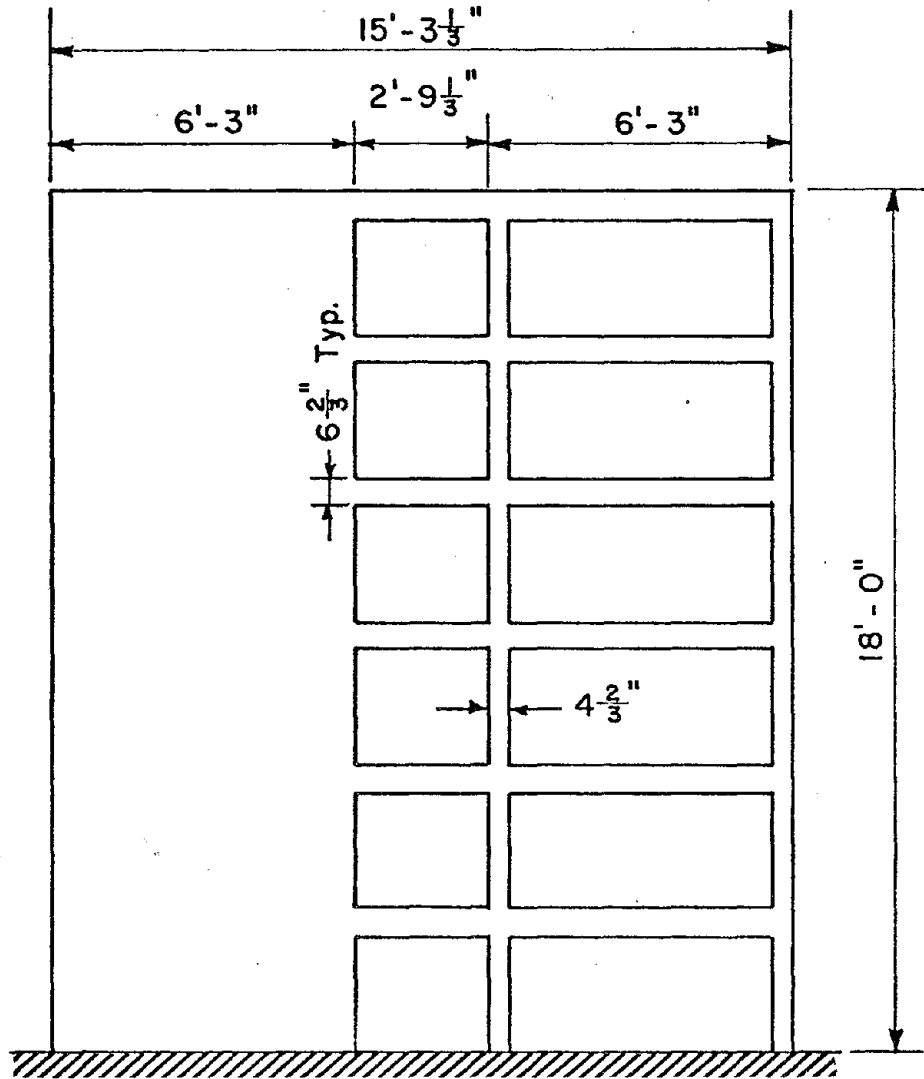
Fig. 85   System 4 - Wall-Frame System

System 3, shown in Fig. 84, differs from System 1 and System 2 in that it is designed to behave as a single isolated wall. The wall is pierced with a row of vertical openings. Dimensions of the connecting elements above and below these openings are the inverse of those in System 1. This gives them an overall length-to-depth ratio of 0.4, placing them below the proportions of elements tested by Paulay.[6,7] Their strength is expected to be governed by shear. The vertical elements in this system have the same overall dimensions as the walls in Systems 1 and 2.

As shown in Fig. 85, System 4 consists of a wall interacting with a frame. The geometry of this system is similar to that of System 2. However, very large openings have been placed in one wall element to form the frame. The beam elements connecting the wall to the frame have overall length-to-depth ratios of five, the same as the connecting beams in System 2. The vertical wall element is the same as those used in System 1 and System 2. Overall dimensions of the frame are the same as those of the wall.

Design Criteria. A significant portion of the total effort during the first twelve months of the project has been directed toward proportioning the four systems. These were selected with the intent of extending the work done by other investigators and avoiding unnecessary duplication of effort. Criteria defining desired modes of behavior for each system were established. Based on these criteria, an analysis was performed

to obtain element proportions and reinforcing steel requirements in each system. An explanation of the manner in which this approach was applied to each system follows.

The behavioral criteria for System 1 and System 2 require that hinging in all coupling beams occur prior to yielding in the walls. This is desirable since damage confined to the coupling beams can be repaired easily. It also results in the most efficient use of the energy dissipating capacity of the system.

Diagonal reinforcement, as shown in Fig. 86, will be placed in the expected hinging region of the beams in System 1 and System 2. Sufficient amounts of diagonal steel to carry the total shear force will be provided. The primary purpose of this reinforcement will be to prevent "sliding shear" failures similar to those observed by other researchers.[5,6,7] The diagonal reinforcement will be embedded in the walls. Closed vertical hoops will provide confinement of the beam concrete.

System 3 was designed to behave as an isolated wall. This requires that the connecting elements remain stiff so that the capacity of the system is governed by flexure at the base.

The design of System 4 was based on the requirement that the hinges should form in the beams, rather than the columns. This mode of behavior is considered necessary to maintain overall lateral stability of the system under earthquake loading.

Design of Systems

Coupled Walls. Equal amounts of top and bottom flex-
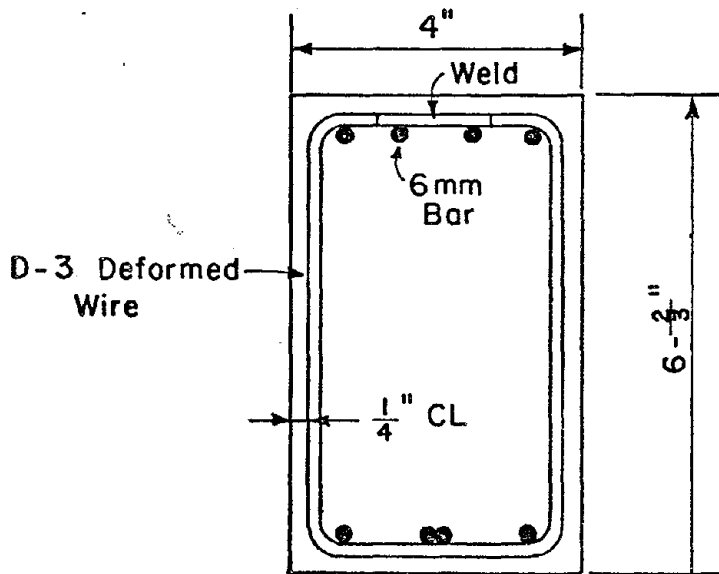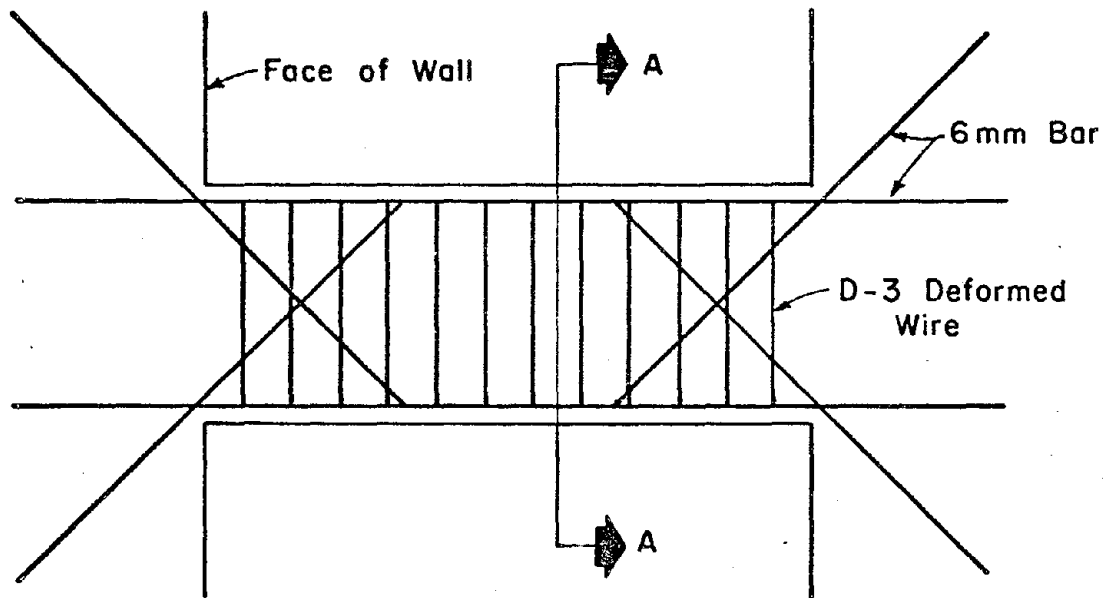
SECTION A-A

Fig. 86 Proposed Details of Coupling Beam for System 1

ural reinforcement will be provided in the coupling beams of System 1 and System 2. This reinforcement was selected to control the magnitudes of the shear stresses in these members. The coupling beams in System 1, having an overall length-to-depth ratio of 2.5, will have a maximum shear stress of $6.5\sqrt{f'_c}$ based on 3000 psi concrete and using 60,000 psi reinforcing steel with a 50% increase assumed for strain hardening. This shear stress is near the maximum suggested by Bertero and Popov[8] for this type of member. The maximum shear stress in the coupling beams of System 2 will be $2.6\sqrt{f'_c}$. Behavior of the coupling beams in both System 1 and System 2 will be determined by element tests.

The rectangular wall elements in System 1 and System 2 are similar to Specimen R2 scheduled for testing in Part I of the investigation. A detail of the wall cross section is shown in Fig. 87. These walls, designed in accordance with the 1971 ACI Building Code,[1] contain 4% local vertical reinforcement in the outer edges and 0.25% reinforcement elsewhere. Closed hoops are provided to confine the local vertical reinforcement in the hinging region at the base of the wall.

Both System 1 and System 2 were analyzed to determine that hinging in the coupling beams would preceed yield in the wall elements. The effects of cracking in both the coupling beams and the walls were considered. In the analysis, one wall of each system was isolated and subjected to the maximum possible coupling beam forces in combination with the lateral
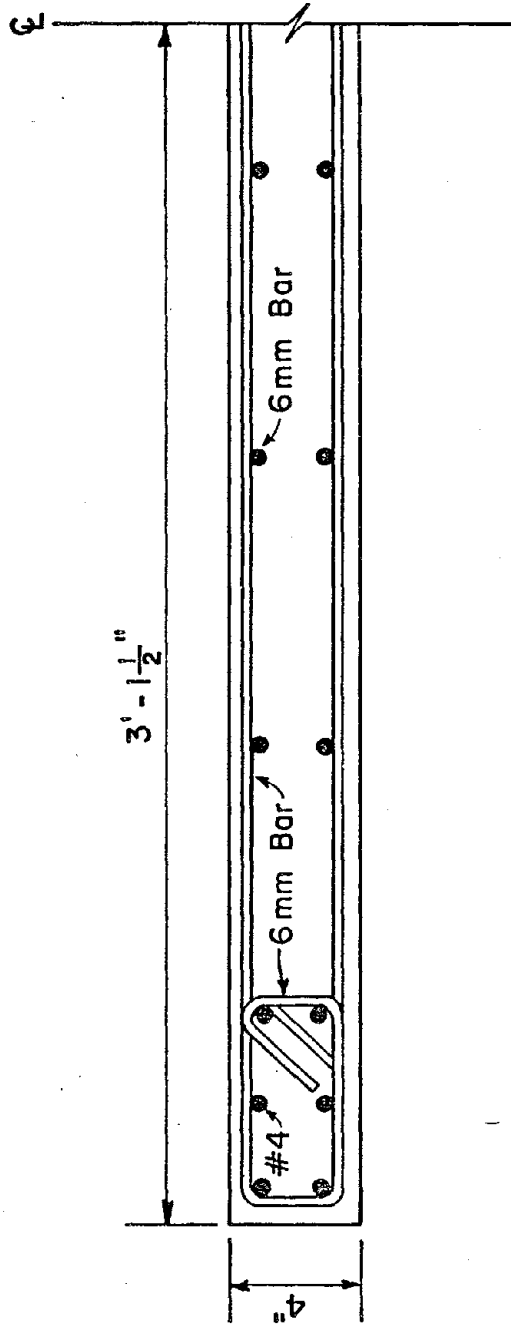
Fig. 87 Cross Section of Wall Element

load causing yield in the wall. Deflections and rotations were calculated along the face of the wall at coupling beam locations. A similar analysis was carried out for the other wall. Coupling beam end rotations were then calculated and compared to those required to cause yielding. Rotations were greater than those required, indicated that all coupling beams hinge prior to wall yielding. Finally, the capacities of each system were calculated by assuming a mechanism with hinges at the base of the wall elements.

Wall with Central Openings. System 3 was designed with 4% local reinforcement at its outer edges. To satisfy equilibrium, the total shear in all the connecting elements was equated to the tensile capacity of the vertical reinforcement at the base of one vertical element. The proportionate distribution of shear force carried by each connecting element was determined by the so called "laminar" method of analysis. (9,10,11) A maximum shear stress of $20\sqrt{f'_c}$ has been calculated for the critical connecting element. Reinforcement to resist shear was proportioned by shear friction.

Wall-Frame System. The wall-frame system was analyzed using an available computer program[12] to determine conditions at first yield. This analysis indicated that first yield occurs at the base of the wall element instead of in the connecting beams as for System 1 and System 2. This is attributed to the fact that the frame is much more flexible than a wall. Consequently, less restraint is provided at the ends of the connecting beams. To ensure overall lateral stability

-124-

of the frame, the columns were designed with a greater moment capacity than the beams. The capacity of the system was calculated using limit analysis.

Selection of Scale

Selection of an appropriate scale for the coupled wall systems was dependent on several factors. A scale large enough to permit use of hot rolled deformed reinforcement was needed. However, physical dimensions of the laboratory required that less than full-scale structures be tested. A 1/3 scale was selected to best satisfy these requirements. Testing to this scale has an additional advantage in that dimensions of the walls are similar to those of the isolated walls in Part I. Therefore, the results of the two parts of the investigation can be easily compared.

Fabrication

Plans for fabricating the test specimens were made during the period. For ease of construction, the specimens will be cast horizontally and rotated into the upright position for testing. The design of the formwork to facilitate this procedure is nearing completion.

Test Apparatus

Figure 88 shows an elevation of the planned test set-up. Loading abutments consisting of pairs of reinforced concrete panels will be located on each side of the test specimens. These will be post-tensioned to the test floor to provide lateral resistance for loading the specimens. The fabrication of the panels is underway.
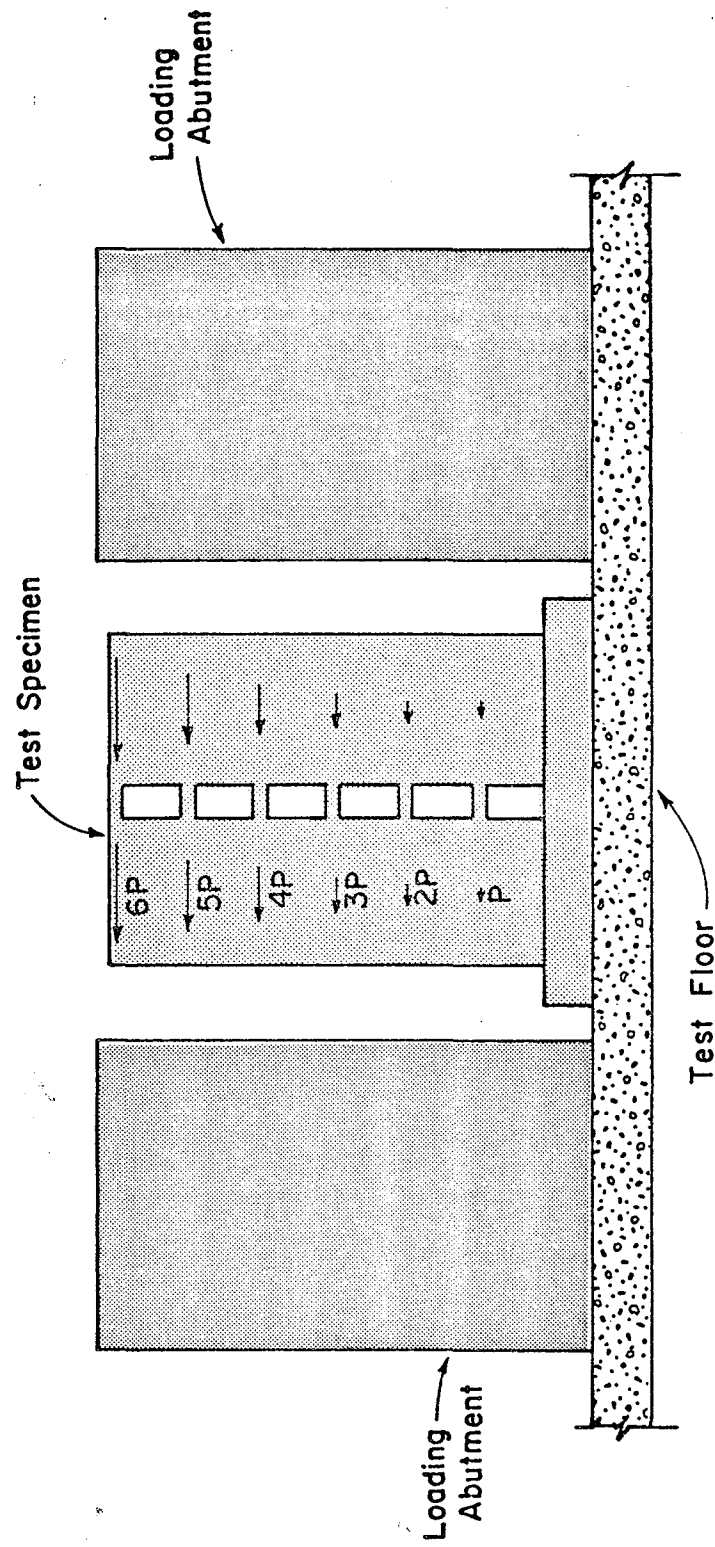
Fig. 88 Setup for Systems Tests

Lateral loads will be applied to the test specimens
to create a triangular distribution of force. The direction of
the forces will be reversed during alternate load cycles. Loads
will be applied equally to the centroids of the vertical wall
elements at each floor level to simulate the effect of inertia
forces. The magnitude of the applied loads will be controlled
hydraulically. The design of the loading apparatus is nearly
complete.

PART III - ELEMENTS

Objective and Scope

The objective of this part of the investigation is to perform tests on elements of wall systems to provide information on effectiveness of confinement reinforcement. In this Progress Report, results are given for an initial investigation of the effects of lateral confinement on the stress-strain curves of concrete in compression.

In this investigation, tests are being carried out on 17 specimens representing the compression zones of walls. Test cross sections are provided with lateral confinement reinforcement in the form of closed rectangular hoops. The effective stress-strain curve for the confined concrete is being determined from the data to obtain a measure of the added ductility available from confinement.

Test Program

Design of Test Specimens. The tests were performed using C-shaped specimens as shown in Fig. 89. These were adopted from the design first used by Hognestad, Hanson and McHenry[2] to determine the stress-strain curve of plain concrete.

In the tests carried out to date, the variables include spacing of confinement reinforcement, size of confinement, strength of concrete, amount of longitudinal reinforcement, and size of the test specimen. Values chosen for the different variables are shown in Table 7.
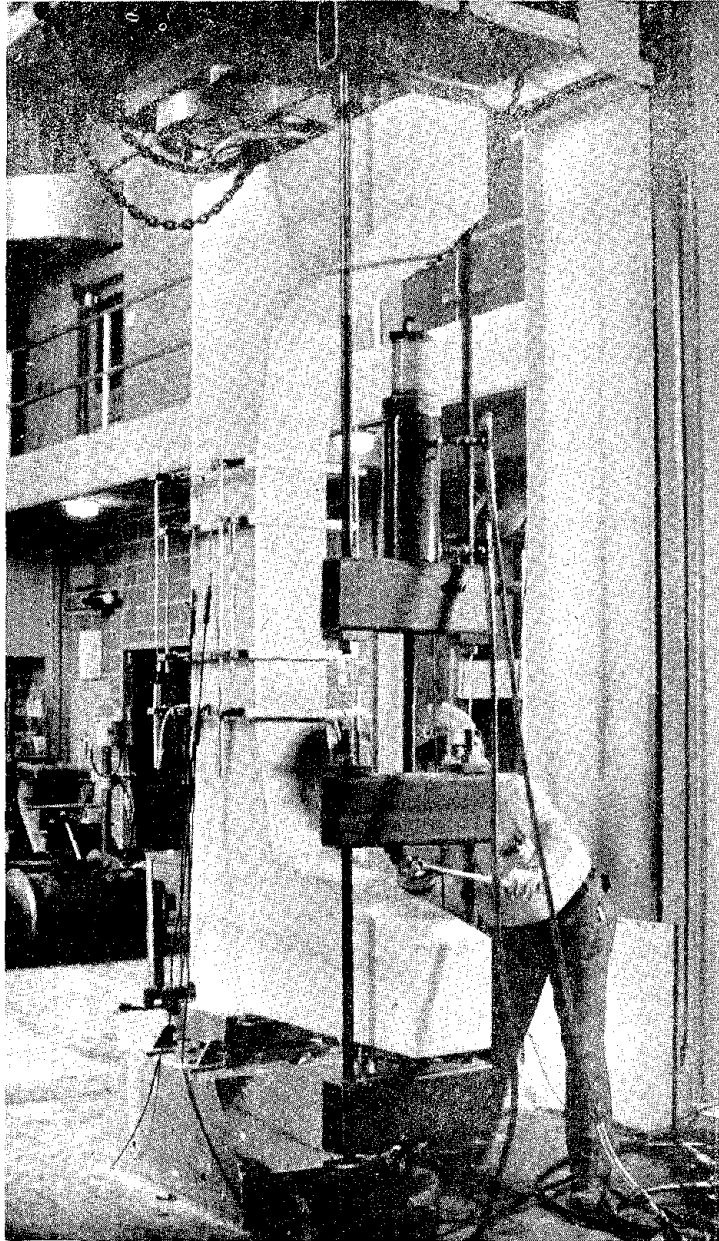
Fig. 89   Test Specimen Ready for Testing

TABLE 7   DETAILS OF TEST SPECIMENS

Group	Test Cross Section in.	Long. Reinf. %	Concrete Comp.Str. ksi	Hoop Size Bar No.	Hoop Spacing in. 2	4	8	∞	Comments
1	10x16	0	3					X*	Plain Concrete
2	10x16	0.5	3	3		X			
				4	X	X*	X		
				5		X			
3	10x16	3.9	3	3		X			
				4	X	X*	X		
				5		X			
4	5x8	0	3					X	Plain Concrete
5	5x8	0.5	3	2	X				
6	5x8	4.4	3	2	X				
7	5x8	0	6					X	Plain Concrete
8	5x8	0.5	6	2	X				
9	5x8	4.4	6	2	X				

Notes: 1. Groups 4, 5 and 6 are repetitions, in half scale, of the specimens marked with asterisk* in Groups 1, 2, and 3, respectively

2. Groups 7, 8 and 9 are repetitions in 6 kis concrete, of Groups 4, 5 and 6, respectively

The two sizes of test specimens were 5x8 in. and 10x16 in. For the larger size specimen the central value for the hoop size and spacing is No. 4 bars at 4 in. This met the requirements of ACI 318-71[1] for lateral confinement as specified in Appendix A, Section A.6.4.3. The hoop size and spacing were increased and decreased from this value to determine the influence on the effective stress-strain curve of the concrete. The specimens were constructed using concrete having a design cylinder strength of 3000 psi.

Longitudinal reinforcement consisted of four bars, one in each corner of the cross section. Two sizes of bars were used; No. 4 and No. 11. This gave vertical reinforcement percentages of 0.5 and 3.9, respectively. These values were chosen to approximate the extreme range that might be used in practice. In addition, specimens having the central values of the variables will also be constructed in half size using 3000 psi and 6000 psi concrete. Specimens with hoop reinforcement of No. 2 bars at 2-in. spacing will be tested with 0.5% or 4.4% longitudinal reinforcement.

A plain concrete specimen of the larger size using 3000 psi concrete was tested. Specimens in the smaller size using 3000 and 6000 psi concrete strengths are also included to provide a basis for comparison.

Results described in this report cover the tests in which confinement reinforcement size and spacing were varied in the larger size specimen having a 0.5% longitudinal rein-

forcement. Results for the plain concrete control specimen are also included.

Description of Test Specimens. The larger specimens shown in Fig. 89 were 104-in. high and 10x16 in. in cross section

Hoops were held in place at the desired spacing by tying to the longitudinal reinforcement. The four longitudinal bars were placed at the rectangular hoop corners so that the hoop cover was 3/4 in. Flexural and shear reinforcement was added to the arms of the "C" shaped specimen to prevent distress in this region during the test. A photograph of a reinforcing cage is shown in Fig. 90.

Materials. The concrete contained a blend of Type I portland cements and 3/4-in. maximum size Elgin sand and gravel aggregate. Each specimen was moist cured under plastic sheet at 73F for three days after casting. Subsequently the concrete was cured at 73F and 50% relative humidity. The concrete cylinder strengths ranged from 3040 to 3430 psi for the specimens reported. Strengths given are the average of three 6x12-in. cylinders taken from the concrete region on which strain measurements were made during the test. The arms of the specimen were cast at the same time as the test portion, but using higher strength concrete.

All reinforcement met the requirements of ASTM Designation A615[13] Grade 60.
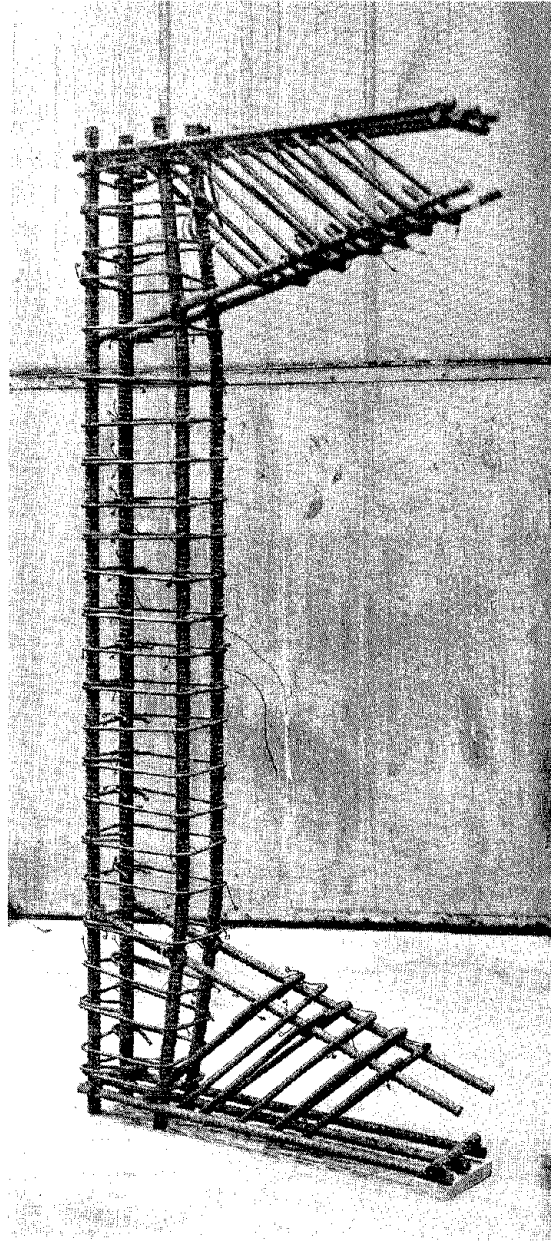
Fig. 90   Reinforcing Cage for Confined
          Concrete Test Specimen

Construction of Test Specimens. Reinforcement cages were constructed as shown in Fig. 90. Details of the completed cage are shown in Fig. 91. The cage was placed in a plywood form and the specimen cast in a horizontal position as shown in Fig. 92.

Test Apparatus The major load P_1, shown in Fig. 91, was applied by a testing machine having a million pound capacity. Force was applied through a system of bearing plates and rollers that accommodated rotation of the specimen during the test.

The minor load P_2, shown in Fig. 91, was applied by a hydraulic ram through a system of rods, cross-heads and rollers. This apparatus is also visible in the foreground of Fig. 89.

Test Procedure. During the test, the major load P_1 was increased at a constant rate. By manually controlling the value of the minor load P_2, strain at the extreme fibers at the back of the cross section, the left side in Fig. 91, was kept at zero. The back face represented the neutral axis boundary of the compression zone of the cross section. On the opposite side of the cross section, the right side in Fig. 91, the extreme fibers are subjected to a monotonically increasing compressive strain, thus representing the extreme compressive fiber of the cross section.

Instrumentation. Direct current differential transformers (DCDT) measuring the distances between reference frames mounted transversely on the specimen were used to determine
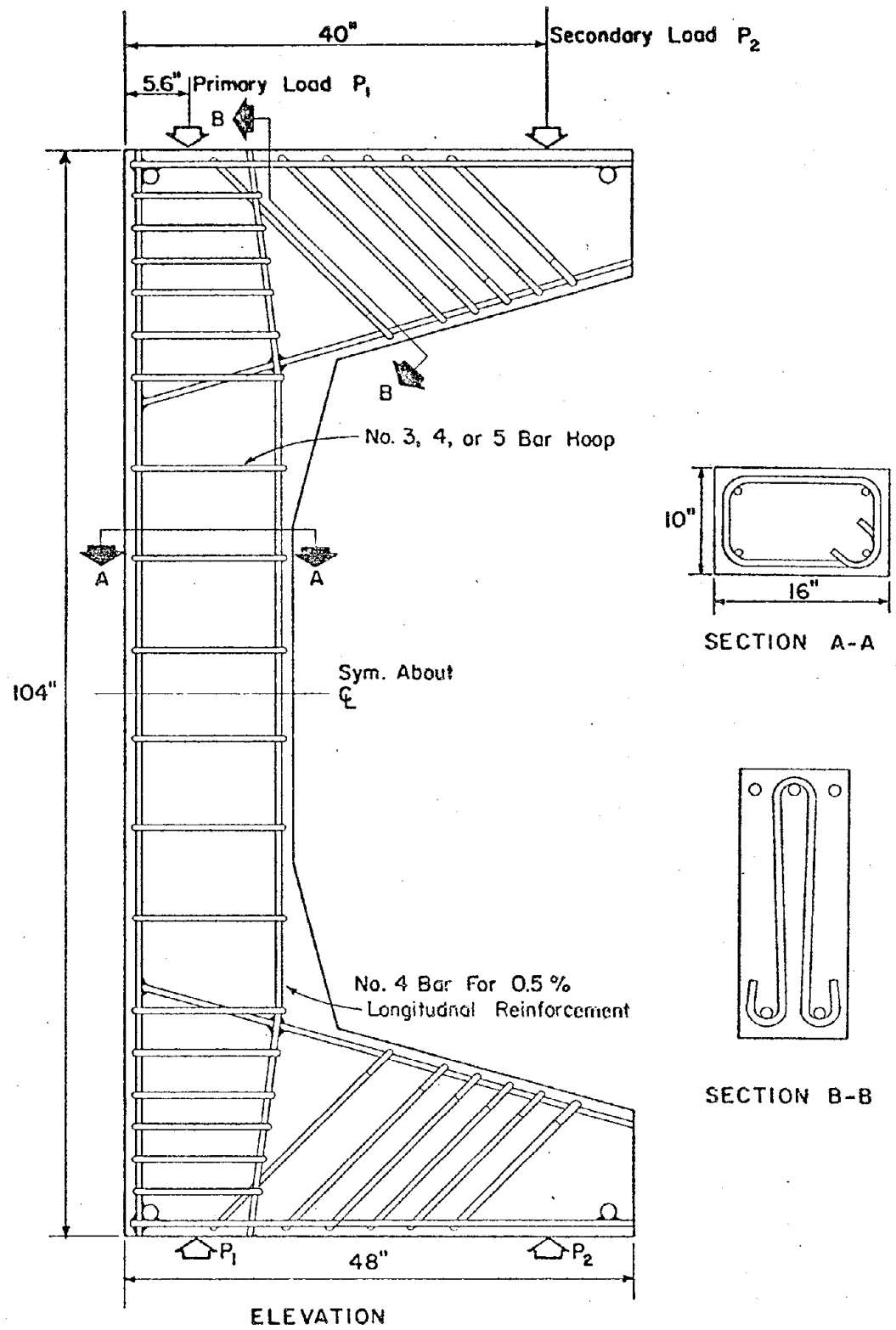
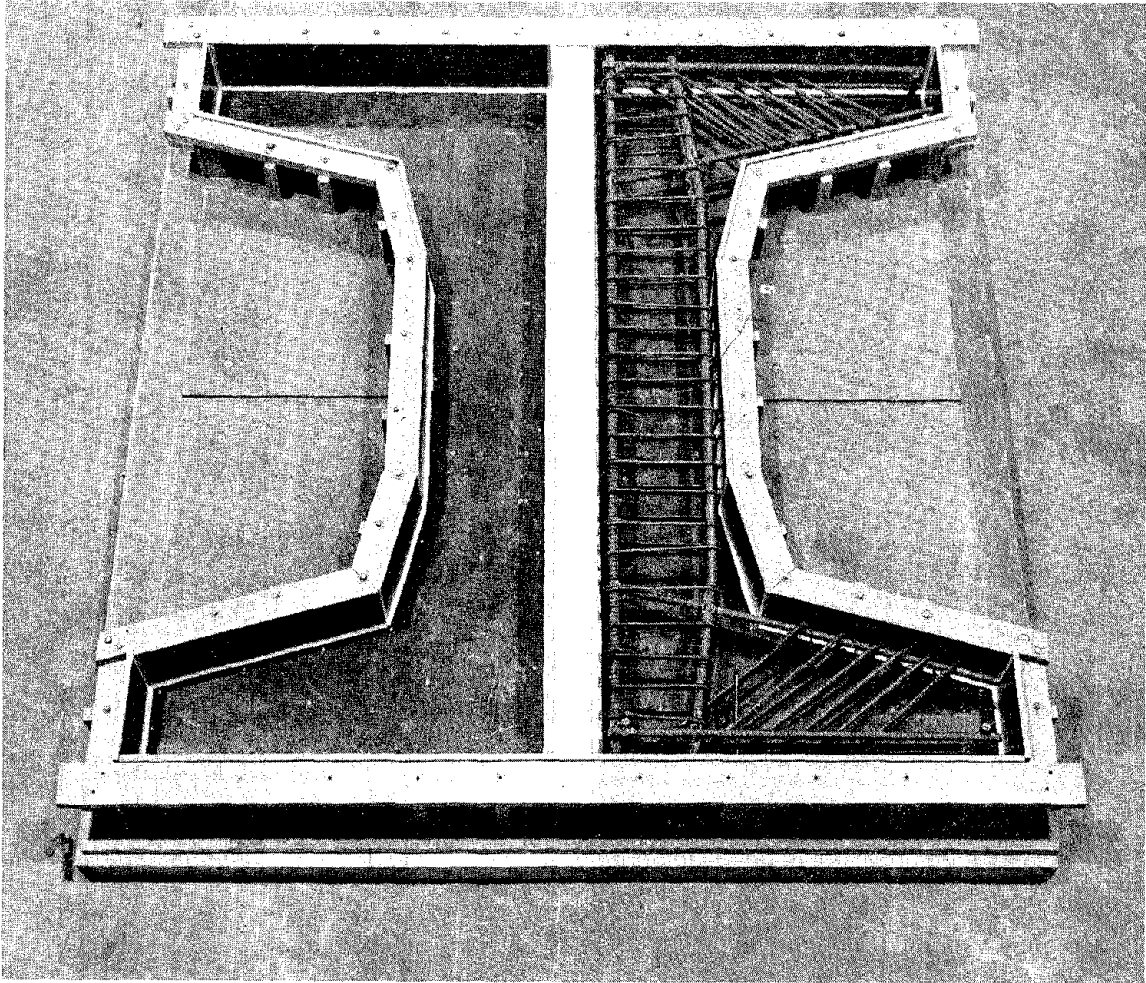Fig. 91   Confined Concrete Specimen Details

Fig. 92 Reinforcing Cage in Form

strain both in the plane of the compression face and in the plane of the neutral face. Two pairs of frames were used over gage lengths initially at 16 in. and at 30 in. An additional horizontal DCDT was used to monitor the bending distortion from loading. This information was used to determine changes in the load lever arms.

Signals from the DCDT's were monitored at regular intervals during the continuous loading of the specimen. Loads were also monitored by sensors described elsewhere[14]. Electrical resistance strain gages mounted on most specimens provided confirming information on strain distributions prior to spalling of the concrete cover. Data was both printed and punched on paper tape. The punched tape was read into an META 4/1130 computer for data reduction and analysis.

Analysis. Stresses in the longitudinal reinforcement were calculated from strain data. Resultant reinforcement loads and moments were then subtracted from total loads and moments so that loads and moments on the concrete could be determined.

With loads and moments on the concrete determined, analysis followed that used by Hognestad, Hanson, and McHenry[2]. Closely spaced readings of data during the test enabled the differentials in the following equations to be approximated by finite differences $\Delta f_o / \Delta \epsilon_c$ and $\Delta m_o / \Delta \epsilon_c$

$$f_c = \epsilon_c \frac{df_o}{d\epsilon_c} + f_o \qquad (1)$$

$$f_c = \epsilon_c \frac{dm_o}{d\epsilon_c} + 2\, m_o \qquad\qquad (2)$$

where

    f_c = compressive stress in concrete

    ϵ_c = strain in concrete

    f_o = average compressive stress in concrete

    $m_o = \dfrac{\text{applied monent}}{bc^2}$

    b = width of rectangular member

    c = distances from neutral axis to compression
         edge of member

Concrete stresses are calculated on the basis of small differences between large numbers. This process naturally produced some scatter in the data. By using two independent methods to calculate the relationship between stress f_c and strain ϵ_c the accuracy of the test data is checked since several experimental sources of error affect the two equations differently.

To produce the final plots, results of the data analysis were condensed by eliminating readings for which the two values of f_c did not substantially agree. These selected points were then plotted and a smooth curve drawn. The results are shown in Figs. 93 and 94 for variations in hoop spacing and hoop size, respectively. A sample plot of selected points is shown in Fig. 95.
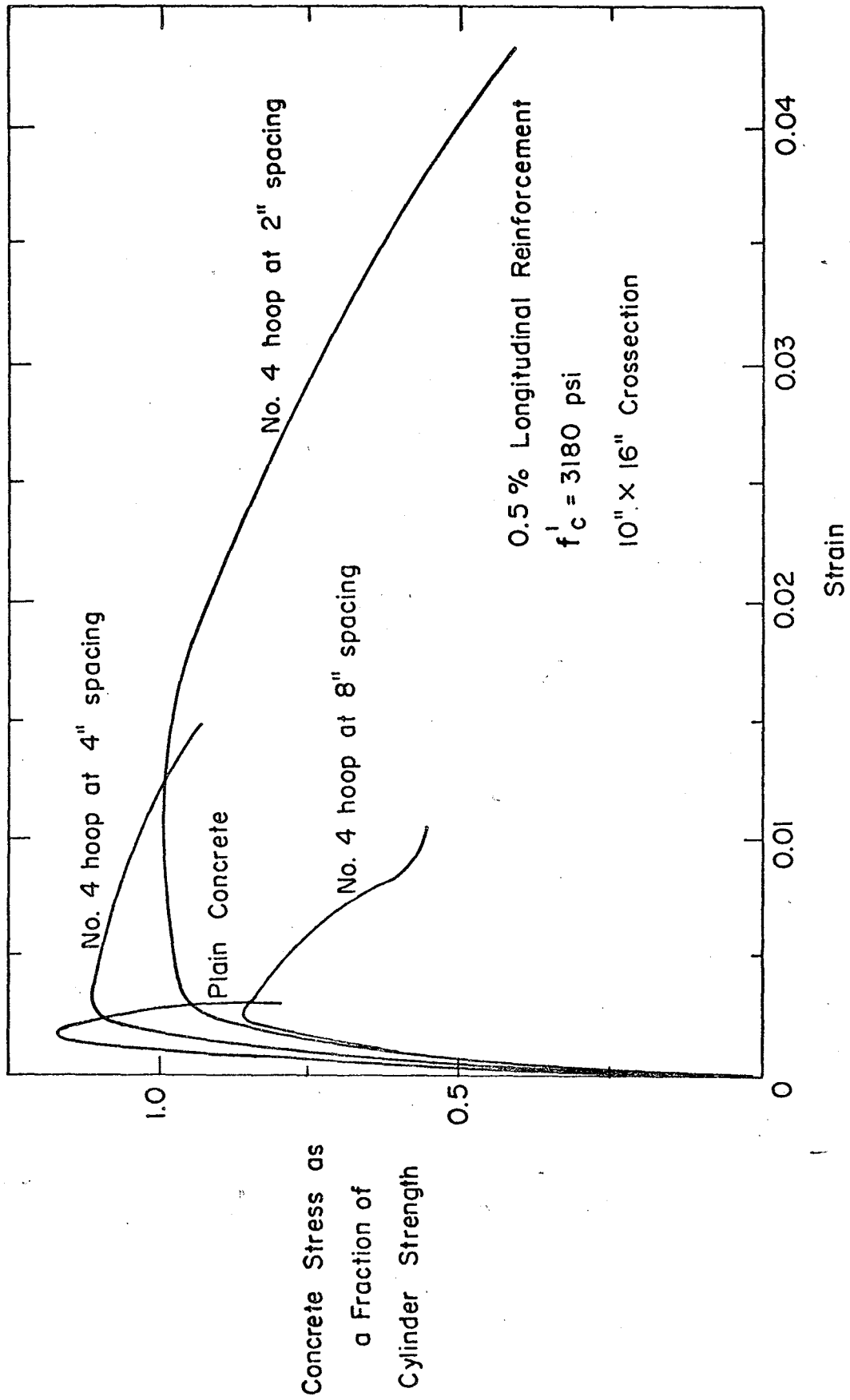
-138-

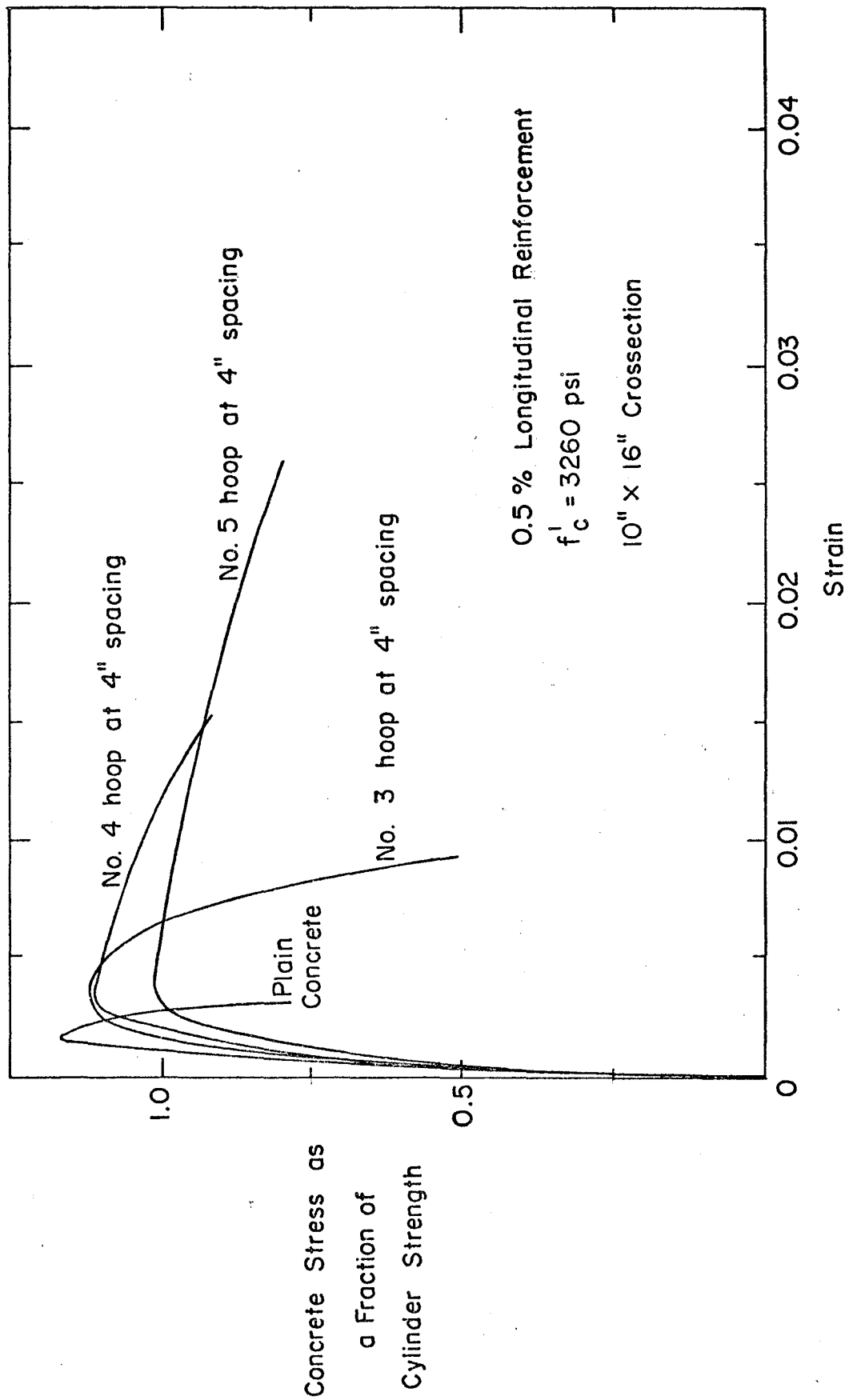Fig. 93 Stress-Strain Relationship of Confined Concrete – Effect of Hoop Spacing

Fig. 94 Stress-Strain Relationship of Confined Concrete –
Effect of Hoop Size

Fig. 95   Data Forming Basis of Faired Curve Shown in Fig. 94

Test Results

Test results shown in Figs. 93 and 94 illustrate the effect on stress-strain relation of hoop spacing and size of hoops for specimens reinforced with 0.5% longitudinal reinforcement. The stress-strain relation of a plain concrete specimen is shown for reference. The ordinate to all plots is in terms of the ratio of concrete stress to concrete cylinder strength.

Regardless of spacing, hoops did have a beneficial effect upon the stress-strain relation. Even specimens containing hoops with 8-in. spacing showed capacity remaining at strains of 0.010, a value well above the 0.003 strain often assumed for plain concrete and observed once again in the control specimen.

All failure modes of confined concrete specimens were gradual while unreinforced concrete specimens failed suddenly. Maximum strain in the confined specimens was attained when the longitudinal reinforcement buckled. Figure 96 shows the buckled bar in each region of the confined concrete specimens after testing. In no case did the confined concrete specimens fracture into two sections as did the plain concrete specimens shown in Fig. 97 after testing. This continuity is a necessary prerequisite for ductile behavior.
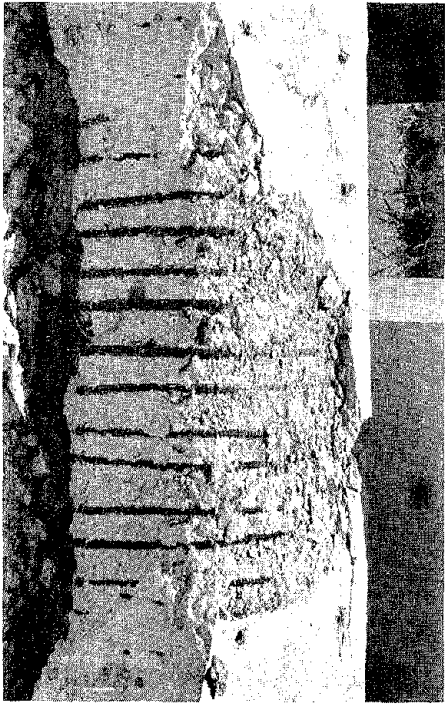
a) 2-in. Hoop Spacing
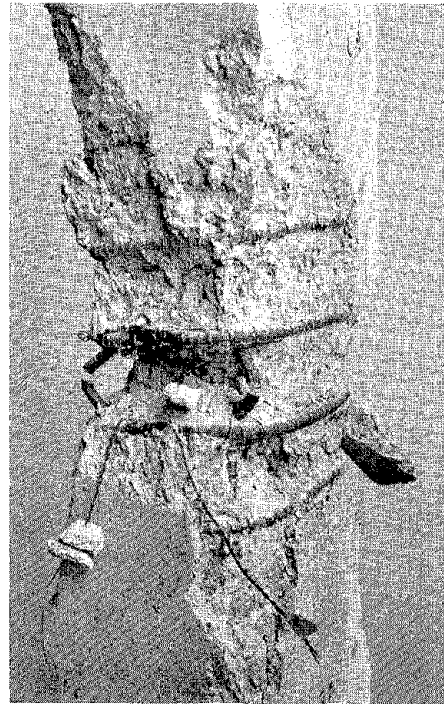
b) 4-in. Hoop Spacing

c) 8-in. Hoop Spacing
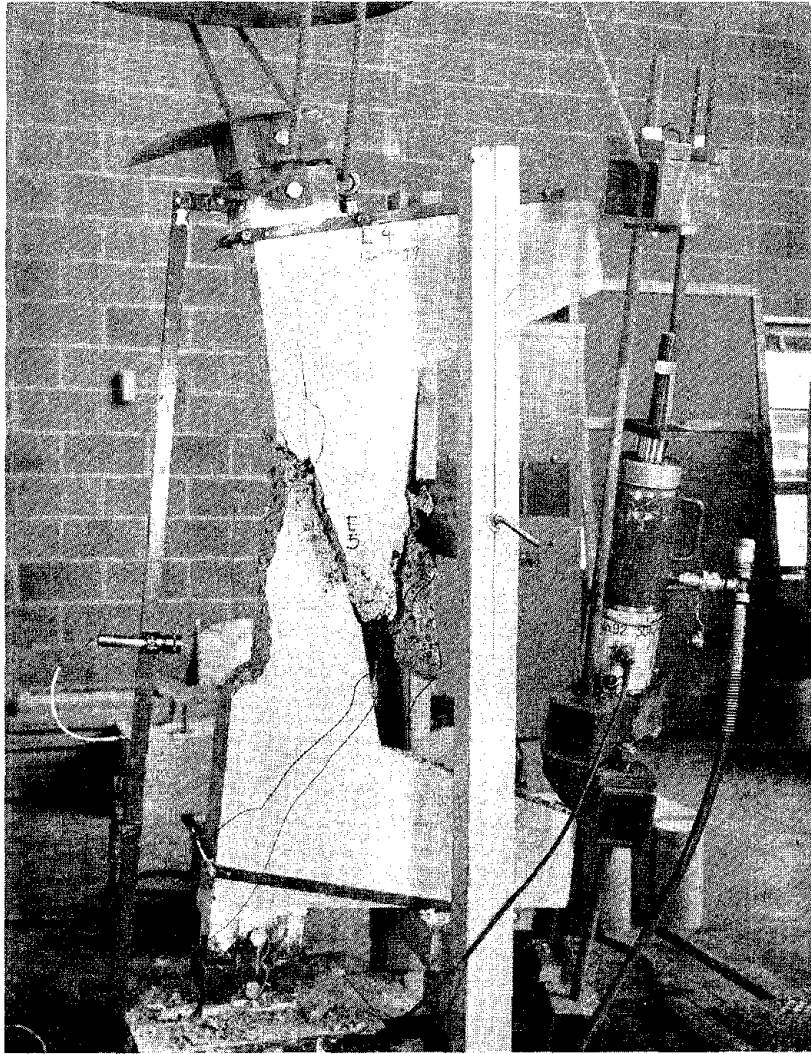
Fig. 96 Buckled Bar Region of Specimens

Fig. 97   Plain Concrete Specimen After Test

REFERENCES

1. "Building Code Requirements for Reinforced Concrete (ACI 318-71)," American Concrete Institute, Detroit 78 pp.

2. Hognestad, E., Hanson, N. W., and McHenry, D., "Concrete Stress Distribution in Ultimate Strength Design,, Journal of the American Concrete Institute, December 1955, Proceedings, Vol. 52, pp. 455-479. Also PCA Development Bulletin D6.

3. "Manual of Standard Practice for Detailing Reinforced Concrete Structures (ACI 315-74)," American Concrete Institute, Detroit, 1974, 167 pp.

4. "Specifications for Structural Concrete for Buildings (ACI 301-72)," American Concrete Institute, Detroit, 1972, 36 pp.

5. Santhakumar, A. R., and Paulay, T., "Ductility of Coupled Shear Walls," University of Canterbury, Civil Engineering Research Report No. 74-10, Christchurch, New Zealand, 1974.

6. Paulay, T., "Coupling Beams of Reinforced Concrete Shear Walls,, Journal of the Structural Division, ASCE, Vol. 97, No. ST3, Proceedings Paper 7984, March 1971, pp. 843-862.

7. Paulay, T., "Simulated Seismic Loading of Spandrel Beams," Journal of the Structural Division, ASCE, Vol. 97, No. ST9, Proceedings Paper 8365, September, 1971, pp. 2407-2419.

8. Bertero, Vitelmo V., and Popov, Egor P., "Hysteretic Behavior of Reinforced Concrete Flexural Members with Special Web Reinforcement," Proceedings, U. S. National Conference on Earthquake Engineering, Ann Arbor, 1975, pp. 316-326.

9. Chitty, L., "On the Cantilever Composed of a Number of Parallel Beams Interconnected by Cross Bars," London, Edinburgh and Dublin Philosophical Magazine and Journal of Science, Vol. 38, October 1947, pp. 685-699.

10. Coull, A., and Choudhury, J. R., "Stresses and Deflections in Coupled Shear Walls," Proceedings, American Concrete Institute, Vol. 64, February, 1967, pp. 65-72.

11. Coull, A., and Choudhury, J. R., "Analysis of Coupled Shear Walls," Proceedings, American Concrete Institute, Vol. 64, September, 1967, pp. 587-593.

12. Derecho, Arnaldo T., "Analysis of Plane Multistory Frame-Shear Wall Structures Under Lateral and Gravity Loads," Portland Cement Association, Research and Development Bulletin SR097, 01D, 1971.

13. ASTM Designation: A615-74a, "Standard Specification for Deformed and Plain Billet-Steel Bars for Concrete Reinforcement. American Society for Testing and Materials, Philadelphia, Pennsylvania.

14. Hognestad, E., Hanson, N. W., Kriz, L. B. and Kurvits, O. A., "Facilities and Test Methods of PCA Structural Laboratory," papers under various titles in Journal of the PCA Research and Development Laboratories, Vol. 1, No. 1, Jan. 1959, pp. 12-20, 40-44; Vol. 1, No. 2, May 1959, pp. 30-37; and Vol. 1, No. 3, Sept. 1959, pp. 35-41; reprinted jointly as PCA Development Department Bulletin D33.

ACKNOWLEDGMENTS